

University of Rhode Island

DigitalCommons@URI

Open Access Dissertations

2022

ADVANCED DETECTION OF MICROPLASTICS AND PER- AND POLYFLUOROALKYL SUBSTANCES IN SEDIMENTS FROM THE NARRAGANSETT BAY WATERSHED

Michaela A. Cashman

University of Rhode Island, Cashman.Michaela@epa.gov

Follow this and additional works at: https://digitalcommons.uri.edu/oa_diss

Recommended Citation

Cashman, Michaela A., "ADVANCED DETECTION OF MICROPLASTICS AND PER- AND POLYFLUOROALKYL SUBSTANCES IN SEDIMENTS FROM THE NARRAGANSETT BAY WATERSHED" (2022). *Open Access Dissertations*. Paper 1364.

https://digitalcommons.uri.edu/oa_diss/1364

This Dissertation is brought to you by the University of Rhode Island. It has been accepted for inclusion in Open Access Dissertations by an authorized administrator of DigitalCommons@URI. For more information, please contact digitalcommons-group@uri.edu. For permission to reuse copyrighted content, contact the author directly.

ADVANCED DETECTION OF MICROPLASTICS AND PER- AND
POLYFLUOROALKYL SUBSTANCES IN SEDIMENTS FROM THE
NARRAGANSETT BAY WATERSHED

BY

MICHAELA A. CASHMAN

A DISSERTATION SUBMITTED IN PARTIAL FULFILLMENT OF THE
REQUIREMENTS FOR THE DEGREE OF
DOCTOR OF PHILOSOPHY
IN
BIOLOGICAL AND ENVIRONMENTAL SCIENCES

UNIVERSITY OF RHODE ISLAND

2022

DOCTOR OF PHILOSOPHY IN BIOLOGICAL AND ENVIRONMENTAL
SCIENCES

OF

MICHAELA A. CASHMAN

APPROVED:

Dissertation Committee:

Major Professor THOMAS B. BOVING

KAY HO

VINKA CRAVER

Brenton DeBoef
DEAN OF THE GRADUATE SCHOOL

UNIVERSITY OF RHODE ISLAND
2022

ABSTRACT

Sediments underlay most waterbodies and make up a vital part of aquatic habitats. Due to their physical and chemical properties, sediments can act as a sink for many types of contaminants. Sediments must be routinely assessed for their possible interaction with emerging contaminant classes. But the identification of emerging contaminants in sediments is often hindered by a lack of analytical standards or standardized methods. The research herein develops methods for the detection of two classes of emerging contaminants from sediment, namely microplastics (MPs) and per- and polyfluoroalkyl substances (PFAS). These methods are then used to analyze sediments within the Narragansett Bay watershed, Rhode Island, USA.

The first chapter of this dissertation focuses on microplastics. Microplastics are small (<5 mm) plastic particles which pose a threat to marine ecosystems. Identifying MPs in marine sediments is crucial for understanding their fate and effects. Many MP extraction methods exist, but procedural differences prevent meaningful comparisons across datasets. Chapter one examines the efficiency of five methods for extracting MPs (45–1,000 μm) from marine sediments. Known quantities of MPs were spiked into sediments. The MPs were extracted and enumerated to demonstrate percent recovery. Findings determined that sediment matrix, MP properties, and extraction method affect the percent recovery of MPs from sediments. Average recoveries of spiked microplastics were between 0 % and 87.4% and varied greatly by sediment type, microplastic,

and method of extraction. In general, larger particle and lower density MPs were more effectively recovered. Marine sediments low in organic matter and with larger grain size also had higher percent recoveries of MPs. These findings support the need for method optimization and unified procedures.

In chapter two, a hybridized method was developed for the extraction of microplastics (45-1,000 μm) from marine sediments using sodium bromide solution for density separation. Method performance was tested using spiked microplastics as internal standards. The method was then tested by extracting MPs from sediments collected from Narragansett Bay, Rhode Island, USA. Suspect microplastics were analyzed with Raman spectroscopy. Microplastic abundance ranged from 40 particles/100 g sediment to 4.6 million particles/100 g sediment (wet weight). Cellulose acetate fibers were the most abundant microplastic. These results are some of the first data for microplastics in Rhode Island marine sediments.

Chapter three shifts focus to a different class of contaminants: Per- and polyfluoroalkyl substances (PFAS) are a diverse set of synthetic fluorinated chemicals. The use of PFAS in industrial applications predates accessible analytical techniques for their identification in environmental matrices. Therefore, identifying sources of PFAS in environmental matrices can be challenging. Characterizing PFAS from radiometrically dated sediment cores is one mechanism to determine past PFAS deposition and provide a better understanding of the fate of this complex class of contaminants in aquatic environments. In this study, three sediment cores were collected from a

dammed section of the Pawtuxet River in West Warwick, Rhode Island, USA. The coring location was chosen for its proximity to former manufacturing facilities suspected to use PFAS. Sediments from the cores were radiometrically dated using ^{137}Cs and ^{210}Pb and analyzed for 24 PFAS compounds using a targeted analytical method. A modified Total Oxidizable Precursor (TOP) assay was performed to identify the presence of PFAS precursors. Suspect and non-targeted analysis was performed to identify additional PFAS missed in targeted analysis. Initial sediment concentrations showed temporal trends of PFAS preserved within the sediment record ranging from <1-50 ng/g sediment. These data identify legacy PFAS compounds previously used in manufacturing processes over several decades, particularly long-chain perfluorinated carboxylic acids (PFCAs). This type of investigation provides a window into the transport behavior and longevity of PFAS once they enter the sedimentary environment.

ACKNOWLEDGMENTS

There are many people I must thank for helping me through this chapter of my life. In seven years, I completed both my MS and PhD while working full time at the EPA. This would have never been possible without a core group of people who supported me through the entire process. I'd like to first thank my advisor, Dr. Thomas Boving. I consider myself lucky to have worked under his direction for both my master's and doctoral degrees. Thank you for shaping my education, expanding my capabilities, and providing such remarkable mentorship. I look forward to our continued collaborations. I must also thank my first EPA advisors, Dr. Kay Ho and Dr. Robert Burgess. Thank you for taking me on as your assistant nearly ten years ago. I am so grateful that you encouraged me to pursue research science and go back to school. I owe many thanks to Dr. Mark Cantwell. Thank you for being an excellent mentor and confidant. I can't believe how much research we've accomplished in two years, and how much fun we've had along the way. And thank you to Dr. Vinka Craver for serving on both committees and providing encouragement when I needed it.

I owe many thanks to each of my co-authors, collaborators, co-workers, and co-conspirators. Thank you for making me a better scientist and human. Thank you to the staff and students of the URI Geosciences Department. Like the Vishnu Schist, you have always been a great foundational support. A

special thanks goes to Julie Smallridge, who came to my rescue every time I locked myself out of my office.

Thank you to my friends and family, for your encouragement and patience as I navigated this process. And thank you to my dog Rocky, for bringing much needed brightness into the process.

Most importantly, thank you to my husband Andrew. I would have never made it through this process without your support. Thank you for always making sure that I took the time to care for myself first. And thank you for your unwavering care and understanding. Your trust in my dreams means the world to me.

DEDICATION

I dedicate this dissertation to my parents. My desire to become an environmental scientist started with our many hikes, paddles, and outdoor adventures. Thanks for always cheering me on, even when I'm grumpy.

PREFACE

This dissertation is written in manuscript format in accordance with the requirements of the Graduate School of the University of Rhode Island. This dissertation contains three chapters as three separate manuscripts formatted for the journals, *Marine Pollution Bulletin* and *Environmental Science & Technology*. Chapter one, *Comparison of microplastic isolation and extraction procedures from marine sediments* was published in *Marine Pollution Bulletin* in October 2020. Chapter two, *Quantification of microplastics in sediments from Narragansett Bay, Rhode Island USA using a novel isolation and extraction method* was published in *Marine Pollution Bulletin* in February 2022. Chapter three is entitled, *Temporal Distribution of PFAS in Sediments Cores from an Urban River: Relation to Water and Fish Tissue Data* and is formatted for the anticipated submission to *Environmental Science & Technology*.

TABLE OF CONTENTS

ABSTRACT	ii
ACKNOWLEDGMENTS	v
DEDICATION	vii
PREFACE	viii
TABLE OF CONTENTS	ix
LIST OF TABLES	xii
LIST OF FIGURES	xiv
Chapter 1	1
Introduction	2
Materials and Methods	6
<i>Experimental Set-Up</i>	6
<i>Quality Control</i>	8
<i>Methods Compared</i>	8
<i>Plastic Characterization</i>	11
<i>Nile Red Addition</i>	12
<i>Statistical Analysis</i>	13
Results and Discussion	14
<i>Overall Trends</i>	14
<i>Comparison of Recovery to a Standard</i>	17
<i>Variability Associated with the Methods</i>	18
<i>Effectiveness of Nile Red</i>	19
<i>Factors Affecting Method Efficacy</i>	20
<i>Recommendations</i>	21
Conclusion	24
References	26
Tables	30
Figures	32

Supplemental Information	35
<i>Quality Assurance</i>	35
SI Figures	37
SI Tables	38
Chapter 2	43
Introduction	44
<i>Narragansett Bay</i>	45
Methods	46
<i>Method Development & Validation</i>	46
<i>Narragansett Bay Sediments</i>	50
<i>Raman Analysis</i>	51
Results	53
<i>Assessing Extraction Efficiency using Internal Standards</i>	53
<i>MPs in Narragansett Bay Sediments</i>	54
Discussion	56
<i>Presence of Cellulose Acetate</i>	57
<i>Challenges with Microfibers</i>	59
Conclusion	61
References	62
Figures	69
Tables	75
Supplemental Information	77
<i>The Hybrid Extraction Method</i>	77
SI Figures	90
SI Tables	92
Chapter 3	99
Introduction	100
<i>The Pawtuxet River</i>	106
Methods	107
<i>Stable Isotope & Grain Size Analysis</i>	108
<i>Radiometric Dating</i>	108

<i>Chlorinated Pesticides</i>	109
<i>PFAS Targeted Analysis</i>	110
<i>TOP Assay</i>	112
<i>Extractable Organic Fluorine</i>	112
<i>Nontargeted Analysis</i>	113
<i>Water and Fish Matrices</i>	114
Results	114
Discussion	118
<i>Sediment PFAS</i>	118
<i>Water & Fish Matrices</i>	121
<i>TOP & EOF</i>	123
Conclusion	125
References	128
Figures	135
Tables.....	140
Supplemental Information.....	141
SI Figures	141
SI Tables.....	146
CONCLUSION	156

LIST OF TABLES

Table 1-1. Physical properties and sampling locations for representative sediments: Long Island Sound and Narragansett Beach. Sediment sizes classified using grainsize diameter 10, 50, and 90% cumulative percentile value.....	30
Table 1-2. Properties of microplastics used in this investigation.	31
Table 1-3. Table of basic statistical analysis performed on MP mean recovery including recovery mean (M), standard deviation (SD), and coefficient of variance (CV). Plastic polymers include polyvinyl chloride (PVC), polyethylene (PE), polystyrene (PS), polyethylene terephthalate (PET), and polypropylene (PP).....	38
Table 1-4. Raw data and percent recoveries of individual samples used to calculate values in SI Table 3.....	39
Table 1-5. Mean recoveries and standard deviations of MPs detected before and after staining with Nile Red as seen in Figure 3.	41
Table 1-6. Raw data of individual samples used to calculate values for NR used in Figure 3.	42
Table 2-1. Sampling Station Locations of Sediments collected from Narragansett Bay in July 2019. Sediment sizes classified using grainsize diameter (μm) 10% (D10), 50% (D50), and 90% (D90) cumulative percentile value.....	75
Table 2-2. Percent recovery of internal spiked MPs from environmental samples.....	76
Table 2-3. Physical properties and sampling locations for representative sediments: Long Island Sound and Narragansett Beach. <i>Sediment sizes classified using grainsize diameter 10, 50, and 90% cumulative percentile value</i>	92
Table 2-4. Properties of microplastics used in this investigation.	93
Table 2-5. Spiked and recovered MPs in method development to determine percent recovery.	94
Table 2-6. Mean (M) and relative standard deviation (RSD) recoveries of MPs by sediment and polymer type.	95
Table 2-7. Mean (M) recoveries of spiked MPs at each Station within Narragansett Bay.	96
Table 2-8. Number of synthetic particles found in air blanks and water blank for quality control.....	97
Table 2-9. Raw data from Raman Analysis.....	98
Table 3-1. Targeted analysis of PFAS in surface sediment, fish muscle, and water from sediment coring location.....	140
Table 3-2. List of PFAS analytes and isotopically labeled standards for targeted analysis on LC-MS/MS.....	146
Table 3-3. Minimum Detection Limits calculated for sediment and water samples on LC-MS/MS.	148

Table 3-4. PFAS concentrations in sediment targeted analysis. Concentrations reported in ng/ g dry sediment. Nondetect (ND) and concentrations below the minimum detection limit (MDL) are not reported.	149
Table 3-5. PFAS concentrations in fish tissue. Concentrations reported in ng/g dry sediment. Nondetect (ND) and concentrations below the minimum detection limit (MDL) are not reported.	151
Table 3-6. Grainsize of select sediment samples. All values are mean of 3 replicates.	152
Table 3-7. Analysis of 2,4-DDD, 4,4-DDT, and 2,4-DDT (ng/g) for sediment age depth.	153
Table 3-8. PFAS concentrations in sediment targeted analysis from the TOP assay. Concentrations reported in ng/ g dry sediment. Non-detect (ND) and concentrations below the minimum detection limit (MDL) are not reported..	154
Table 3-9. Total Fluorine (F) in ng from targeted analysis, TOP Assay, and EOF for surface water and sediment core.....	155

LIST OF FIGURES

Figure 1-1. Suggested pathways for microplastics in marine environments...	32
Figure 1-2. Mean percent recoveries of microplastics. Different letters represent statistical differences between polymer recovery ($p < 0.05$) per sediment type and method. Group “a” mean percent recovery is significantly greater than group “b”, which is significantly greater than group “c”. Bars with two letters are not significantly different from either group. Orange bar color signifies samples with significantly greater ($p < 0.05$) than 70% recovery. X-axis is organized first by plastic type (PVC= polyvinyl chloride, PE= polyethylene, PS= polystyrene, PET= polyethylene terephthalate, and PP= polypropylene), and further subdivided by extraction method (C=Coppock, F=Fries, N=Nuelle, G=Gilbreath, and Z=Zobkov).....	33
Figure 1-3. Mean recovery of microplastics using visual spectroscopy prior to staining (“No Stain”) vs. after staining (“Nile Red”). “*” = $p < 0.05$ T-test.	34
Figure 1-4. Schematic of SMI unit constructed at EPA Atlantic Coastal Environmental Sciences Division for MP extraction. The SMI unit was constructed using 63mm PVC piping and ball valve. The unit was designed so that all internal sides were smooth. Dimensions of the PVC pipe were 63 mm OD, 53 mm ID, and both PVC pipes were 140 mm h each. The total height of the SMI unit was 380 mm.....	37
Figure 2-1. A map of sampling locations in Narragansett Bay, RI, USA.	69
Figure 2-2. A wet sediment sample (2a) is poured over a set of stacked sieves and rinsed through with DI water. The sieves are stacked from top to bottom, 1,000, 250, and 45 μ m. Sediment that pass through all three sieves or is retained on 1000 μ m sieve are discarded. Materials retained on the 250 μ m sieve are retained as size class 250-1000 μ m (2b). Materials retained on the 45 μ m sieve are retained as size class 250-45 μ m (2c). Each size class undergoes two density separations. MPs are retained on 4 filters for each sample (2d, 2e, 2f, 2g).	70
Figure 2-3. Number of Microplastics (MPs) per 100g sediment sample at each station. Total number of MPs per sediment displayed in text above bars.....	71
Figure 2-4. Percent frequency of Microplastics (MPs) by polymer type at each station.....	72
Figure 2-5. Select Microplastics (MPs) displayed as number of MPs by the five most frequently occurring plastic types: cellulose acetate (CA) gold, polyurethane (PU) blue), Methyl cellulose (MC) orange, polypropylene (PP) green, and polyester (PO) purple. CA, PU, MC, PP, and PO non-detects are not shown on this figure.	73
Figure 2-6. Breakdown of Microplastics (MPs) by physical characteristics: percent frequency of MP by color (6A), shape (6B), and size (6C).	74
Figure 2-7. Mean percent recovery of MPs recovered from NAR and LIS sediments during method development. Error bars show relative standard deviation (RSD). N=5 for both sediment types.	90

Figure 2-8. Microscope picture of cellulose acetate fibers retained on filter from Station 4.....	91
Figure 3-1. A map of the Pawtuxet River in central Rhode Island, USA. The location of field sampling is denoted as the “Coring Location” on the map...	135
Figure 3-2. Stable isotope and elemental analysis of Carbon (C) and Nitrogen (N) in sediment cores as a function of depth.	136
Figure 3-3. Σ PFAS by compound class in sediment core in ng/g and % proportionality.....	137
Figure 3-4. Total F abundance in Targeted Analysis, TOP Analysis, and EOF. Results from target-ed analysis and the TOP Assay are shown in blue. The chart on the right includes F abundance in EOF.	138
Figure 3-5. Kendrick Mass Defect Plot (KMD) of suspected fluorinated features based on insource fragmentation patterns.	139
Figure 3-6. Radiometric Isotope data from 210-Pb and Cs-137 used to develop a Constant Rate of Supply (CRS) piecewise model.	141
Figure 3-7. Σ PFAS by compound in sediment core in ng/g and % proportionality.....	142
Figure 3-8. Percent change of PFAS deposition in sediment core. Percent change was calculated by comparing sediment sample concentration (x2) to underlying sediment ((x1) as $(x2-x1)/(x1)$).....	143
Figure 3-9. Percent frequency of PFAS found in surface sediment, fish muscle, and surface water.....	144
Figure 3-10. Upstream water concentrations of targeted PFAS. Samples were taken from (1) Pilgrim Avenue, (2) Washington Street, (3) Crompton Pier, and (4) Rhodes on the Pawtuxet in January 2021. Note - (3) Crompton Pier is the sediment coring location.....	145

Chapter 1

Quantification of microplastics in sediments from Narragansett Bay, Rhode Island USA using a novel isolation and extraction method

Michaela Cashman^{1,2}, Troy Langknecht³, Dounia El Khatib³, Robert M. Burgess¹, Thomas B. Boving^{2,4}, Sandra Robinson¹, Kay T. Ho¹

¹ U.S. Environmental Protection Agency
ORD/CEMM Atlantic Coastal Environmental Sciences Division
27 Tarzwell Drive
Narragansett, Rhode Island, USA 02882

² University of Rhode Island
Department of Geosciences
9 E Alumni Avenue
Kingston, Rhode Island, USA 02881

³ Oak Ridge Institute of Science Education
c/o U.S. Environmental Protection Agency
ORD/CEMM Atlantic Coastal Environmental Sciences Division
27 Tarzwell Drive
Narragansett, Rhode Island, USA 02882

⁴ University of Rhode Island
Department of Civil Engineering
9 E Alumni Avenue
Kingston, Rhode Island, USA 02881

This chapter was prepared for and published by *Marine Pollution Bulletin* in October of 2020

Introduction

Oceanic plastic pollution has garnered international attention as an example of waste mismanagement. Over 8.3 billion metric tons of plastic have been produced globally since the 1950s. Plastic consumption has surpassed the capacity of modern recycling infrastructure, leading to mismanaged disposal and environmental pollution. It is estimated that 8 million tons of plastic enter the oceans from land each year (Jambeck et al. 2015). However, floating plastics account for only 1% of the expected 8 million tons of plastic entering oceans annually (Van Sebille et al. 2015). Much of the 99% of the remaining plastics are expected to degrade into plastic fragments <5mm, known as microplastics (MPs) (Murphy 2017) through a series of physical, chemical, and biological processes (Van Cauwenberghe et al. 2013), and ultimately accumulate in sediments (Figure 1) (Andrady 2011, Browne et al. 2011, Hidalgo-Ruz et al. 2012, Kowalski et al. 2016). MPs are quickly rising to the forefront of emerging contaminant studies due to their unique quantification challenges and unknown toxic effects. Given this situation and their potential for environmental impacts, it is critical for researchers to have scientifically robust methods for extracting and isolating MPs from sediments.

There is an extensive list of published methods for isolating MPs from sediments (Mai et al. 2018, Prata et al. 2019). The variety of published procedures reflect the unique challenges associated with isolating MPs from marine sediments. Differences in extraction and isolation procedures

ultimately determine the ability of various MPs to be accurately recovered and quantified, resulting in a wide range of recovery efficiencies. Therefore, it is difficult to compare MP recovery rates (number of plastic particles per sample) between environmental samples using different procedures. Developing methods to address a range of sediment and plastic matrices has resulted in a wide variety of extraction techniques. Procedural differences include the mass of sediment samples, sample preparation, and sample handling. With no sediment standard reference material for MPs, methods are developed with an array of sediment and plastic matrices. Sediments may go through pretreatment steps including oven drying (Gilbreath et al. 2019, Nuelle et al. 2014, Su et al. 2018), pre-sieving of coarse or fine materials (Gilbreath et al. 2019, Zobkov and Esiukova 2017), or chemical oxidation (Hurley et al. 2018, Maes et al. 2017, Masura et al. 2015, Zobkov and Esiukova 2017). The method efficacy is often dependent on sediment composition. Sediment properties such as grainsize, organic matter content, and mineralogy largely affect results and method complexity. Differentiating between plastic and non-plastic particles in environmental samples is another major obstacle in isolating and visually identifying microplastics (Shaw and Day 1994, Tamminga et al. 2017). Recent studies indicate that using selective fluorescent stains, such as Nile Red, may improve the detection of MPs in environmental samples (Maes et al. 2017, Shim et al. 2016). Nile Red is a fluorescent stain that adheres to hydrophobic substances including lipids and

plastic. Hypothetically, staining environmental samples with Nile Red reduces the likelihood of false positive identification (Vianello et al. 2013).

This research assessed five current methods for the extraction and isolation of MPs from marine sediments. Two sediments (one sandy and one silty) were used as representative matrixes for amending known quantities of five common types of MPs. These matrices are considered representative of the types of sediments found along the coasts of the United States including sand occurring at beaches and typical subtidal temperate silty muds. Microplastics are known to accumulate in these types of sediments. Consequently, methods for isolating and extracting MPs from sediments would need to be functional with these types of matrices. The MPs were chosen to represent a range of MP polymer types, shapes, sizes, densities, and colors. Nile Red was also evaluated for improving MP visibility during extraction and isolation. We present a comparison of the efficiency of commonly used methods to characterize the number and types of MPs in marine sediments.

Most techniques used to isolate MPs from marine and estuarine sediments involve density separation (i.e., floatation) by agitating sediment samples with aqueous salt solutions (Thompson et al. 2004). Methods that rely on floatation separations are restricted by the density of their respective salt solutions. Common plastics range in density from 0.8-2.35 g/cm³ (Hidalgo-Ruz et al. 2012). Low density salt solutions such as sodium chloride may be insufficient to separate higher density plastics from sediment (Coppock et al.

2017, Hidalgo-Ruz et al. 2012). However, high density salts (e.g., NaBr, NaI, ZnCl₂) may not allow differentiation among plastics and other sediment components making separation from sediment particles difficult. In addition, the various salts used in density separation methods vary greatly in price, toxicity, reactivity, and waste disposal. These considerations can be restrictive or prohibitive to laboratories seeking to use higher density salts.

Many extraction methods favor low density plastic particles, but environmental microplastics include a myriad of high-density plastic polymers, including polyester, (Browne et al. 2011, Lusher et al. 2013, Lusher et al. 2014, Nor and Obbard 2014) polyethylene terephthalate (PET), (Nor and Obbard 2014, Peng et al. 2017) and polyethylene (PE) (Rios et al. 2007). Small variations in plastic chemical composition lead to large differences in polymer properties (Brydson 1999). It is important to consider that many methods may inadvertently select for specific polymer fragments (i.e., microplastic spheres versus fibers) based on their physical properties (Nel et al. 2018). Another complication is microplastics stimulate biofilm formation. MPs with biofilm will increase their particle mass and complicate density separation (Rummel et al. 2017, Zettler et al. 2013). Surficial biofilms often mask the polymer type from spectrometers and can effectively camouflage plastic particles embedded within sediments. While this study does not address the complications of polymer spectrometry, many isolation methods use chemical oxidation as a means of further separating organic material and removing biofilms from the microplastic-sediment matrix (Coppock et al. 2017,

Gilbreath et al. 2019, Masura et al. 2015, Zobkov and Esiukova 2017). In summary, several factors greatly affect the overall method performance for recovering MPs from marine sediments. Many isolation and extraction methods exist, but there is no information on their relative performance.

Materials and Methods

Experimental Set-Up

Methods were chosen to represent a wide range of commonly used, literature documented procedures, and for the ability to be performed easily and inexpensively. Other considerations included minimal waste generation, low start-up costs, simple equipment and instrumentation set-up, and overall quick processing time. Each method was assessed using two model sediments, silty sediment from Long Island Sound, New York (USA) and beach sand from Narragansett Beach, Rhode Island (USA). Long Island Sound sediment (LIS) is a well characterized, fine-grained sediment, collected using a Smith MacIntyre grab sampler (0.1 m²) in September 2010 (Ho et al. 2000). Narragansett Beach sand (NAR) was collected by hand from the intertidal zone using a metal shovel in January of 2018. Sediments were press sieved through a 2 mm sieve prior to analysis to remove any coarse fragments, and the NAR was heated in a muffle oven at 550°C for six hours to remove organic material. Representative samples were analyzed for particle size distributions using a Restech CamSizer P4 (Haan, Germany) (Table 1).

Five representative MPs were amended in known quantities into each sediment sample to evaluate the recovery efficiency of the selected microplastic extraction methods. The representative microplastics reflect a wide variety of polymer type, fragment shape, and particle size. For this study, we analyzed MPs ranging from 40-710 μm . The plastics used for spiking included polystyrene (PS), PE, polyvinyl chloride (PVC), PET, and polypropylene (PP) (Table 2). Fluorescent colored MPs were chosen for their ability to be easily enumerated as spiked reference materials. Both the PS and PE microbeads were purchased from Cospheric LLC (Santa Barbara, CA, USA). The other three microplastics purchased were PVC pipe (Home Depot, GA, USA), PET embroidery floss (J&P Coats, Middlesex, UK), and PP rope (SeaChoice, Pompano Beach, FL, USA). These three plastics were ground or cut into small pieces and sieved through a series of stacked mesh sieves to obtain desired size classes (Table 2). MPs were stored in a glass jar containing filtered seawater (20 μm) from Narragansett Bay (Narragansett, RI, USA) for a minimum of two weeks at 20°C to develop a biofilm. Prior to sediment addition, each MP particle was individually inspected microscopically (Nikon SMZ745-T, Nikon, Minato, Tokyo, Japan) for shape abnormalities or fragmentation by two analysts. After inspection, a minimum of twenty plastic pieces per polymer type were carefully transferred to a sediment sample (20 pieces * 5 plastic types = 100 pieces of plastic/sample). The plastic-amended sediments were mixed on a roller mill (4 RPM) at 4°C for a minimum of 48h.

Quality Control

Each method was evaluated with a total of 12 spiked sediment samples. An additional two sediment blanks (one sediment blank per sediment type) and a water blank were used per method to assess background and cross contamination during extraction. Airborne background contamination was assessed with one air blank per sample extraction. Air blanks were collected by wetting a 20 µm polycarbonate track etched (PCTE) filter (Poretics, GVS North America, Sanford, ME, USA) with deionized water and placing the filter into a glass petri dish covered in aluminum foil. The foil cover was removed whenever the working samples were exposed to air to assess possible air-born contamination. Each filter was inspected under the microscope with both normal light and UV excitation using a NightSea (Lexington, MA, USA) fluorescence filter (Excitation 360-380 nm, emission 415 nm long pass) to quantify the number of particles adhered to the filter. Further information on clean laboratory setup and quality control can be found in the Supplemental Information section.

Methods Compared

The following section outlines the general approach of each method. Each method was explicitly followed as described by the authors unless stated below. Detailed extraction steps can be found in published methods. Methods will be referred to by the last name of the first author for the remainder of this manuscript.

Fries et al. (2013): This method is a density separation approach using sodium chloride (NaCl) solution ($\rho=1.2 \text{ g/cm}^3$). Wet sediment samples (175g) underwent extraction in 2L glass separatory funnels with the NaCl solution. Samples were vigorously shaken to float microplastics to the NaCl solution surface. After a settling period, sediment was removed through the bottom port of the separatory funnel. Suspended MPs in NaCl solution were filtered onto a 20 μm PCTE membrane filter and visually inspected using a Nikon SMZ745-T microscope.

Gilbreath et al. (2019): This manuscript extracts MPs from bioretention ponds, but uses a methodology commonly used to extract MPs from sediments. This method is a modified version of Stolte et al. (2015) that extracts MPs $>45 \mu\text{m}$ using a calcium chloride (CaCl_2) solution ($\rho=1.4 \text{ g/cm}^3$). Sieved ($>45 \mu\text{m}$) sediment samples (150 g) were split into size fractions (45-500 μm , 501-1,000 μm) and placed in 600 mL glass beakers with CaCl_2 solution. Samples were stirred vigorously and left to settle. All floating materials were transferred using a metal spoon to 1-L glass separatory funnels filled with CaCl_2 . From there, separatory funnels were shaken, and the suspension allowed to settle. After settling, floating materials were filtered onto a 20 μm PCTE membrane filter and visually inspected using a Nikon SMZ745-T microscope.

Nuelle et al. (2014): This method is a density separation approach that uses both NaCl ($\rho=1.2 \text{ g/cm}^3$) and sodium iodide (NaI) ($\rho =1.8 \text{ g/cm}^3$) solutions. Sieved ($<1 \text{ mm}$) and dried (60° C) sediment samples (1 kg) were

initially separated with air induced overflow (AIO), which uses an aerated NaCl solution for density separation. Sediment samples were fluidized using the AIO method, which floats the MPs out of the fluidized sample causing them to overflow into secondary containment. All materials in secondary containment were transferred to 500 mL glass volumetric flasks filled with NaI solution. The volumetric flasks were shaken and decanted after a settling period. All decanted materials were filtered onto a 20 μm PCTE membrane filter and visually inspected using a Nikon SMZ745-T microscope.

Coppock et al. (2017): This method is a density separation approach that uses zinc chloride (ZnCl_2) solution ($\rho = 1.5 \text{ g/cm}^3$) and a sediment microplastics isolation (SMI) unit. The SMI unit was constructed in our laboratory. Sediment samples (70 g) were placed in the SMI unit with ZnCl_2 and a stir bar. Plastics were separated through density separation driven by mixing with the stir bar. After settling, all floating materials were filtered onto 20 μm PCTE filters and underwent oxidation (30% H_2O_2) for 1 week. Oxidized samples were filtered onto new 20 μm PCTE filters and visually inspected using a Nikon SMZ745-T microscope.

The referenced ball valve used by Coppock et al. (2017) to construct the SMI was not commercially available in the United States. Therefore, our laboratory opted for a PVC ball valve constructed from a 6.4 cm slo-close valve made by Colonial Engineering Inc. (Portage, MI, USA). The unit was constructed using 63 mm outer diameter PVC piping with the ISO ball valve

fixture adhered to a PVC plate (SI Figure 4). Details for construction and operation can be found in Coppock et al. (2017).

Zobkov & Esiukova (2017): This method is an adaptation of the laboratory method published by the National Oceanic and Atmospheric Administration (NOAA) (Masura et al. 2015) that uses ZnCl_2 ($\rho = 1.6 \text{ g/cm}^3$) for density separation followed by oxidation catalyzed with a heated water bath. Sediment samples (400 g) were added to glass beakers containing aqueous ZnCl_2 solution. After stirring with stainless steel spoons and settling, floating debris and supernatant were filtered through a 170 μm stainless steel sieve. Debris retained on the sieve were rinsed into clean glass beakers by tilting the sieve and rinsing into a clean beaker with the addition of a 30% H_2O_2 and Fe (II) catalyst solution. Beakers were covered with aluminum foil and placed in a hot water bath (75 °C) for 15 hours. A solution containing 4.5% hydrochloric acid (4.5%) was then added to each beaker. Samples underwent another round of density separation with ZnCl_2 and then were filtered onto 20 μm PCTE filters and visually inspected using a Nikon SMZ745-T microscope.

Plastic Characterization

Each sample was ultimately filtered onto a 20 μm PCTE membrane filter for visual inspection. Samples high in organic matter and sediment were often filtered onto several separate filters to more evenly distribute the debris. Filters were visually inspected under the microscope (Nikon SMZ745-T) using 2x magnification and identified as spiked MPs with white and fluorescent light.

Physical properties of spiked MPs (color, fluorescence, shape, and size) made them easily identifiable with microscopy. Two people verified each MP count using both normal light and cyan excitation with a NightSea (Lexington, MA, USA) fluorescence filter (excitation 490-515 nm, emission 550 nm long pass). Samples were recounted if there were discrepancies between the MP counts by both analysts. Spiked microplastics were counted on each filter and tallied by polymer type. Filters from sediment blank samples and water blank samples were visually inspected in the same manner. All filters were stored at 20° C in glass petri dishes with foil lids after identification.

Nile Red Addition

A secondary objective of this study was to determine the effects of Nile Red (NR) staining on the observational counting of microplastics from each sample. Lipophilic dyes such as Nile Red help differentiate microplastics from their environmental matrices during visual observation. Nile Red was purchased from Thomas Scientific (MP Biomedicals, Solon, OH, USA). A NR stock solution was prepared at 0.05 g/L in acetone according to methods developed by Maes et al. (2017). Prior to staining experimental samples, a laboratory trial was performed to determine an appropriate staining concentration and temporal duration to effectively stain the five model plastics. The best results were obtained with a concentration of 0.025 g/L NR for a staining duration of 10 minutes.

As described previously, post-processed filters from each method were analyzed to determine percent recovery of MPs. After analyzing percent recovery, a subset of these filters were stained with NR and recounted to determine if NR staining affects percent recovery based on visual observation. Two samples (one sandy and one silty) from each method were randomly selected for staining. Samples were mounted onto a vacuum filter apparatus and stained with 10 mL of 0.025 g/L NR solution for ten minutes, ensuring the entire filter was covered with stain. After ten minutes, the samples were filtered and thoroughly rinsed with DI water to remove all NR stain. The filters were then inspected under on a Nikon SMZ745-T microscope equipped with NightSea fluorescence filter (excitation 490-515 nm, emission 550 nm long pass) to recount microplastics. MP counts were compared for each filter pre- and post- NR staining to determine whether NR affected percent recovery.

Statistical Analysis

Mean percent recovery of microplastics achieved by each method was determined as a function of polymer and sediment type using Microsoft Excel (2016). All analyses of variance (ANOVA) were performed using the SAS statistical software (SAS Institute Inc., Cary, NC, USA; Version 9.4). Statistically significant differences ($p < 0.05$) among methods were determined for each polymer and sediment type using ANOVA. Significant differences identified by the ANOVA were further analyzed with a Bonferroni f-test to identify significant differences among recovery rates. A recovery threshold of

70% was determined before the start of experiments as a desirable recovery rate to evaluate the effectiveness of each method. A one-way t-test was used to compare each mean recovery to the 70% threshold between method, sediment type, and plastic. Samples with average percent recoveries of 0% were excluded from the t-test. Mean recoveries of MPs pre- and post-Nile Red staining were determined for each polymer type and then analyzed using a one-way t-test to determine significant ($p < 0.05$) differences.

Results and Discussion

Overall Trends

Recovered MPs were compared against known spiked MP quantities to determine percent recovery for each sample (SI Table 3; SI Table 4). Overall, mean recoveries were slightly better in the sandy sediment with non-zero values ranging from 5% to 87% in the NAR sand compared to 2% to 77% in the silty LIS sediment (Figure 2). In addition, 36% of the recoveries in the NAR exceeded 50% while only 20% of the recoveries from the silty sediment exceeded 50% (Figure 2). Mean recoveries for PVC ranged from 33-86% for sand and 11-68% for silt. PE recoveries ranged from 32-61% for sand and 0-52% for silt. For both types of sediments, recoveries of PS were very low ranging from 0% to less than 20%. Mean recovery of PET ranged from 5-68% for sand and 2-58% for silt. Finally, for PP, recoveries ranged from 23-87% for sand and 0-77% for silt.

Across all methods, the hierarchical ranking of mean recovery of MPs by polymer was the same for both sediment types. PVC had the highest recovery (i.e., $59 \pm 25\%$ sand; $43 \pm 35\%$ silt), followed by PP ($53 \pm 27\%$ sand; $40 \pm 29\%$ silt), PE ($48 \pm 29\%$ sand; $34 \pm 29\%$ silt), PET ($43 \pm 29\%$ sand; $23 \pm 25\%$ silt), and PS ($6 \pm 9\%$ sand; $8 \pm 10\%$ silt). Mean recoveries across methods were higher in sandier sediment than silty sediments for each polymer, except for PS as the small size of PS ($40 \mu\text{m}$) prevented high recoveries for all methods. In general, the quantitative ranking of polymer recovery followed the size-ranking of each MP. That is, PVC and PP were the largest MPs ($500\text{-}710 \mu\text{m}$), and the most highly recovered from both sediments. PE ($96\text{-}106 \mu\text{m}$) was the next highest recovered, followed by PET ($250\text{-}500 \mu\text{m}$). Although PET was classed as a larger particle than PE, the fiber diameter ($20 \mu\text{m}$) in contrast to their long length made their recovery more difficult. PS was generally the most difficult MP to recover and was also the smallest plastic studied ($40 \mu\text{m}$). There was no recovery of PS from either the Zobkov ($170 \mu\text{m}$) or Gilbreath ($45 \mu\text{m}$) methods, as the initial sieve step for both methods removed smaller-sized particles.

There was no statistically significant trend of quantitative ranking of polymer recovery based on MP density. The ranking of density from greatest to least (Table 2) was PET, PVC, PE, PS, and PP, whereas the ranking of mean recovery from greatest to least was PVC, PP, PE, PET, and PS. However, it is challenging to draw comparisons among MPs based on properties without noting that MP color and shape may also affect recovery

efficacy (i.e., colorful plastics are easier to see microscopically). There was no consistent pattern of quantitative ranking of polymer recovery based on method for either sediment type. More specifically, there was no recovery of PE from the Zobkov method, and no recovery of PS from the Zobkov or Gilbreath methods.

In a quantitative ranking of methods based on mean percent recovery, the Gilbreath method was the most successful at recovering dense plastics (PVC and PET) from silty sediments. The Coppock method was the most effective method for recovering light plastics (PP and PE) from silty sediments. The Nuelle method recovered the most PET, PS, and PE from sandy sediments, as well as PS from silty sediments. Overall, the Zobkov method was found to be the least effective for the isolation and extraction of our preselected microplastics. This is likely due to the higher size fraction cutoff of their samples (45 μm Gilbreath and 175 μm Zobkov). It should be stressed that these quantitative rankings are not method recommendations. The difference in ranking was often a vanishingly small margin, and this ranking does not consider the method's efficacy or recovery rate variability.

The Zobkov method consistently ranked the lowest in recovery per polymer and sediment type, but this is likely due to method constraints from size cutoffs. Many of the MPs tested for this study were smaller than the detection limit for this method (i.e. <175 μm). Overall, the Fries method and Nuelle method had higher recoveries for most plastic polymers in sand. The Fries method yielded the highest mean recoveries for PET ($59 \pm 25\%$), PP (87

$\pm 9\%$) and PE ($59 \pm 35\%$) while the Nuelle method ranked the highest for mean recoveries of PE ($62 \pm 27\%$), PET ($68 \pm 20\%$), and PS ($13 \pm 12\%$). However, the Coppock method achieved a mean 86% recovery of PVC in sand, the second highest recovery of any polymer by any method. The Coppock method and Gilbreath method generally have the highest mean recoveries of plastic polymers in silty sediments. In addition, the Coppock method had the highest mean recoveries for PE ($53 \pm 25\%$), PP ($77 \pm 16\%$), and PS ($17 \pm 12\%$). The Gilbreath method had highest mean recovery for PE (tied with Coppock, $53 \pm 25\%$), PET ($55 \pm 22\%$), and PVC ($76 \pm 25\%$).

Comparison of Recovery to a Standard

When performing relative comparisons, we established a target goal of $\geq 70\%$ recovery as achievable and desirable. No singular method effectively or consistently recovered $>70\%$ of each polymer in either sediment. The mean recovery was significantly greater than 70% in only two extractions from NAR sand. PP plastic was extracted with a mean efficiency of 87% ($\pm 9\%$) using the Fries method and PVC was extracted with a mean efficiency of 86% ($\pm 11\%$) using the Coppock method. This analysis indicates that less than 10% of the isolation and extraction procedures meet the sandy sediment 70% standard and none of the procedures met the silty sediment standard. Had the standard been set at the low value of $\geq 50\%$ recovery, 40% of the isolation and extraction procedures have met or exceeded the standard for sandy sediment.

For the silty sediment, the procedures meeting the standard was approximately 30%.

Variability Associated with the Methods

Coefficients of variance ($CV = (\text{standard deviation}/\text{mean}) * 100$) were calculated to measure the relative variability of the recoveries (Supplemental Information Table 1). CVs ranged from 6-141%, indicating large variation in recovery of MPs. Mean recovery values of 0 were excluded from this analysis. For PET extracted using the Zobkov method, the CVs of 141% for both sand and silt indicated higher variability of percent recoveries compared with other polymers and methods. CVs for PVC, PET and PP were consistently lower in sand. CVs for PS were consistently lower in silty sediment, and CVs for PE extractions were method dependent. In general, CV values for PP and PVC were lower than PE, PET, and PS. This suggests that the recoveries of PP and PVC were more consistent with variability. Consequently, PVC and PP were on average, the most highly recovered MPs independent of sediment and method.

Several of the individual recovery replicates were greater than 100%. This highlights the important issue of MP fragmentation during isolation and extraction. Both the ground PVC and manufactured PE beads were noted as highly friable. Methods that used abrasive measures such as dry sieving likely caused these plastics to break down further and resulted in artificially high recoveries (i.e., >100%). Several methods had consistent recoveries of 0%,

especially for smaller sized microplastics. As previously noted, Gilbreath and Zobkov methods had higher size cut-off ranges (45 μm and 175 μm , respectively) that caused the loss of small MPs from sediments. None of the plastics tested in this evaluation were greater than the 1 mm upper size threshold used by several methods.

The variability in mean recovery is much larger in this evaluation than the variability reported by each author's individual methodology validation in the scientific literature. For the four published methods, reported MP mean recoveries ranged from 70-100% (Nuelle (91-99%), Fries (80-100%), Zobkov (85-99%), and Coppock (70-100%)). The discrepancies between published recoveries and our laboratory trials clearly highlights the influence of sediment matrix, and MP properties of size, shape and density when reporting microplastic abundance in environmental samples. Standardization of isolation and extraction techniques need to be paired with explicit limitations of recovery. Based on this comparison, it is unreasonable to assume that one method will extract all MPs from all matrices with the same level of efficiency. As discussed above, statistical analyses indicated PP extracted from sandy sediment by the Fries method and PVC extracted from silt by the Coppock method were the only two mean recoveries significantly greater than 70%.

Effectiveness of Nile Red

There was no statistically significant benefit to using NR to identify MPs on filters (Figure 3). Initial investigations from Maes et al. used NR to recover

an average of 96.6% spiked MPs from various sediments.(Maes et al. 2017) In our study, mean recovery was higher before NR staining for PE (50.6 vs. 44.9%), PET (42.6 vs. 38.7%), and PP (52.9 vs 44.9%). Mean recovery of PVC (60.7 vs. 67.9%) and PS (14.8 vs 15.5%) was higher after staining with NR (SI Table 5; SI Table 6). NR did not uniformly stain the spiked plastics on each filter. This suggests the potential to miss certain MPs due to low stain uptake. Another major difficulty in using NR to stain MPs came from the incidental false-positive staining of organic debris such as benthic organisms and diatoms also present in the final filter samples. The silty sediment's high organic carbon content made identifying stained plastics particularly difficult, especially when differentiating smaller plastics such as PS and PE. These results suggest that the use of NR may confuse MP identification in high organic carbon sediments rather than providing improved identification.

Factors Affecting Method Efficacy

Based on this investigation, we suspect physical properties (i.e., grain size and distribution, mineralogy and % carbon) play a significant role in microplastic extraction efficacy. For example, the beach sand with its large grainsize and lack of organic matter consistently generated better mean recoveries than the silty sediment. Silty sediment samples consistently took longer to extract and had lower percent recoveries. High sediment cohesion complicated procedural steps involving bulk sediment transfer, sediment suspension, and/or oven drying. As noted regarding the NR stain, moderate

levels of organic matter add complexity to the plastic identification in the silty sediment. It is important to note the challenges of working with fine grained sediments because they represent a large fraction of global sediment inventories, (Thorp 1937) particularly in low energy depositional environments such as estuaries and protected bays where MPs and other anthropogenic contaminants will likely settle (Hume and Herdendorf 1992, Pettijohn and Ridge 1932, Reineck and Wunderlich 1968). In addition, sediment property variation can inadvertently influence microplastic visual identification. Plastics that mimic or are masked by sediment composition may be under-reported depending on the isolation and extraction method. Sandy beaches are distributed globally and represent an important aesthetic, recreational, economic and ecological resource. Some of the methods compared here demonstrated considerable promise with sandy sediments.

Recommendations

The diversity of MPs and range of sediment matrixes may be too broad to standardize recoveries for isolation and extraction (e.g., 70%) with a single extraction procedure. While we saw positive aspects of each extraction method, we cannot make a recommendation for a single method that functions best for all sediment and microplastic types. Therefore, it is imperative that researchers first define what types (particularly size) of plastics they would like to quantify and how their environmental samples may affect the extraction process. In terms of method efficacy, the Gilbreath method was the easiest to

use with sandier sediments, whereas the Coppock method and Fries method were the easiest to apply with silty sediments. However, efficacy does not reflect best percent recovery, nor does it describe the total number of nonpolymer particles (e.g., sediment, natural organic carbon) that remain on the final filters for polymer analysis. In these instances, laboratories conducting polymer spectral analysis (e.g., Raman, FT-IR) after MP extraction need to perform organic matter oxidation to reduce the number of particles on each filter. Oxidation steps do lengthen the processing time, but they were crucial for sediment high in organic matter. The biofilms were often removed in oxidation, and some MP particles with surficial dyes lost some of their coloration. These points may be notable if researchers are looking to identify MP surface characteristics. The Zobkov method is an adaptation of the NOAA sediment method and would work well on larger MPs (Masura et al. 2015). Given our laboratory setup, we found the Nuelle method most challenging to replicate; however, the Nuelle method is the only one that examined sediment sample masses in the 1 kg range. The other four methods were easier to perform partly due to their smaller sediment mass. This method is advantageous for larger sediment samples.

Even though these five methods are a small fraction of the existing methods in use, they represent distinct processes common to many methods. Readers may also find these results helpful in developing their own extraction methods, but we emphasize that these are only opinions of the laboratory researchers. MPs were frequently lost from the samples in extraction steps

that involved transferring the sample from one container to another. In addition, methods that limit the amount of sediment transfer are easier to perform. Many MPs were also observed as sticking to the walls of containers during density separation. Therefore, extraction methods need multiple rinsing steps to ensure complete transfer. The fine-grained sediment was consistently more difficult to work with. Methods that included sediment drying are not recommended for silty sediments, as this resulted in sediment “bricks” that were difficult to sieve and further process. Wet sediment matrixes with high amounts of fine silts and clay are often difficult to sieve and filter. We recommend removing the fine fraction of MPs, sediments, and organic matter from samples (<45 μm) prior to analysis to greatly improve method efficacy. MPs smaller than 45 μm in size cannot be easily seen under current stereomicroscopes. While this investigation did not look at polymer spectral analysis, many methods implore researchers to transfer suspected MPs with tweezers off of filters and onto clean surfaces prior to spectral analysis. Researchers interested in MPs <45 μm might consider further delineating size fractions to help with visual observations. A positive aspect of all five methods is that salt solutions for density separation can be reused. For these studies, used salt solutions were filtered, reconstituted up to appropriate density, and re-filtered to cutdown on the purchasing of salts and generation of waste.

Potential observation bias must be documented when reporting data on MP abundance in sediments. It may be ultimately necessary to move towards developing a MP internal standard for sediments to help identify bias in MP

isolation. Our recommendation is to develop a suite of MPs that are representative of, and span the types of MP particles (size, shape) of interest. This suite could be amended into environmental matrixes and extracted along with environmental MPs to estimate efficiency. This suite of MPs should be determined by the research project objectives. Recovery rates for the internal standard MPs should extrapolate the estimated recovery of environmental MPs isolated from environmental samples. An internal standard would allow for better standardization of data across environmental sampling and a better understanding of challenges posed by sediment matrices.

Conclusion

The comparison of five methods to extract varying MPs from two sediment types indicate that method, sediment matrix, and plastic properties play substantial roles in the isolation of MPs from environmental sediment matrixes. Sediments high in organic matter and with smaller grain sizes were generally more difficult to extract MPs from and had lower mean recoveries when compared to MP recoveries from sand. In addition, most methods reviewed had higher mean recoveries for larger and low-density plastics. These findings highlight potential biases in the current approximations of MP distribution in sediments worldwide. Further, the variability associated with each method was elevated with CVs ranging from 8% to 140% and 6% to 110% for the silt and sand, respectively. These CVs suggest that larger MPs (>500 μm) are easier and more consistently recovered than smaller MPs. The

isolation and extraction of MPs from sediments is a crucial first step in the identification of MPs by polymer. Differences in MP extraction procedures prevent meaningful comparisons across field analyses. Further, differences in sediment matrix and MP properties can substantially affect extraction efficacy of MPs from sediments. The development of an internal standard composed of multiple types of MPs is urgently needed to allow standardization of MP extractions in marine sediments.

References

1. Andrady, A.L. (2011) Microplastics in the marine environment. *Marine pollution bulletin* 62(8), 1596-1605.
2. Browne, M.A., Crump, P., Niven, S.J., Teuten, E., Tonkin, A., Galloway, T. and Thompson, R. (2011) Accumulation of microplastic on shorelines worldwide: sources and sinks. *Environmental science & technology* 45(21), 9175-9179.
3. Brydson, J.A. (1999) *Plastics materials*, Elsevier.
4. Coppock, R.L., Cole, M., Lindeque, P.K., Queirós, A.M. and Galloway, T.S. (2017) A small-scale, portable method for extracting microplastics from marine sediments. *Environmental Pollution* 230, 829-837.
5. Fries, E., Dekiff, J.H., Willmeyer, J., Nuelle, M.-T., Ebert, M. and Remy, D. (2013) Identification of polymer types and additives in marine microplastic particles using pyrolysis-GC/MS and scanning electron microscopy. *Environmental Science-Processes & Impacts* 15(10), 1949-1956.
6. Gilbreath, A., McKee, L., Shimabuku, I., Lin, D., Werbowski, L.M., Zhu, X., Grbic, J. and Rochman, C. (2019) Multiyear Water Quality Performance and Mass Accumulation of PCBs, Mercury, Methylmercury, Copper, and Microplastics in a Bioretention Rain Garden. *Journal of Sustainable Water in the Built Environment* 5(4), 04019004.
7. Hidalgo-Ruz, V., Gutow, L., Thompson, R.C. and Thiel, M. (2012) Microplastics in the Marine Environment: A Review of the Methods Used for Identification and Quantification. *Environmental Science & Technology* 46(6), 3060-3075.
8. Ho, K.T., Kuhn, A., Pelletier, M., McGee, F., Burgess, R.M. and Serbst, J. (2000) Sediment toxicity assessment: Comparison of standard and new testing designs. *Archives of Environmental Contamination and Toxicology* 39(4), 462-468.
9. Hume, T.M. and Herdendorf, C.E. (1992) Factors controlling tidal inlet characteristics on low drift coasts. *Journal of Coastal Research*, 355-375.
10. Hurley, R.R., Lusher, A.L., Olsen, M. and Nizzetto, L. (2018) Validation of a method for extracting microplastics from complex, Organic-Rich, Environmental Matrices. *Environmental science & technology* 52(13), 7409-7417.

11. Jambeck, J.R., Geyer, R., Wilcox, C., Siegler, T.R., Perryman, M., Andrady, A., Narayan, R. and Law, K.L. (2015) Plastic waste inputs from land into the ocean. *Science* 347(6223), 768-771.
12. Kowalski, N., Reichardt, A.M. and Waniek, J.J. (2016) Sinking rates of microplastics and potential implications of their alteration by physical, biological, and chemical factors. *Marine pollution bulletin* 109(1), 310-319.
13. Lusher, A., Mchugh, M. and Thompson, R. (2013) Occurrence of microplastics in the gastrointestinal tract of pelagic and demersal fish from the English Channel. *Marine pollution bulletin* 67(1-2), 94-99.
14. Lusher, A.L., Burke, A., O'Connor, I. and Officer, R. (2014) Microplastic pollution in the Northeast Atlantic Ocean: Validated and opportunistic sampling. *Marine pollution bulletin* 88(1-2), 325-333.
15. Maes, T., Jessop, R., Wellner, N., Haupt, K. and Mayes, A.G. (2017) A rapid-screening approach to detect and quantify microplastics based on fluorescent tagging with Nile Red. *Scientific Reports* 7.
16. Mai, L., Bao, L.-J., Shi, L., Wong, C.S. and Zeng, E.Y. (2018) A review of methods for measuring microplastics in aquatic environments. *Environmental Science and Pollution Research* 25(12), 11319-11332.
17. Masura, J., Baker, J.E., Foster, G., Arthur, C. and Herring, C. (2015) Laboratory methods for the analysis of microplastics in the marine environment: recommendations for quantifying synthetic particles in waters and sediments, US Department of Commerce, National Oceanic and Atmospheric Administration, [National Ocean Service], NOAA Marine Debris Program.
18. Murphy, M. (2017) Microplastics Expert Workshop Report, US Environmental Protection Agency.
19. Nel, H.A., Dalu, T. and Wasserman, R.J. (2018) Sinks and sources: Assessing microplastic abundance in river sediment and deposit feeders in an Austral temperate urban river system. *Science of The Total Environment* 612, 950-956.
20. Nor, N.H.M. and Obbard, J.P. (2014) Microplastics in Singapore's coastal mangrove ecosystems. *Marine pollution bulletin* 79(1-2), 278-283.
- Nuelle, M.-T., Dekiff, J.H., Remy, D. and Fries, E. (2014) A new analytical approach for monitoring microplastics in marine sediments. *Environmental pollution* 184, 161-169.

21. Peng, G., Zhu, B., Yang, D., Su, L., Shi, H. and Li, D. (2017) Microplastics in sediments of the Changjiang Estuary, China. *Environmental Pollution* 225, 283-290.
22. Pettijohn, F.J. and Ridge, J.D. (1932) A textural variation series of beach sands from Cedar Point, Ohio. *Journal of Sedimentary Research* 2(2), 76-88.
- Prata, J.C., da Costa, J.P., Duarte, A.C. and Rocha-Santos, T. (2019) Methods for sampling and detection of microplastics in water and sediment: A critical review. *TrAC Trends in Analytical Chemistry* 110, 150-159.
23. Reineck, H.E. and Wunderlich, F. (1968) Classification and origin of flaser and lenticular bedding. *Sedimentology* 11(1-2), 99-104.
24. Rios, L.M., Moore, C. and Jones, P.R. (2007) Persistent organic pollutants carried by synthetic polymers in the ocean environment. *Marine pollution bulletin* 54(8), 1230-1237.
25. Rummel, C.D., Jahnke, A., Gorokhova, E., Kühnel, D. and Schmitt-Jansen, M. (2017) Impacts of biofilm formation on the fate and potential effects of microplastic in the aquatic environment. *Environmental Science & Technology Letters* 4(7), 258-267.
26. Shaw, D.G. and Day, R.H. (1994) Colour-and form-dependent loss of plastic micro-debris from the North Pacific Ocean. *Marine pollution bulletin* 28(1), 39-43.
27. Shim, W.J., Song, Y.K., Hong, S.H. and Jang, M. (2016) Identification and quantification of microplastics using Nile Red staining. *Marine pollution bulletin* 113(1-2), 469-476.
28. Stolte, A., Forster, S., Gerdts, G. and Schubert, H. (2015) Microplastic concentrations in beach sediments along the German Baltic coast. *Marine pollution bulletin* 99(1-2), 216-229.
29. Su, L., Cai, H., Kolandhasamy, P., Wu, C., Rochman, C.M. and Shi, H. (2018) Using the Asian clam as an indicator of microplastic pollution in freshwater ecosystems. *Environmental Pollution* 234, 347-355.
30. Tamminga, M., Hengstmann, E. and Fischer, E. (2017) Nile Red staining as a subsidiary method for microplastic quantification: a comparison of three solvents and factors influencing application reliability. *SDRP J Earth Sci Environ Stud* 2(2), 165-172.
31. Thompson, R.C., Olsen, Y., Mitchell, R.P., Davis, A., Rowland, S.J., John, A.W., McGonigle, D. and Russell, A.E. (2004) Lost at sea: where is all the plastic? *Science* 304(5672), 838-838.

32. Thorp, E.M. (1937) Description of deep-sea bottom samples from the western north Atlantic and the Caribbean sea, University of California press.
33. Van Cauwenberghe, L., Claessens, M., Vandegehuchte, M.B., Mees, J. and Janssen, C.R. (2013) Assessment of marine debris on the Belgian Continental Shelf. *Marine pollution bulletin* 73(1), 161-169.
34. Van Sebille, E., Wilcox, C., Lebreton, L., Maximenko, N., Hardesty, B.D., Van Franeker, J.A., Eriksen, M., Siegel, D., Galgani, F. and Law, K.L. (2015) A global inventory of small floating plastic debris. *Environmental Research Letters* 10(12), 124006.
35. Vianello, A., Boldrin, A., Guerriero, P., Moschino, V., Rella, R., Sturaro, A. and Da Ros, L. (2013) Microplastic particles in sediments of Lagoon of Venice, Italy: First observations on occurrence, spatial patterns and identification. *Estuarine Coastal and Shelf Science* 130, 54-61.
36. Zettler, E.R., Mincer, T.J. and Amaral-Zettler, L.A. (2013) Life in the "plastisphere": microbial communities on plastic marine debris. *Environmental science & technology* 47(13), 7137-7146.
37. Zobkov, M. and Esiukova, E. (2017) Microplastics in Baltic bottom sediments: Quantification procedures and first results. *Marine Pollution Bulletin* 114(2), 724-732.

Tables

Table 1-1. Physical properties and sampling locations for representative sediments: Long Island Sound and Narragansett Beach. Sediment sizes classified using grainsize diameter 10, 50, and 90% cumulative percentile value.

	D ₁₀ (μ m)	D ₅₀ (μ m)	D ₉₀ (μ m)	Water wt/wt %	Organic Carbon %	GPS Coordinates of Collection Location
Long Island Sound (LIS)	4.1	13.7	62.6	43	2	41° 7'N 72° 52'W
Narragansett Beach (NAR)	179.1	251.6	345.2	<1	0	41° 26'N 72° 27'W

Table 1-2. Properties of microplastics used in this investigation.

	Size (μm)	Density (g/cm^3)	Shape	Color	Source
Polystyrene (PS)	40	0.96	Sphere	Transparent	Cospheric
Polyethylene (PE)	96-106	1.13	Sphere	Blue	Cospheric
Polyvinyl Chloride (PVC)	500-710	1.35	Fragment	Orange	PVC Pipe
Polyethylene Terephthalate (PET)	250-500	1.38	Fiber	Pink	Embroidery Floss
Polypropylene (PP)	500-710	0.91	Fiber	Yellow	Rope

Figures

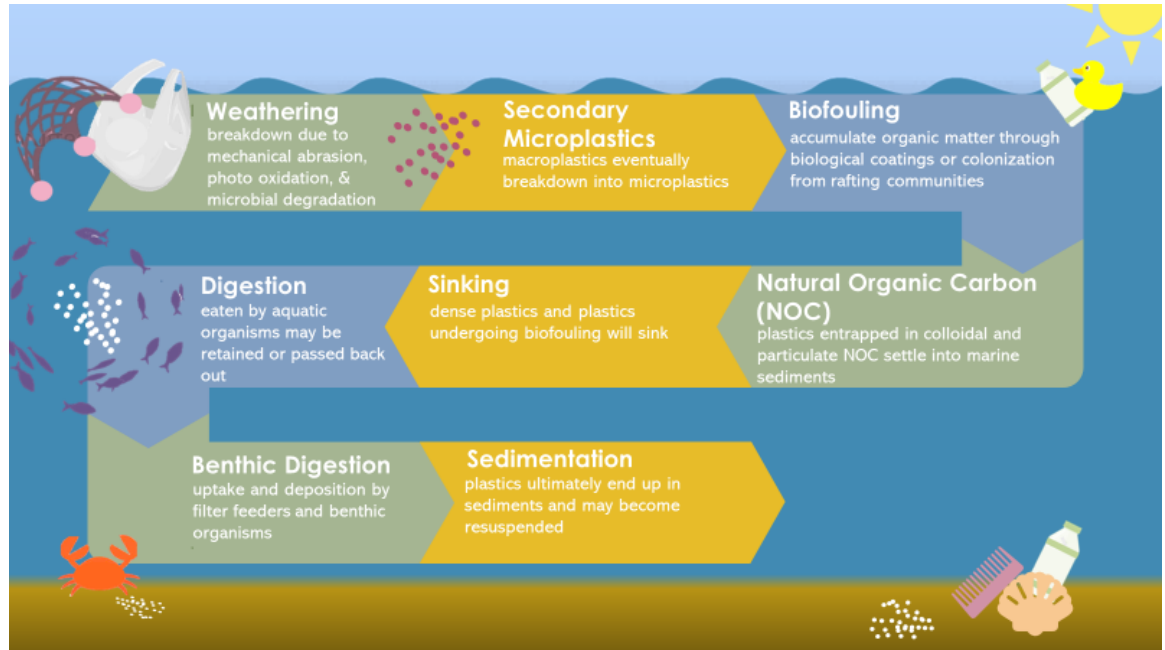


Figure 1-1. Suggested pathways for microplastics in marine environments.

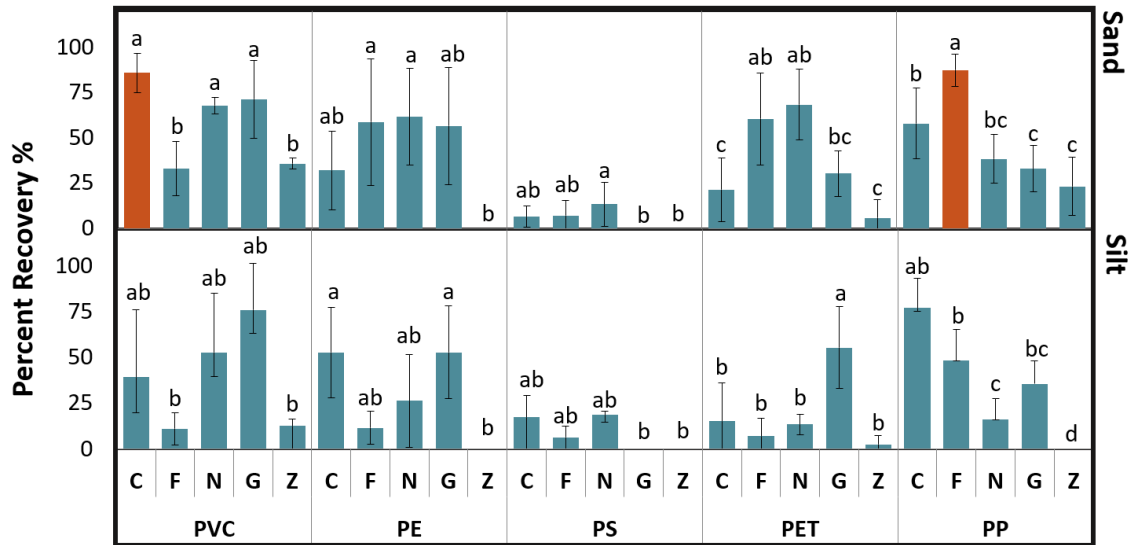


Figure 1-2. Mean percent recoveries of microplastics. Different letters represent statistical differences between polymer recovery ($p < 0.05$) per sediment type and method. Group “a” mean percent recovery is significantly greater than group “b”, which is significantly greater than group “c”. Bars with two letters are not significantly different from either group. Orange bar color signifies samples with significantly greater ($p < 0.05$) than 70% recovery. X-axis is organized first by plastic type (PVC= polyvinyl chloride, PE= polyethylene, PS= polystyrene, PET= polyethylene terephthalate, and PP= polypropylene), and further subdivided by extraction method (C=Coppock, F=Fries, N=Nuelle, G=Gilbreath, and Z=Zobkov).

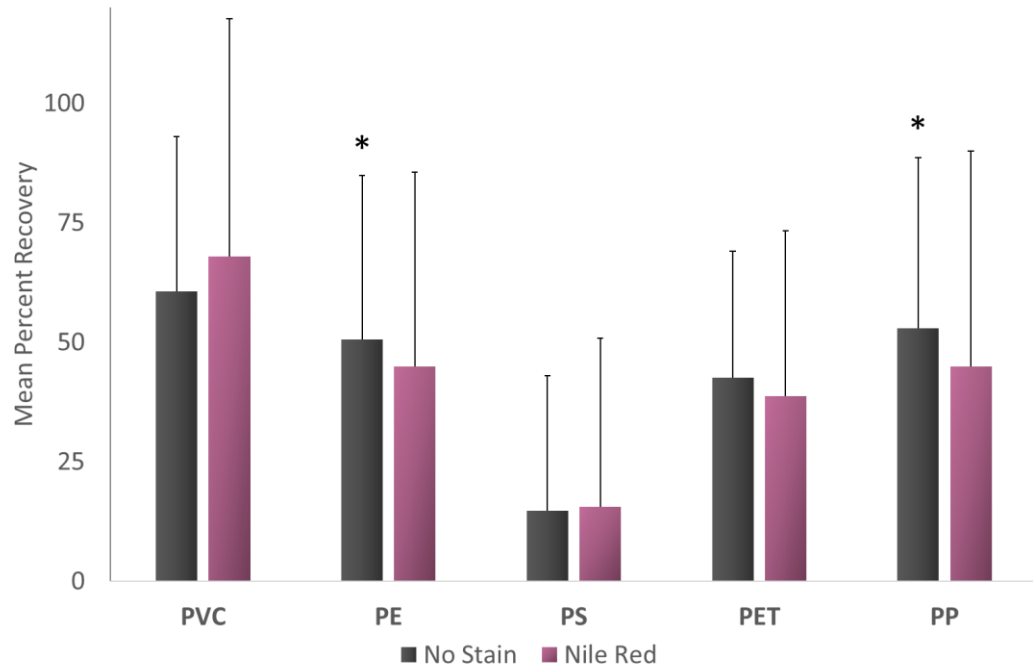


Figure 1-3. Mean recovery of microplastics using visual spectroscopy prior to staining (“No Stain”) vs. after staining (“Nile Red”). “*” = $p < 0.05$ T-test.

Supplemental Information

Quality Assurance

Proper quality assurance is integral to accurate measurements of MPs in environmental matrices. For this study, clean laboratory and forensic approaches were followed to minimize sample contamination. Our lab space is exclusively used for MP analysis which minimizes potential cross contamination. Prior to sample analysis, the lab was retrofitted to remove potential sources of MP contamination. This included the installation of a Minimum Efficiency Reporting Value (MERV)-13 filter which removes 90% of particles in the 3-10 μm range, 90% of particles in the 1-3 μm range and 50% of particles in the range 0.3-1 μm range and deep cleaning of all horizontal surfaces. Lab benches were replaced with marble countertops and all plastic sinks/ basins were exchanged for stainless steel models. A laminar flow hood was put into the laboratory to conduct vacuum filtration. Lab disposables such as paper towels were replaced with 100% cotton cleaning cloths, and other plastic items were removed from the laboratory. All persons entering the lab were required to wear brightly colored 100% cotton lab coats over their clothing to prevent shedding of synthetic microfibers. Lab spaces were wiped down with DI water and cotton cleaning cloths at the beginning and end of each research day. All lab materials were thoroughly cleaned after use and covered with aluminum foil to prevent airborne MP contamination. Salt solutions were pre-filtered (0.45 μm) before use to remove MPs from solution. All samples and solutions were stored in containers with lids to prevent airborne contamination.

Each extraction method was tried out several times prior to this study to minimize user error. For these trials, sediment samples were spiked with ten pieces of 1 mm PET glitter. These MPs were easy to see during each extraction step and helped visualize potential sources of error. Each method extraction was repeated until 100% recovery of 1 mm PET MPs was achieved.

Air blanks were used with each method to determine possible contamination of spiked samples. Each air blank was analyzed under a microscope by two separate analysts to detect MPs. None of the air blanks contained any of our spiked MP particles. Therefore, none of the percent recoveries were adjusted to account for the air blanks. We note that many of the filters contained cotton fibers from our lab coats. Fiber shedding from lab coats is a particular concern for researchers analyzing environmental samples. As a laboratory protocol, air blanks are monitored weekly for the accumulation of particles. If more than five particles are found on an air blank, lab work is paused so that laboratory spaces are wiped down and re-cleaned. Lab work is resumed after thorough cleaning.

SI Figures

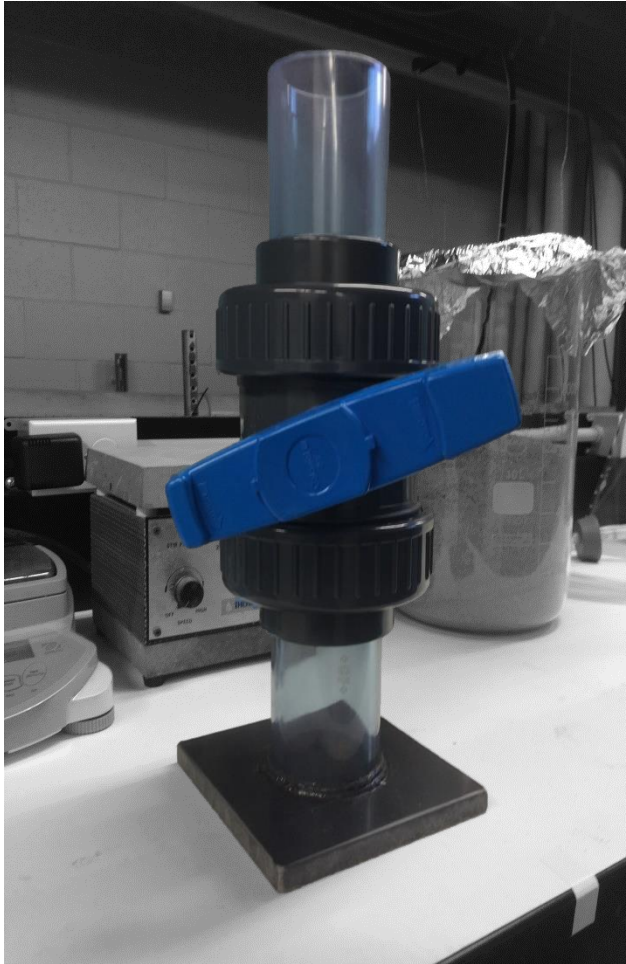


Figure 1-4. Schematic of SMI unit constructed at EPA Atlantic Coastal Environmental Sciences Division for MP extraction. The SMI unit was constructed using 63mm PVC piping and ball valve. The unit was designed so that all internal sides were smooth. Dimensions of the PVC pipe were 63 mm OD, 53 mm ID, and both PVC pipes were 140 mm h each. The total height of the SMI unit was 380 mm.

SI Tables

Table 1-3. Table of basic statistical analysis performed on MP mean recovery including recovery mean (M), standard deviation (SD), and coefficient of variance (CV). Plastic polymers include polyvinyl chloride (PVC), polyethylene (PE), polystyrene (PS), polyethylene terephthalate (PET), and polypropylene (PP).

	Methods	n =	PVC			PE			PS			PET			PP		
			M	SD	CV	M	SD	CV	M	SD	CV	M	SD	CV	M	SD	CV
Silt	Fries	4	11.2	7.6	67.9	11.8	7.8	66.1	6.5	5.5	84.6	7.3	8.2	112.3	48.4	14.7	30.4
	Gilbreath	6	76.1	25.3	33.2	53.0	25.5	48.1	0.0	0.0	n/a	55.5	22.3	40.2	35.7	25.3	70.9
	Nuelle	3	53.0	26.4	49.8	26.5	20.7	78.1	18.8	1.5	8.0	13.7	4.6	33.6	16.2	9.5	58.6
	Coppock	5	39.4	32.8	83.2	52.9	22.1	41.8	17.5	10.8	61.7	15.3	18.8	122.9	77.1	14.5	18.8
	Zobkov	3	12.7	3.3	26.0	0.0	0.0	n/a	0.0	0.0	n/a	2.7	3.8	140.7	0.0	0.0	n/a
Sand	Fries	8	33.1	13.9	42.0	58.8	32.8	55.8	7.2	7.8	108.3	60.5	23.8	39.3	87.4	8.4	9.6
	Gilbreath	6	71.4	21.4	30.0	56.6	32.4	57.2	0.0	0.0	n/a	30.4	12.6	41.4	33.0	12.8	38.8
	Nuelle	6	68.0	4.1	6.0	61.7	24.3	39.4	13.4	11.0	82.1	68.5	18.0	26.3	38.4	12.3	32.0
	Coppock	5	86.0	9.7	11.3	32.1	19.5	60.7	6.6	5.2	78.8	21.6	15.7	72.7	57.9	17.5	30.2
	Zobkov	3	35.8	2.4	6.7	0.0	0.0	n/a	0.0	0.0	n/a	5.8	8.2	141.4	23.3	13.1	56.2

Table 1-4. Raw data and percent recoveries of individual samples used to calculate values in SI Table 3.

Method	Sediment Type	Spiked Plastics by Polymer					Recovered Plastics by Polymer					Percent Recoveries (=recovery/spike)*100				
		PVC	PE	PS	PET	PP	PVC	PE	PS	PET	PP	PVC	PE	PS	PET	PP
Fries	LIS	24	20	32	20	23	2	5	1	4	7	8.3	25.0	3.1	20.0	30.4
		21	25	23	24	20	4	2	2	0	14	19.0	8.0	8.7	0.0	70.0
		21	22	21	20	22	0	2	3	0	9	0.0	9.1	14.3	0.0	40.9
		23	20	20	22	23	4	1	0	2	12	17.4	5.0	0.0	9.1	52.2
		22	23	21	29	20	5	14	5	25	19	22.7	60.9	23.8	86.2	95.0
	NAR	20	23	27	20	23	6	9	0	15	18	30.0	39.1	0.0	75.0	78.3
		22	25	21	20	24	7	10	0	13	23	31.8	40.0	0.0	65.0	95.8
		27	25	22	29	21	12	12	2	17	20	44.4	48.0	9.1	58.6	95.2
		20	20	22	23	23	13	4	1	17	17	65.0	20.0	4.5	73.9	73.9
		20	23	34	21	23	5	9	2	2	18	25.0	39.1	5.9	9.5	78.3
		23	34	36	23	34	6	34	5	18	31	26.1	100.0	13.9	78.3	91.2
		30	26	28	24	23	6	32	0	9	21	20.0	123.1	0.0	37.5	91.3
Rochman	LIS	23	21	22	20	20	20	13	0	15	9	87.0	61.9	0.0	75.0	45.0
		20	23	31	34	22	18	21	0	18	10	90.0	91.3	0.0	52.9	45.5
		20	31	26	20	24	10	11	0	18	6	50.0	35.5	0.0	90.0	25.0
		20	25	29	21	26	11	8	0	8	4	55.0	32.0	0.0	38.1	15.4
		20	22	22	20	23	12	6	0	7	10	60.0	27.3	0.0	35.0	43.5
		20	20	23	24	25	23	14	0	10	10	115.0	70.0	0.0	41.7	40.0
	NAR	20	20	28	28	21	20	12	0	3	2	100.0	60.0	0.0	10.7	9.5
		20	23	27	30	22	8	12	0	13	10	40.0	52.2	0.0	43.3	45.5
		20	30	20	22	25	14	9	0	7	8	70.0	30.0	0.0	31.8	32.0
		20	34	20	28	22	12	9	0	11	8	60.0	26.5	0.0	39.3	36.4
		22	22	20	24	21	15	12	0	9	9	68.2	54.5	0.0	37.5	42.9
		20	24	29	20	22	18	28	0	4	7	90.0	116.7	0.0	20.0	31.8
Coppock	LIS	21	22	26	24	21	12	20	7	1	17	57.1	90.9	26.9	4.2	81.0
		20	27	22	21	26	19	11	6	11	26	95.0	40.7	27.3	52.4	100.0
		20	20	26	27	20	5	5	6	1	15	25.0	25.0	23.1	3.7	75.0
		20	25	30	25	22	1	12	0	3	12	5.0	48.0	0.0	12.0	54.5
		20	20	20	23	20	3	12	2	1	15	15.0	60.0	10.0	4.3	75.0
	NAR	20	21	28	21	23	19	9	0	5	9	95.0	42.9	0.0	23.8	39.1
		20	22	28	27	25	15	2	1	3	10	75.0	9.1	3.6	11.1	40.0
		20	20	23	22	25	16	9	1	11	18	80.0	45.0	4.3	50.0	72.0
		20	20	21	21	24	20	11	3	4	20	100.0	55.0	14.3	19.0	83.3
		20	24	28	25	20	16	2	3	1	11	80.0	8.3	10.7	4.0	55.0
Nuelle	LIS	23	20	29	27	27	7	3	5	2	8	30.4	15.0	17.2	7.4	29.6
		26	22	24	22	28	10	2	5	4	3	38.5	9.1	20.8	18.2	10.7
		20	27	22	26	24	18	15	4	4	2	90.0	55.6	18.2	15.4	8.3
	NAR	21	22	22	24	28	14	10	6	18	7	66.7	45.5	27.3	75.0	25.0
		22	29	32	22	23	16	17	9	18	14	72.7	58.6	28.1	81.8	60.9
		25	21	37	28	25	16	15	3	12	12	64.0	71.4	8.1	42.9	48.0

		27	22	26	23	30	19	16	0	21	10	70.4	72.7	0.0	91.3	33.3
		21	24	22	24	24	13	24	3	11	8	61.9	100.0	13.6	45.8	33.3
		29	23	31	27	27	21	5	1	20	8	72.4	21.7	3.2	74.1	29.6
Zobkov	LIS	20	20	30	22	20	3	0	0	0	0	15.0	0.0	0.0	0.0	0.0
		20	23	23	22	20	3	0	0	0	0	15.0	0.0	0.0	0.0	0.0
		25	32	23	25	20	2	0	0	2	0	8.0	0.0	0.0	8.0	0.0
	NAR	20	20	32	23	20	7	0	0	4	1	35.0	0.0	0.0	17.4	5.0
		21	22	23	29	20	7	0	0	0	6	33.3	0.0	0.0	0.0	30.0
		23	26	28	21	20	9	0	0	0	7	39.1	0.0	0.0	0.0	35.0

Table 1-5. Mean recoveries and standard deviations of MPs detected before and after staining with Nile Red as seen in Figure 3.

	PVC		PE		PS		PET		PP	
	M	SD								
Before Stain	60.7	32.3	50.6	34.3	14.8	28.3	42.6	26.4	52.9	35.8
Nile Red	67.9	49.7	44.9	40.6	15.5	35.3	38.7	34.6	44.9	45.0

Table 1-6. Raw data of individual samples used to calculate values for NR used in Figure 3.

	Number Spiked Plastics by Polymer					Recovered Plastics by Polymer normal light					Nile Red Recovered Plastics by Polymer				
	PVC	PE	PS	PET	PP	PVC	PE	PS	PET	PP	PVC	PE	PS	PET	PP
Fries- LIS	20	29	21	20	27	4	22	21	20	27	6	0	18	4	8
Fries- NAR	20	20	22	23	23	13	4	1	17	17	14	1	0	16	16
Fries- NAR	30	26	28	24	23	6	32	0	9	21	20	28	21	24	24
Rochman- LIS	20	20	23	24	25	23	14	0	10	10	16	8	0	4	0
Rochman- NAR	22	22	20	24	21	15	12	0	9	9	2	4	0	2	6
Coppock- LIS	20	27	22	21	26	19	11	6	11	26	14	4	0	0	2
Coppock- NAR	20	20	23	22	25	16	9	1	11	18	67	0	0	0	0
Nuelle- LIS	20	27	22	26	24	18	15	4	4	2	40	14	5	4	0
Nuelle- NAR	25	21	37	28	25	16	15	3	12	12	23	12	0	8	0
Zobkov- LIS	20	23	23	22	20	3	0	0	0	0	7	1	0	2	0
Zobkov- NAR	20	20	32	23	20	7	0	0	4	1	11	0	0	0	0

Chapter 2

Quantification of microplastics in sediments from Narragansett Bay, Rhode Island USA using a novel isolation and extraction method

Michaela Cashman^{1,2}, Troy Langknecht³, Dounia El Khatib³, Robert M. Burgess¹, Thomas B. Boving^{2,4}, Sandra Robinson¹, Kay T. Ho¹

¹ U.S. Environmental Protection Agency
ORD/CEMM Atlantic Coastal Environmental Sciences Division
27 Tarzwell Drive
Narragansett, Rhode Island, USA 02882

² University of Rhode Island
Department of Geosciences
9 E Alumni Avenue
Kingston, Rhode Island, USA 02881

³ Oak Ridge Institute of Science Education
c/o U.S. Environmental Protection Agency
ORD/CEMM Atlantic Coastal Environmental Sciences Division
27 Tarzwell Drive
Narragansett, Rhode Island, USA 02882

⁴ University of Rhode Island
Department of Civil Engineering
9 E Alumni Avenue
Kingston, Rhode Island, USA 02881

This was prepared for and published by Marine Pollution Bulletin in February 2022.

Introduction

Microplastics (MPs) are small plastic particles (1nm-5mm) commonly identified as a marine pollutant (Thompson et al. 2004). Many MPs entering the oceans will ultimately end up in sediments (Andrady 2011, Browne et al. 2011, Cózar et al. 2014, Hidalgo-Ruz et al. 2012, Kowalski et al. 2016).

Understanding the distribution and abundance of MPs in sediments is the first step to determine their potential risks to marine environments. However, there are many technical challenges associated with extracting and identifying MPs from marine sediments.

The wide diversity of their physical properties makes MPs a particularly challenging class of contaminants to extract, quantify, and identify in environmental media. While there are dozens of published methods for the extraction of MPs from sediments, procedural differences, sediment characteristics, and MP physical properties can all affect the efficacy of MP extraction and types of MPs reported in environmental samples (Burgess et al. 2017, Rochman et al. 2019). Our prior research compared the extraction efficacy of 5 types of MPs from two sediment types using a range of different extraction procedures from the scientific literature (Cashman et al. 2020). The findings and recommendations from these data were used to develop a new isolation and extraction method to more efficiently capture a wider range of MPs from environmental sediments. Referred to as the “hybrid method”, this new method combines recommendations from Cashman et al. (2020) with characteristics from the methods evaluated in the comparison study (Coppock

et al. 2017, Fries et al. 2013, Gilbreath et al. 2019, Nuelle et al. 2014, Zobkov and Esiukova 2017) to develop a method that is cost efficient, generates minimal hazardous waste, doesn't require equipment fabrication, and successfully extracts MPs from a range of sediments. The research herein uses the hybrid method for the extraction of MPs from marine sediments from Narragansett Bay (NB), Rhode Island.

Narragansett Bay

NB is located on the northeast Atlantic coast of the United States (Figure 1). The greater NB watershed area (4081 km²) is densely populated with an estimated 1.9 million people from both Rhode Island and Massachusetts (NBEP 2017, Vadeboncoeur et al. 2010). Twenty percent of the watershed's population resides in urbanized coastal land. Classified as a coastal plain estuary, NB has an area of 342 km² and an average depth of 9m (Raposa 2009). Plastics have been reported in NB surface waters and coastlines for decades (Carpenter and Smith 1972, Colton et al. 1974, Cundell 1973, Kraimer 2018, STB 2019). While many of these reports confirm MPs through visual observation, advanced analysis of MPs in environmental matrices are often too cost-prohibitive for small-scale research initiatives.

Many studies focus on MP particles composed of conventional plastic polymers, but anthropogenically modified and semi-synthetic particles such as regenerated celluloses can have physical similar properties to conventional petroleum-based particles (Athey and Erdle 2021). Semi-synthetic particles

are considered MPs according to the legal definition adopted by the State of California and are becoming more commonly recognized as MPs in other research (Coffin 2020). Although semi-synthetic particles are derived from natural materials, during production or use they are often modified with chemical additives, dyes, and finishing agents that can include toxic compounds, such as per and polyfluoroalkyl substances (PFAS), formaldehyde, and azo dyes (Remy et al. 2015, Zambrano et al. 2021). Such particles have shown adverse effects to aquatic organisms (Kim et al. 2021), like microfiber pollution from smoked cigarette filters producing leachates toxic to *Daphnia magna* ($EC_{50}=0.017$ smoked filters) (Belzagui et al. 2021). The additives in semi-synthetic particles may also contribute to their persistence in the environment, which can range from months to decades in aquatic systems (Sait et al. 2021) and are found ubiquitously in the marine environment (Grbić et al. 2020). For this study, we use the definition of microplastics adopted by the State of California Code of Regulations on Microplastic Materials, which includes modified cellulose and semi- synthetic particles (2020).

Methods

Method Development & Validation

A key aspect of the present study was development of a hybrid method for the extraction of MPs from marine and estuarine sediments. Previous research showed MP extraction efficacy is impacted by the type of extraction method, as well as the physical properties of the sediment and MPs (Cashman

et al. 2020). Lessons learned from that method comparison study guided the development of a hybrid method for MPs 45-1,000 μm from sediments with different grain sizes and organic carbon content. This methods section gives a brief overview of the procedure, but detailed step-by-step instructions and quality assurance practices are available in the Supplemental Information.

The hybrid extraction procedure efficacy was assessed using two model sediments, silty sediment from Long Island Sound (LIS), New York (USA) (n=5) and beach sand from the coastline of Narragansett Beach (NAR), Rhode Island (USA) (n=5) (Supplemental Information (SI) Table 3) (Cashman et al. 2020). Both sediments were press-sieved through a 2mm sieve prior to analysis to remove any coarse fragments. The NAR sand was heated in a muffle oven at 550 °C for 6 h to remove natural organic material and existing plastics. Each sediment was homogenized using a metal spatula and split into 100 g (wet) samples in glass jars. Each sediment sample was spiked with known quantities of five representative conventional MP types (polyethylene (PE), polystyrene (PS), polyethylene terephthalate (PET), polyvinyl chloride (PVC) and polypropylene (PP)), with various fragment shapes (sphere, fragment, fiber), particle sizes (45 – 710 μm), and densities (0.91-1.38 g/cm^3) (SI Table 4). Plastics were chosen to represent a range of polymers, sizes, shapes and colors of microplastics to more accurately represent environmental microplastics. A minimum of 20 plastic pieces per polymer type were carefully transferred to each sediment sample (20 MP pieces * 5 plastic types = 100 pieces of MP/ sample). The plastic-amended sediments were then

mixed on a roller mill (4 RPM) at 4°C for a minimum of 48h in the dark (Cashman et al. 2020).

Detailed instructions for MP extraction can be found in the SI. Briefly, pre-weighed (100 g, wet) sediment samples were passed through a series of stacked sieves (1 mm, 250 µm, and 45 µm) using deionized (DI) water (Figure 2a) (Gilbreath et al. 2019). Debris >1 mm and <45 µm were discarded. Retained sediments were of two size classes: 251-1,000 µm and 45-250 µm (Figure 2b & 2c). MPs were extracted from both sieve size classes using a two-step density separation technique. For this technique, two sodium bromide (NaBr) solutions with known densities ($\rho = 1.3$ & 1.5 g/mL) were prepared by dissolving anhydrous NaBr (95%, Honeywell Fluka, Fisher Scientific) in DI water. Densities were checked using a Baum hydrometer and filtered through a 0.45 µm PCTE membrane filter to remove suspended solids.

Sediment samples were then transferred to 1-L glass separatory funnels using 300mL of the low density (1.3g/cm^3) NaBr solution (Figure 2b & 2c). Separatory funnels containing the NaBr solution and sediments were capped, tipped at a 90° angle, and vigorously shaken for two minutes. Separatory funnels were then returned to their upright position and rinsed with the low density NaBr solution to ensure no particles adhered to the walls of the separatory funnel. The funnel contents were left to settle until the supernatant was clear and sediment had resettled to the bottom (a minimum of two hours). Sediment that had settled out of each separatory funnel were transferred to a second 1 L separatory funnel by opening the funnel stopcock and allowing the

settled sediment to flow out. The remaining supernatant and floating debris were filtered onto a 20 µm PCTE membrane filter and retained for analysis (Figure 2D & 2F). The separatory funnel was rinsed thoroughly to ensure all particles were removed from the walls of the funnel. Sediment that was transferred to the secondary separatory funnels underwent a second round of shaking and settling with the higher density (1.5 g/cm³) NaBr solution. After another settling period, supernatant and floating debris were filtered onto a second 20 µm PCTE filter (Figure 2E & 2G). Sediment that settled to the bottom of this separatory funnel were discarded.

After extraction, each sediment sample produced four filters representing the two sieve size classes and two density separation steps. Each filter was oxidized with 30% hydrogen peroxide for 2 hours at 60°C to remove natural organic material and then filtered onto new PCTE filters (Masura et al. 2015, Zhao et al. 2018). All filters were stored at room temperature in covered petri dishes to prevent airborne contamination. Filters containing spiked MPs from method development were analyzed (i.e., counted) for MP recovery using a Nikon SMZ-45t stereoscope.

Identification of Internal Standard MPs

Filters containing spiked MPs were visually inspected with a Nikon microscope at 2x magnification count spiked MPs retained on the filters. Two analysts verified each MP count using both normal light and cyan excitation with a NightSea (Lexington, MA, USA) fluorescence filter (excitation 490-515 nm, emission 550 nm long pass). Spiked internal standard MPs were counted

on each filter and tallied by polymer type. Recovered MPs were compared to initial spiked values to determine percent recovery. Samples used for method development did not undergo further analysis with Raman spectroscopy.

Narragansett Bay Sediments

Collection Seven locations within NB were analyzed for MPs (Table 1).

Sampling locations were chosen based on prior knowledge of proximal land use and geomorphology. All sampling equipment was rinsed with DI water prior to use and in-between sampling events. Sediment samples were collected in July of 2019 using a Van Veen sediment grab with a 0.1 m² surface area. The top 5 cm of sediment from each sediment grab sample was collected using a metal spade and transferred to clean, muffled glass jars with foil-lined lids. Upon returning to the laboratory, each sediment sample was homogenized with a metal spatula. Sediment grain size was determined with triplicate analysis using a grain size MasterSizer 3000. Remaining sediment was split into sediment samples weighing 100 g (wet) each. All samples were stored in glass jars at 4°C in the dark until extraction. Quality assurance (QA) procedures for collection are detailed in the SI.

MP Extraction Process NB sediments were extracted using the hybrid method described above. To account for MP loss during extraction, one sediment sample from each sampling location was spiked with known quantities of 3 types of MPs as described above to serve as internal standards. The plastics

used as internal standards included PS spheres, PET fibers, and PE films ranging from 45- 500 μm (SI Table 4). All sediments samples were stored at 4°C in the dark until the time of extraction. Detailed description of QA practices, including air blanks, process blanks, and sediment spiking with internal standards can be found in the SI. The spiked sediment samples from NB underwent the same recovery as described above. Alternatively, sediments extracted for environmental MP analysis were examined using Raman spectroscopy.

Raman Analysis

Environmental MPs extracted from NB sediments were identified and quantified with a Renishaw Qontor Confocal Raman spectrometer with Renishaw Wire software (Renishaw PLC, Wotton-Under-Edge, United Kingdom). All data were post-processed with Wire 5.2 Software. The Raman spectrometer was calibrated each day prior to use with a preloaded silicon sample. All samples were analyzed using a 785nm laser at a power of 1%, an integration time of 10 s, 1 accumulation, a spectral range of 100 to 3200 Raman shift/ cm^{-1} and an objective with 20x, 50x, and 100x magnifications. The Raman spectral libraries used to identify materials included the Renishaw spectral libraries for polymers and inorganics, as well as the SLoPP and SLoPP-E spectral libraries (Munno et al. 2020) and Open Specy (Cowger et al. 2021). Particle analysis parameters were optimized for each sample. All suspected MPs retained on the 251-1,000 μm size class filters were picked

using fine forceps (Excelta 5SA) and placed on a piece of double-sided tape adhered to a slide. Each picked particle was circled with permanent marker, numbered, and had their physical properties (e.g., size, color, and shape) recorded (SI Table 9). Single point analysis was used for the picked particles (i.e., 251-1,000 μm) whereas automated maps were used for the filters' subsections. Information on each spectrum including instrument parameters, spectral library, and quality index can be found in SI Table 9. Particles retained on the 45-250 μm size class filters were too small to pick using forceps. Therefore, a $\frac{1}{4}$ wedge-shaped subsection from each filter was analyzed using the scanning feature to maximize efficiency and reduce the amount of time required to analyze each sample. Prior to analysis, filters containing 45-250 μm particles were re-filtered onto new PCTE filters with SkinTac adhesive as described by Thaysen et al. (2020) to prevent particle movement on the filter. All MPs identified from the $\frac{1}{4}$ filter sections were multiplied by 4 to extrapolate the total particle number per filter.

Evaluation of Raman Data

Particles with a confirmed polymer match and hit quality index (HQI) > 0.4 were accepted as a MP particle. All confirmed MP particles were analyzed further for their size, shape, and color. The extraction method was designed for MPs 40-1,000 μm in diameter. However, some MP particles with smaller diameters, such as fibers, were identified during extraction. These particles were still reported in the data. Many non-anthropogenic particles were also

identified, such as cotton, wool, and silk fibers. These are reported in SI Table 9, but ultimately not presented in our data due to a lack of laboratory controls for these types of particles. Spectra identified as polycarbonate (PC) were also omitted from our data due to background interference resulting from the use of PCTE filters in the extraction procedure.

Results

Assessing Extraction Efficiency using Internal Standards

The hybrid method was assessed by recovering known quantities of internal standard MPs from five replicates for both LIS and NAR sediment samples (SI Figure 7, SI Tables 5& 6). Mean recovery for MPs was >70% for nearly all polymers and both sediment types (i.e., silty and beach sand). The one exception to this was the mean recovery of PET fibers from LIS sediment (\bar{x} =45.14%, RSD=62.1%). The PET fibers used in percent recovery tests had a length of 250-500 μ m, but a fiber diameter of roughly 20 μ m. We suspect PET fiber loss most likely occurred in the initial sieving steps (Figure 2a). Several mean recoveries were >100%. This was due to fragmentation of MPs during the extraction process and is further explained in the discussion.

For the spiked environmental samples from NB, mean recoveries across all types of spiked MPs ranged from 40-100% (Table 2, SI Table 7). The lowest recoveries were observed at Station 1, with a mean recovery of 40%. This was largely due to poor recovery of PS MPs (19%). With the exception of Station 1, PET fibers had the lowest recovery. Station 1 had the

poorest overall MP recoveries (i.e., 40% PE, 19% PS, 63% PET), and Station 3 had the highest overall spiked MP recoveries (i.e., 115% PE, 53% PS, 93% PET). The number of particles found in water and air blanks were below 5 particles per filter (SI Table 8). Particle abundance in the water and air blanks are reported in the SI but are not used to make any baseline subtractions from the data presented.

MPs in Narragansett Bay Sediments

Each station contained a total of 40 to 4.6 million MPs per 100 g (wet) sediment sample (Figure 3). Station 4 had the highest number of total MPs (4.6 million), followed by Station 3 (293), Station 2 (269), Station 7 (189), Station 6 (67), Station 1 (45), and Station 5 (40). Stations 3 and 4 had high abundances of cellulose acetate fibers with 146 and 4.6 million fibers per 100g sample, respectively. A total of 38 different polymer types (semi-synthetic and synthetic) were identified across all stations (Figure 3; SI Table 9). When looking at the summation of MPs across all stations, cellulose acetate was the most commonly identified particle polymer (4.6 million particles), followed by polyester PEY (297 particles), PP (186 particles), methyl cellulose (148 particles), polyurethane (93 particles), PS (33 particles), PE (26 particles), ethyl cellulose (20 particles), and PVC (20 particles) (Figure 4). These nine polymer types accounted for 45-99% of all particles found at each station (Station 1 (84%), Station 2 (75%), Station 3 (83%), Station 4 (99%), Station 5 (70%), Station 6 (45%), and Station 7 (81%) (Figure 4)). All other identified

polymers can be found in SI Table 9. The top five polymer types are mapped separately in Figure 5 to show spatial distribution.

MP color was observed under the stereomicroscope, or by analyzing pictures from the Raman imaging software (SI Table 9). Inconsistencies in nomenclature and technique can result in large discrepancies in reporting MP physical characteristics such as particle color (Lusher et al. 2020). Therefore, colors were reported in broad classes to account for observation variability. A breakdown of MP physical characteristics showed that most MPs were achromatic in color (Figure 6a). Achromatic MPs (black, white, brown, transparent & grey) made up 68-99% of the MPs at each station. MPs were also characterized by shape (Figure 6b) and size (Figure 6c), when possible. Fibers were the dominant MP found at Stations 3 (77%), 4 (>99%), and 5 (45%). Whereas fragments were the dominant MP at Stations 2 (49%), 6 (45%), and 7 (54%). Foams were the most common shape at Station 1 (32%). MPs were measured by their longest length to the nearest 100 μ m. Figure 6c shows these size classes grouped into larger subcategories (45-200, 201-400, 401-600, 601-800, and 801-1000 μ m). MPs in the 45-200 μ m size range were the most identified MP size at Stations 3 (89%), 5 (53%), 6 (43%), and 7 (72%). Station 1 had an equal percentage of MPs in the 45-200 and 201-400 μ m size range (32%). Most MPs found at Station 2 were 201-400 μ m (51%). Due to the large abundance of cellulose acetate fibers found at Station 4, the majority of the MPs at this station were in the 601-800 μ m size range (>99%).

Discussion

Extraction Method Effectiveness The isolation, extraction and identification of MPs from environmental sediments is challenging. Physical characteristics of sediments and MPs, as well as the selected extraction method can greatly affect results of MP extraction and identification. Many existing MP extraction methods focus on MPs >300 μm (Cai et al. 2020, Kowalski et al. 2016, Masura et al. 2015), despite acknowledgement that small (<300 μm) are prevalent in the environment (Corami et al. 2021). This is most likely because the 333 μm neuston net was standard for marine MP trawls for many years (Lindeque et al. 2020). This study aimed to extract and characterize smaller MPs (45-1,000 μm) to better understand their presence in marine sediments. Recovery of spiked MPs from NAR and LIS sediments extracted with hybrid method development had >80% mean recovery for all MPs except PET fibers (SI Figure 7). PET fiber recovery was 40% (LIS sediment) and 70% (NAR sediment) during method development. Fibers can be very difficult to recover from sediments due to their small diameter. Many fibers were noted to pass through sieving steps in the spiked MP recovery tests. The spiked MP recoveries from environmental samples ranged from 18-114% for the polymer types and sediments investigated herein (Table 2). One possible explanation for the large variations are the different physical characteristics of each sediment. Station 1 had the smallest grainsize distribution (Table 1) and the lowest mean percent recovery of spiked MPs (SI Table 5). Station 3 had the largest grainsize distribution and the best mean recovery of spiked MPs.

However, it is more difficult to sieve and process finer grained sediments, which in turn may result in lower MP recovery. A regression analysis showed no significant relationship between the grainsize and MP recovery, indicating that grainsize is not the only influence on extraction efficacy. The use of the internal standards suggests strongly that some of the environmental MPs were lost or unidentified during the extraction process and reported MP values for NB sediments are under-representations of true MP quantities. In addition, this method did not analyze MPs below and above the range 45-1,000 μm . The PVC fragments used as spiking material were fragile and were fragmented during the extraction process. This explains why their % recoveries were >100%. These PVC fragments were not ideal, and therefore not used as spiking materials for the environmental samples. But this does point to the likelihood of MP fragmentation during the extraction process.

Presence of Cellulose Acetate

Perhaps the biggest surprise in analyzing NB sediments was the high abundance of cellulose acetate fibers. The reporting units for MPs in sediment vary by study, but the concentration of MPs found in NB are substantially higher than many existing sediment studies. Some of the highest reported MP concentrations in sediment include 27,606 MPs/ m^2 in South Korea (Lee et al. 2013), 8,000 MPs/ kg in Nova Scotia (Mathalon and Hill 2014), 5,000-7,000 MPs/ m^3 in Portugal (Ballent et al. 2012), and 4,205 MPs/kg in China (Wang et al. 2019). Our data are reported in MP/100g wet weight or 0.03 m^2 surface

area. Extrapolating our results from Station 4 would result in 46 million MPs/kg sediment, or 153 million MPs/ m². Other studies note that cellulose acetate and other regenerated cellulose fibers make up a large portion of recovered MPs (Bridson et al. 2020, Lusher et al. 2013). The cellulose acetate fibers from NB were uniform in size, shape, and color (SI Figure 8). Their uniformity and high abundance lead us to believe that they likely entered NB from a proximal source.

This study was unable to determine the exact source or transport mechanism of the cellulose acetate MPs into NB. Most plastic pollution enters the marine environment from land through rivers (Jambeck et al. 2015). Sediment transported by rivers is often deposited in estuarine and deltaic sedimentary environments (Coleman and Wright 1975), which may explain why coastal environments exhibit such high MP concentrations (Harris 2020). Semi-enclosed marine regions can result in high sequestration of MPs (Alosairi et al. 2020). For these reasons, there is strong evidence observed MPs likely came from nearby land sources. Station 2's sampling location was chosen for its proximity to NB's largest WWTP discharge, and we had originally hypothesized the highest number of MPs would be observed at this station. High fiber abundances are often associated with sewage discharge (Browne et al. 2011). However, very few cellulose acetate fibers were detected at this station. This leads us to believe that these fibers did not come from NB's major WWTP. Cellulose acetate fibers have many industrial uses, including fiberglass for boats (Spaulding Jr 1966), cigarette filters (Shen et al.

2021), and textiles (Law 2004). The collected cellulose acetate fibers were visually compared against weathered and pristine cigarette filters to establish visual similarities. The size and texture of the cellulose acetate fibers did not match the cigarette filters, leading us to believe these fibers did not come from cigarette filters. Narragansett Bay supports many services, including recreational and commercial boating, beaches, small-scale industry, commercial fishing, and residential housing (Dalton et al. 2010). Numerous textile manufacturers and processing companies within NB are known to have worked with cellulose fibers over the past century. The station with the highest MP abundance was Station 4, Arnold Point (Figure 5). This sampling station is on the northwestern point of Aquidneck Island and south of Mount Hope Bay. Geographically this region has a strong history of textile production and boating industry. We believe these fibers could be from the manufacturing of cellulose acetate textiles used in marine industries.

Challenges with Microfibers

Microfibers are often the dominant shape of MPs found in environmental samples (Claessens et al. 2011, Cole and Strawhecker 2014, Lusher et al. 2014, Nel and Froneman 2015, Nor and Obbard 2014, Sanchez-Vidal et al. 2018, Willis et al. 2017, Woodall et al. 2014). Due to the high loss of microfibers in QA recovery samples, we believe our estimates of microfibers underestimate of microfiber occurrence in these sediments. Microplastic research techniques are constantly advancing capabilities to extract and

identify MPs from sediments. Earlier studies that focused on MPs >300 µm may have missed many of the fibers that were caught in finer sieves or filters. This investigation was a survey of sediments across Narragansett Bay. To better understand the variability associated with the measurements reported here, a more intensive and expensive study would be required. However, despite this, these results are some of first to identify MPs in marine sediments from the North Atlantic Region. Further, these results show the wide variability of MP abundance, polymer type, size, shape, and color.

Modified cellulose particles are increasingly noted as one of the most commonly identified MP morphologies in environmental samples (Lenaker et al. 2020, Lusher et al. 2013, Remy et al. 2015), but the toxicity and effects of these fibers are not well understood (Athey and Erdle 2021). Semisynthetic particles were previously thought to readily degrade and be less concerning than their synthetic counterparts. However, several studies have shown MPs often are ingested by benthic organisms including polychaetes (Wright et al. 2013), crustaceans (Watts et al. 2014), and bivalves (Von Moos et al. 2012) and studies by Bour et al. (2018) and Kim et al. (2021) demonstrated acute toxicity to benthic organisms. In addition, more recent studies note that semisynthetic fibers are digested and cause negative impacts in brine shrimp (Kim et al. 2021). The data emerging about the toxicity of modified cellulose fibers and other semisynthetic particles clearly demonstrates the need for further research. The stress of ingestion, retention, and exposure of associated chemicals are of great concern given the high MP concentrations

(Andrady 2011, Remy et al. 2015, Wright et al. 2013). This is especially true for particles with additional additives such as dyes and finishing additives (Athey and Erdle 2021). The concentrations of MPs are particularly concerning to benthic deposit feeders (Morét-Ferguson et al. 2010).

Conclusion

Advancing methodologies for the extraction and identification of MPs from sediment is vital for predicting their impacts in the marine environment. The hybrid method presented here represents a harmonization of existing methods to extract a broad range of MPs from sediments. While no singular method can ensure complete recovery of all MPs from sediment, we believe the hybrid method is advantageous for its low cost, minimal waste generation, and favorable MP recovery. Using the hybrid method to extract MPs from Narragansett Bay sediments revealed very high concentrations of MPs, particularly cellulose acetate fibers. With the exception of Station 4, MPs 45-200 μm in size accounted for 42-88% of all MPs (Figure 6c). This size class is not often reported in traditional extraction methods. We expect that higher MP abundances will continue to be reported as extraction methods advance. This suggests studies evaluating the toxicity of MPs may need to reassess the thresholds for environmental relevance in order to select spiking concentrations which realistically represent potential threats. These results signify the importance of adequately assessing MP abundance in sediments to better understand their risk and effects.

References

1. (2020) Adoption of Definition of 'Microplastics in Drinking Water'. Board, C.S.W.R.C. (ed).
2. Alosairi, Y., Al-Salem, S.M. and Al Ragum, A. (2020) Three-dimensional numerical modelling of transport, fate and distribution of microplastics in the northwestern Arabian/Persian Gulf. *Marine pollution bulletin* 161, 111723.
3. Andrady, A.L. (2011) Microplastics in the marine environment. *Marine pollution bulletin* 62(8), 1596-1605.
4. Athey, S.N. and Erdle, L.M. (2021) Are We Underestimating Anthropogenic Microfiber Pollution? A Critical Review of Occurrence, Methods, and Reporting. *Environmental toxicology and chemistry*.
5. Ballent, A., Purser, A., de Jesus Mendes, P., Pando, S. and Thomsen, L. (2012) Physical transport properties of marine microplastic pollution. *Biogeosciences Discussions* 9(12).
6. Belzagui, F., Buscio, V., Gutiérrez-Bouzán, C. and Vilaseca, M. (2021) Cigarette butts as a microfiber source with a microplastic level of concern. *Science of The Total Environment* 762, 144165.
7. Bour, A., Haarr, A., Keiter, S. and Hylland, K. (2018) Environmentally relevant microplastic exposure affects sediment-dwelling bivalves. *Environmental Pollution* 236, 652-660.
8. Bridson, J.H., Patel, M., Lewis, A., Gaw, S. and Parker, K. (2020) Microplastic contamination in Auckland (New Zealand) beach sediments. *Marine pollution bulletin* 151, 110867.
9. Browne, M.A., Crump, P., Niven, S.J., Teuten, E., Tonkin, A., Galloway, T. and Thompson, R. (2011) Accumulation of microplastic on shorelines worldwide: sources and sinks. *Environmental science & technology* 45(21), 9175-9179.
10. Burgess, R.M., Ho, K.T., Mallos, N.J., Leonard, G.H., Hidalgo-Ruz, V., Cook, A.M. and Christman, K. (2017) Microplastics in the aquatic environment—Perspectives on the scope of the problem. *Environmental toxicology and chemistry* 36(9), 2259-2265.
11. Cai, H., Chen, M., Chen, Q., Du, F., Liu, J. and Shi, H. (2020) Microplastic quantification affected by structure and pore size of filters. *Chemosphere* 257, 127198.

12. Carpenter, E.J. and Smith, K.L. (1972) Plastics on the Sargasso Sea surface. *Science* 175(4027), 1240-1241.
13. Cashman, M.A., Ho, K.T., Boving, T.B., Russo, S., Robinson, S. and Burgess, R.M. (2020) Comparison of microplastic isolation and extraction procedures from marine sediments. *Marine pollution bulletin* 159, 111507.
14. Claessens, M., De Meester, S., Van Landuyt, L., De Clerck, K. and Janssen, C.R. (2011) Occurrence and distribution of microplastics in marine sediments along the Belgian coast. *Marine pollution bulletin* 62(10), 2199-2204.
15. Coffin, S. (2020) Status of Legislation and Regulatory Drivers for Microplastics in California. *To Protect Water Quality Around the World* (54), 17.
16. Cole, D.P. and Strawhecker, K.E. (2014) An improved instrumented indentation technique for single microfibers. *Journal of Materials Research* 29(9), 1104-1112.
17. Coleman, J.M. and Wright, L.D. (1975) Modern river deltas: variability of processes and sand bodies.
18. Colton, J.B., Knapp, F.D. and Burns, B.R. (1974) Plastic particles in surface waters of the northwestern Atlantic. *Science* 185(4150), 491-497.
19. Coppock, R.L., Cole, M., Lindeque, P.K., Queirós, A.M. and Galloway, T.S. (2017) A small-scale, portable method for extracting microplastics from marine sediments. *Environmental Pollution* 230, 829-837.
20. Corami, F., Rosso, B., Morabito, E., Rensi, V., Gambaro, A. and Barbante, C. (2021) Small microplastics (< 100 μm), plasticizers and additives in seawater and sediments: Oleo-extraction, purification, quantification, and polymer characterization using Micro-FTIR. *Science of The Total Environment* 797, 148937.
21. Cowger, W., Steinmetz, Z., Gray, A., Munno, K., Lynch, J., Hapich, H., Primpke, S., De Frond, H., Rochman, C. and Herodotou, O. (2021) Microplastic Spectral Classification Needs an Open Source Community: Open Specy to the Rescue! *Analytical chemistry*.
22. Cózar, A., Echevarría, F., González-Gordillo, J.I., Irigoien, X., Úbeda, B., Hernández-León, S., Palma, Á.T., Navarro, S., García-de-Lomas, J. and Ruiz, A. (2014) Plastic debris in the open ocean. *Proceedings of the National Academy of Sciences* 111(28), 10239-10244.

23. Cundell, A.M. (1973) Plastic materials accumulating in Narragansett Bay. *Marine pollution bulletin* 4(12), 187-188.
24. Dalton, T., Thompson, R. and Jin, D. (2010) Mapping human dimensions in marine spatial planning and management: An example from Narragansett Bay, Rhode Island. *Marine Policy* 34(2), 309-319.
25. Fries, E., Dekiff, J.H., Willmeyer, J., Nuelle, M.-T., Ebert, M. and Remy, D. (2013) Identification of polymer types and additives in marine microplastic particles using pyrolysis-GC/MS and scanning electron microscopy. *Environmental science: processes & impacts* 15(10), 1949-1956.
26. Gilbreath, A., McKee, L., Shimabuku, I., Lin, D., Werbowski, L.M., Zhu, X., Grbic, J. and Rochman, C. (2019) Multiyear water quality performance and mass accumulation of PCBs, mercury, methylmercury, copper, and microplastics in a bioretention rain garden. *Journal of Sustainable Water in the Built Environment* 5(4), 04019004.
27. Grbić, J., Helm, P., Athey, S. and Rochman, C.M. (2020) Microplastics entering northwestern Lake Ontario are diverse and linked to urban sources. *Water research* 174, 115623.
28. Harris, P.T. (2020) The fate of microplastic in marine sedimentary environments: A review and synthesis. *Marine pollution bulletin* 158, 111398.
- Hidalgo-Ruz, V., Gutow, L., Thompson, R.C. and Thiel, M. (2012) Microplastics in the marine environment: a review of the methods used for identification and quantification. *Environmental science & technology* 46(6), 3060-3075.
29. Jambeck, J.R., Geyer, R., Wilcox, C., Siegler, T.R., Perryman, M., Andrady, A., Narayan, R. and Law, K.L. (2015) Plastic waste inputs from land into the ocean. *Science* 347(6223), 768-771.
30. Kim, L., Kim, S.A., Kim, T.H., Kim, J. and An, Y.-J. (2021) Synthetic and natural microfibers induce gut damage in the brine shrimp *Artemia franciscana*. *Aquatic Toxicology* 232, 105748.
31. Kowalski, N., Reichardt, A.M. and Waniek, J.J. (2016) Sinking rates of microplastics and potential implications of their alteration by physical, biological, and chemical factors. *Marine pollution bulletin* 109(1), 310-319.
32. Kraimer, M.T., Eva; McLaughlin, Dave (2018) Clean Ocean Access 2016 - 2018 Marina Trash Skimmer Report.
33. Law, R.C. (2004) Applications of cellulose acetate: Cellulose acetate in textile application, pp. 255-266, Wiley Online Library.

34. Lee, J., Hong, S., Song, Y.K., Hong, S.H., Jang, Y.C., Jang, M., Heo, N.W., Han, G.M., Lee, M.J. and Kang, D. (2013) Relationships among the abundances of plastic debris in different size classes on beaches in South Korea. *Marine pollution bulletin* 77(1-2), 349-354.
35. Lenaker, P.L., Corsi, S.R. and Mason, S.A. (2020) Spatial distribution of microplastics in surficial benthic sediment of Lake Michigan and Lake Erie. *Environmental science & technology* 55(1), 373-384.
36. Lindeque, P.K., Cole, M., Coppock, R.L., Lewis, C.N., Miller, R.Z., Watts, A.J.R., Wilson-McNeal, A., Wright, S.L. and Galloway, T.S. (2020) Are we underestimating microplastic abundance in the marine environment? A comparison of microplastic capture with nets of different mesh-size. *Environmental Pollution* 265, 114721.
37. Lusher, A.L., Burke, A., O'Connor, I. and Officer, R. (2014) Microplastic pollution in the Northeast Atlantic Ocean: validated and opportunistic sampling. *Marine pollution bulletin* 88(1-2), 325-333.
38. Lusher, A.L., McHugh, M. and Thompson, R.C. (2013) Occurrence of microplastics in the gastrointestinal tract of pelagic and demersal fish from the English Channel. *Marine pollution bulletin* 67(1-2), 94-99.
39. Lusher, A.L., Munno, K., Hermabessiere, L. and Carr, S. (2020) Isolation and extraction of microplastics from environmental samples: an evaluation of practical approaches and recommendations for further harmonization. *Applied spectroscopy* 74(9), 1049-1065.
40. Masura, J., Baker, J., Foster, G. and Arthur, C. (2015) *Laboratory Methods for the Analysis of Microplastics in the Marine Environment: Recommendations for quantifying synthetic particles in waters and sediments.*
41. Mathalon, A. and Hill, P. (2014) Microplastic fibers in the intertidal ecosystem surrounding Halifax Harbor, Nova Scotia. *Marine pollution bulletin* 81(1), 69-79.
42. Morét-Ferguson, S., Law, K.L., Proskurowski, G., Murphy, E.K., Peacock, E.E. and Reddy, C.M. (2010) The size, mass, and composition of plastic debris in the western North Atlantic Ocean. *Marine pollution bulletin* 60(10), 1873-1878.
43. Munno, K., De Frond, H., O'Donnell, B. and Rochman, C.M. (2020) Increasing the accessibility for characterizing microplastics: Introducing new application-based and spectral libraries of plastic particles (SLoPP and SLoPP-E). *Analytical chemistry* 92(3), 2443-2451.

44. NBEP, N.B.E.P. (2017) State of Narragansett Bay and its Watershed. Technical Report, Providence, Rhode Island.
45. Nel, H.A. and Froneman, P.W. (2015) A quantitative analysis of microplastic pollution along the south-eastern coastline of South Africa. *Marine pollution bulletin* 101(1), 274-279.
46. Nor, N.H.M. and Obbard, J.P. (2014) Microplastics in Singapore's coastal mangrove ecosystems. *Marine pollution bulletin* 79(1-2), 278-283.
47. Nuelle, M.-T., Dekiff, J.H., Remy, D. and Fries, E. (2014) A new analytical approach for monitoring microplastics in marine sediments. *Environmental Pollution* 184, 161-169.
48. Raposa, K.B. (2009) Ecological geography of Narragansett Bay. An Ecological Profile of the Narragansett Bay National Estuarine Research Reserve, 77-88.
49. Remy, F., Collard, F., Gilbert, B., Compère, P., Eppe, G. and Lepoint, G. (2015) When microplastic is not plastic: the ingestion of artificial cellulose fibers by macrofauna living in seagrass macrophytodebris. *Environmental science & technology* 49(18), 11158-11166.
50. Rochman, C.M., Brookson, C., Bikker, J., Djuric, N., Earn, A., Bucci, K., Athey, S., Huntington, A., McIlwraith, H. and Munno, K. (2019) Rethinking microplastics as a diverse contaminant suite. *Environmental toxicology and chemistry* 38(4), 703-711.
51. Sait, S.T.L., Sørensen, L., Kubowicz, S., Vike-Jonas, K., Gonzalez, S.V., Asimakopoulou, A.G. and Booth, A.M. (2021) Microplastic fibres from synthetic textiles: Environmental degradation and additive chemical content. *Environmental Pollution* 268, 115745.
52. Sanchez-Vidal, A., Thompson, R.C., Canals, M. and de Haan, W.P. (2018) The imprint of microfibrils in southern European deep seas. *PloS one* 13(11), e0207033.
53. Shen, M., Li, Y., Song, B., Zhou, C., Gong, J. and Zeng, G. (2021) Smoked cigarette butts: Unignorable source for environmental microplastic fibers. *Science of The Total Environment*, 148384.
54. Spaulding Jr, K.B. (1966) Fiberglass boats in naval service. *Naval Engineers Journal* 78(2), 333-340.
- STB, S.T.B. (2019) Trawling for Microplastics. Bay, S.t. (ed), Savebay.org.

55. Thaysen, C., Munno, K., Hermabessiere, L. and Rochman, C.M. (2020) Towards Raman automation for microplastics: Developing strategies for particle adhesion and filter subsampling. *Applied spectroscopy* 74(9), 976-988.
56. Thompson, R.C., Olsen, Y., Mitchell, R.P., Davis, A., Rowland, S.J., John, A.W.G., McGonigle, D. and Russell, A.E. (2004) Lost at sea: where is all the plastic? *Science* 304(5672), 838-838.
57. Vadeboncoeur, M.A., Hamburg, S.P. and Pryor, D. (2010) Modeled nitrogen loading to Narragansett Bay: 1850 to 2015. *Estuaries and Coasts* 33(5), 1113-1127.
58. Von Moos, N., Burkhardt-Holm, P. and Köhler, A. (2012) Uptake and effects of microplastics on cells and tissue of the blue mussel *Mytilus edulis* L. after an experimental exposure. *Environmental science & technology* 46(20), 11327-11335.
59. Wang, J., Wang, M., Ru, S. and Liu, X. (2019) High levels of microplastic pollution in the sediments and benthic organisms of the South Yellow Sea, China. *Science of The Total Environment* 651, 1661-1669.
60. Watts, A.J.R., Lewis, C., Goodhead, R.M., Beckett, S.J., Moger, J., Tyler, C.R. and Galloway, T.S. (2014) Uptake and retention of microplastics by the shore crab *Carcinus maenas*. *Environmental science & technology* 48(15), 8823-8830.
61. Willis, K.A., Eriksen, R., Wilcox, C. and Hardesty, B.D. (2017) Microplastic distribution at different sediment depths in an urban estuary. *Frontiers in Marine Science* 4, 419.
62. Woodall, L.C., Sanchez-Vidal, A., Canals, M., Paterson, G.L.J., Coppock, R., Sleight, V., Calafat, A., Rogers, A.D., Narayanaswamy, B.E. and Thompson, R.C. (2014) The deep sea is a major sink for microplastic debris. *Royal Society open science* 1(4), 140317.
63. Wright, S.L., Thompson, R.C. and Galloway, T.S. (2013) The physical impacts of microplastics on marine organisms: a review. *Environmental Pollution* 178, 483-492.
64. Zambrano, M.C., Pawlak, J.J., Daystar, J., Ankeny, M. and Venditti, R.A. (2021) Impact of dyes and finishes on the aquatic biodegradability of cotton textile fibers and microfibers released on laundering clothes: correlations between enzyme adsorption and activity and biodegradation rates. *Marine pollution bulletin* 165, 112030.

65. Zhao, S., Ward, J.E., Danley, M. and Mincer, T.J. (2018) Field-based evidence for microplastic in marine aggregates and mussels: implications for trophic transfer. *Environmental science & technology* 52(19), 11038-11048.

66. Zobkov, M. and Esiukova, E. (2017) Microplastics in Baltic bottom sediments: quantification procedures and first results. *Marine pollution bulletin* 114(2), 724-732.

Figures

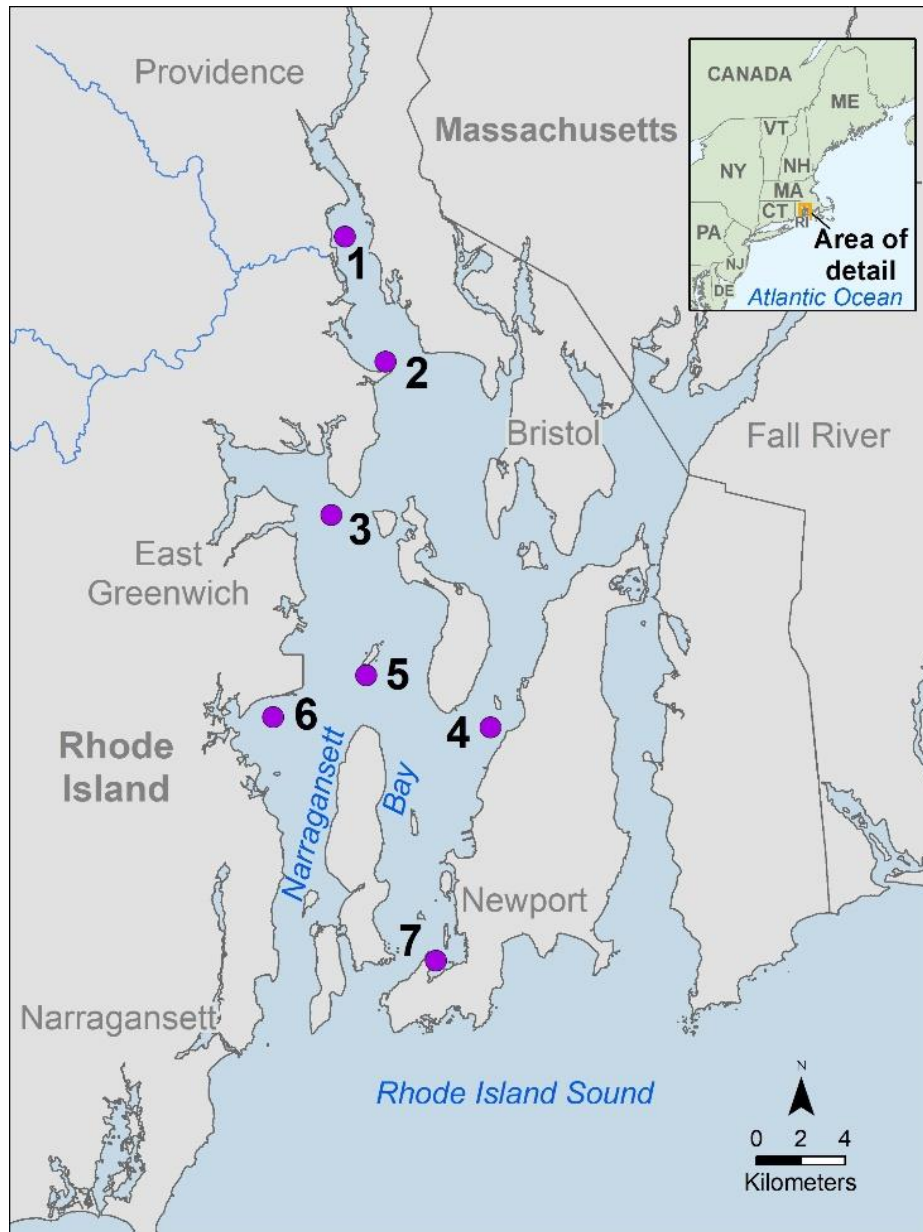


Figure 2-1. A map of sampling locations in Narragansett Bay, RI, USA.

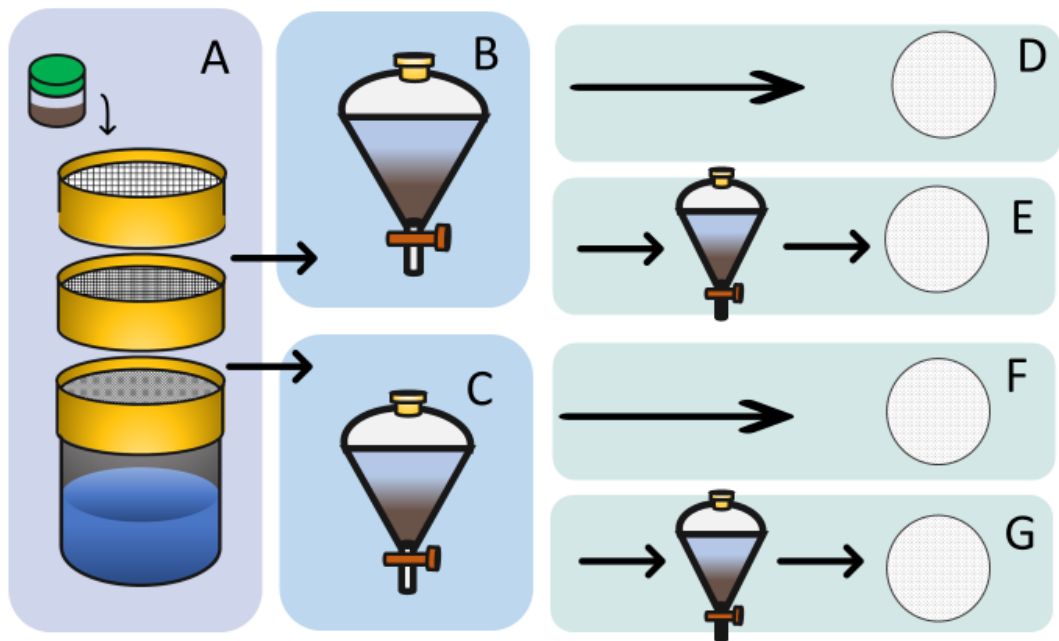


Figure 2-2. A wet sediment sample (2a) is poured over a set of stacked sieves and rinsed through with DI water. The sieves are stacked from top to bottom, 1,000, 250, and 45 μ m. Sediment that pass through all three sieves or is retained on 1000 μ m sieve are discarded. Materials retained on the 250 μ m sieve are retained as size class 250-1000 μ m (2b). Materials retained on the 45 μ m sieve are retained as size class 250-45 μ m (2c). Each size class undergoes two density separations. MPs are retained on 4 filters for each sample (2d, 2e, 2f, 2g).

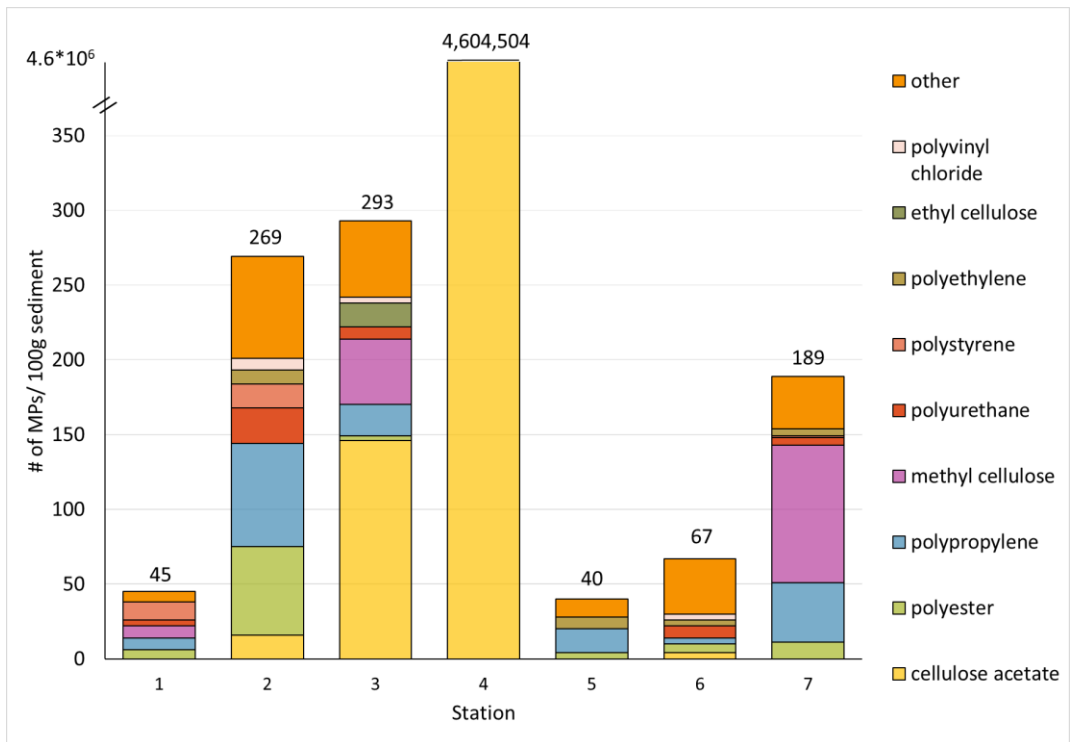


Figure 2-3. Number of Microplastics (MPs) per 100g sediment sample at each station. Total number of MPs per sediment displayed in text above bars.

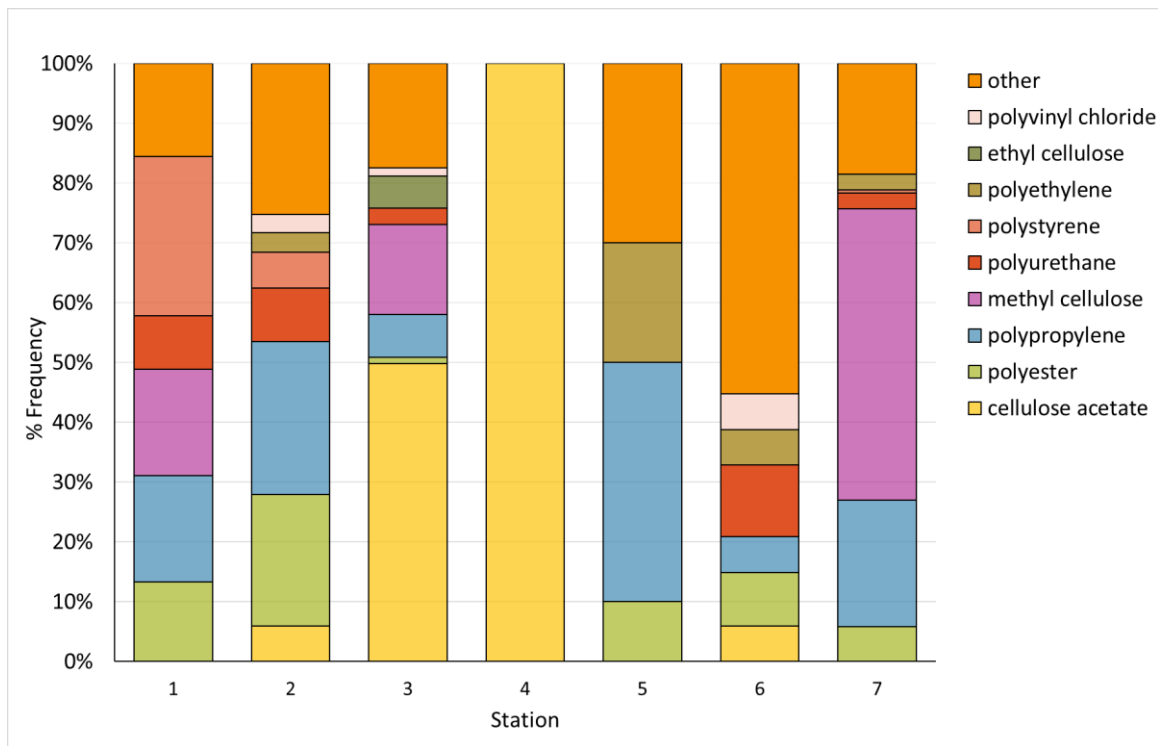


Figure 2-4. Percent frequency of Microplastics (MPs) by polymer type at each station.

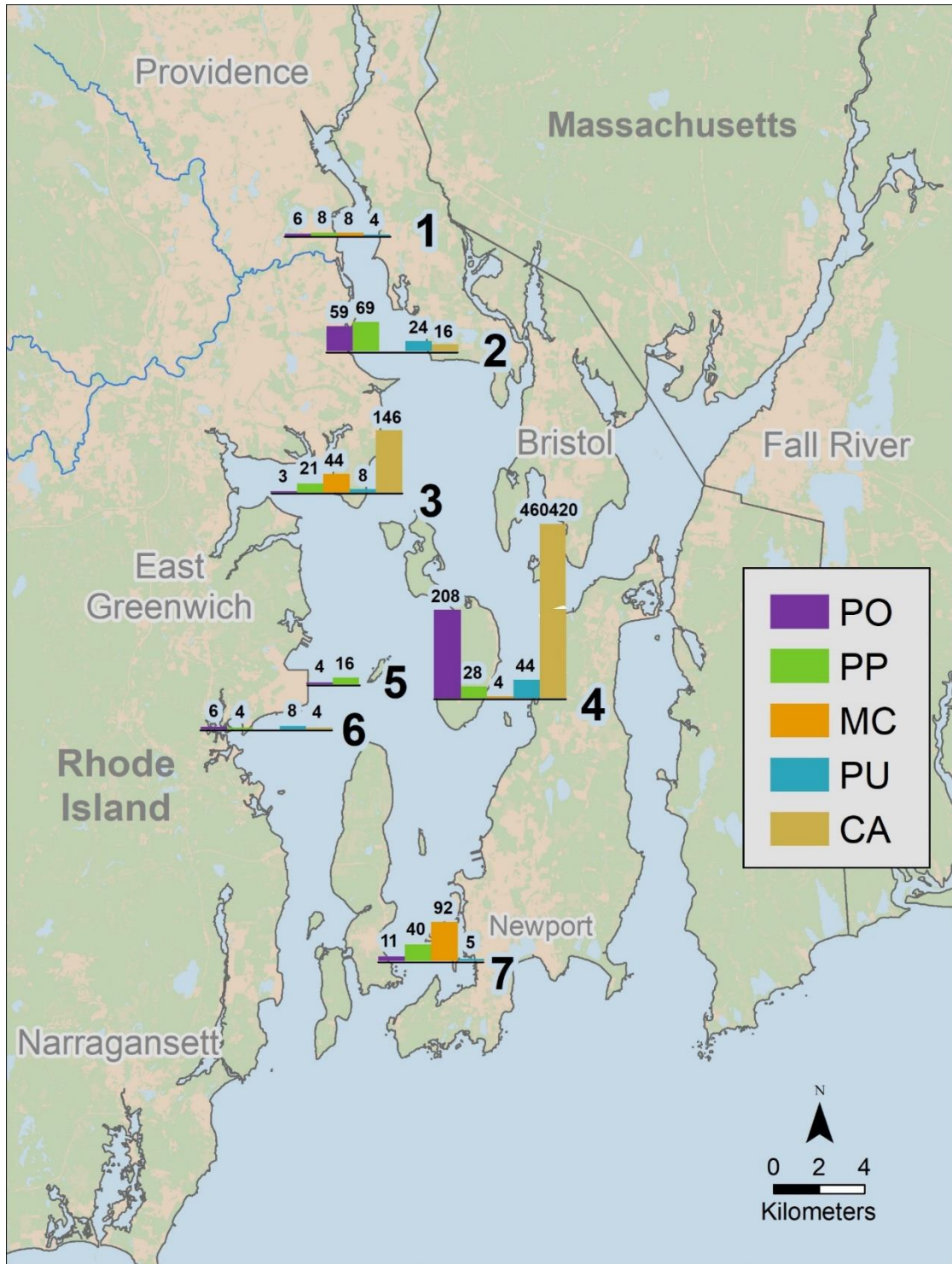


Figure 2-5. Select Microplastics (MPs) displayed as number of MPs by the five most frequently occurring plastic types: cellulose acetate (CA) gold, polyurethane (PU) blue), Methyl cellulose (MC) orange, polypropylene (PP) green, and polyester (PO) purple. CA, PU, MC, PP, and PO non-detects are not shown on this figure.

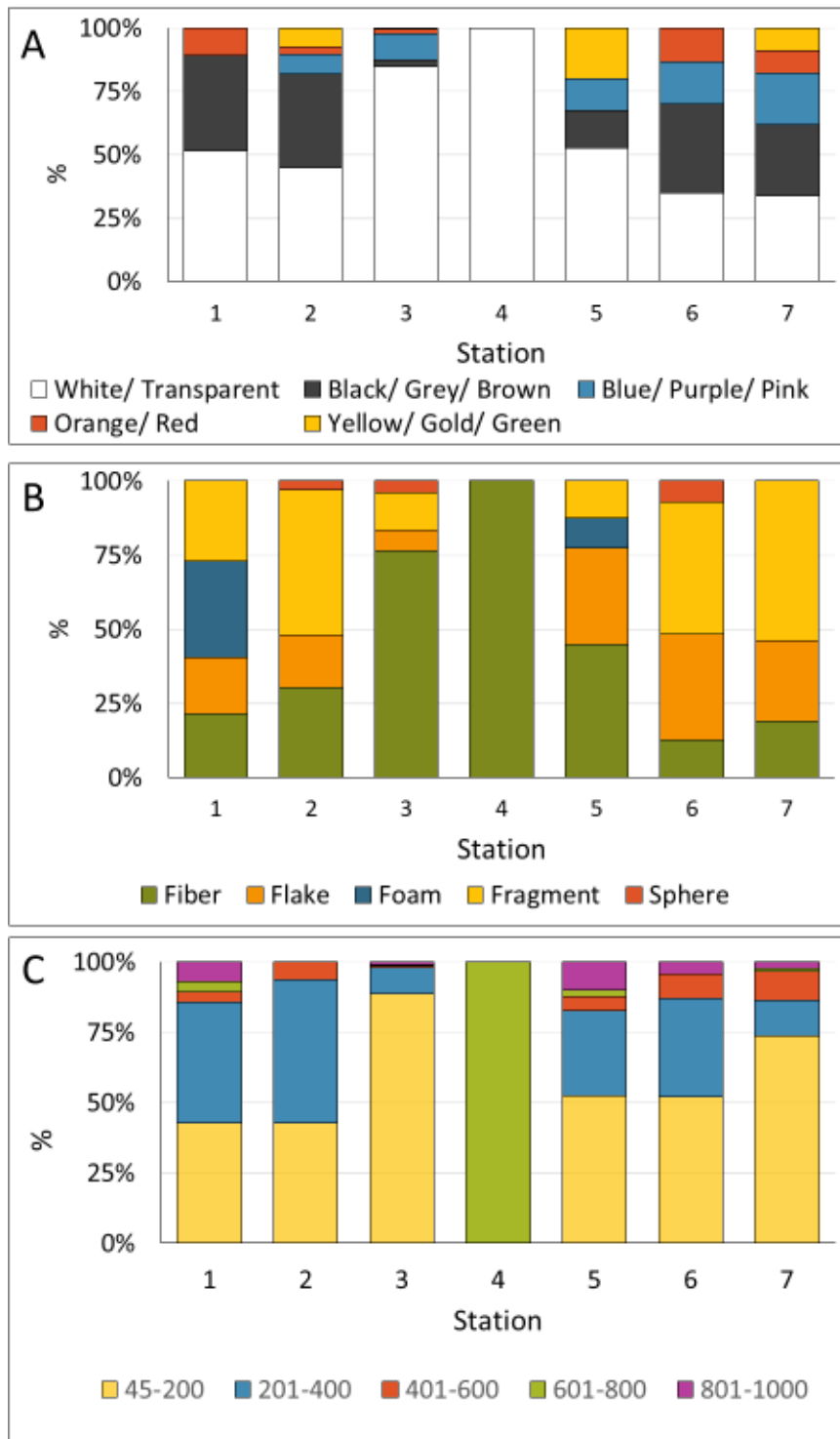


Figure 2-6. Breakdown of Microplastics (MPs) by physical characteristics: percent frequency of MP by color (6A), shape (6B), and size (6C).

Tables

Table 2-1. Sampling Station Locations of Sediments collected from Narragansett Bay in July 2019. Sediment sizes classified using grainsize diameter (μm) 10% (D10), 50% (D50), and 90% (D90) cumulative percentile value.

Station Number	Location (Decimal Degrees)	Description	Water Depth (m)	D ₁₀	D ₅₀	D ₉₀
1	41.772233, -71.381617	Fields Point	3.3	6.57	27.9	127
2	41.721517, -71.359733	Conimicut Point Reach	4	6.68	51.7	340
3	41.659233, -71.389233	Rocky Point	3.8	78.1	240	556
4	41.572983, -71.303400	Arnold Point	5	5.14	22.3	494
5	41.594250, -71.370500	Hope Island	7.3	6.77	31.4	129
6	41.577283, -71.420767	Wickford Harbor	4.5	13.8	99.5	288
7	41.478333, -71.332950	Fort Adams State Park	6.5	6.64	56.9	339

Table 2-2. Percent recovery of internal spiked MPs from environmental samples.

Station	% Recovery			
	PE	PS	PET	Mean Recovery (PE, PS & PET)
1	37.9	18.8	62.5	39.7
2	114.7	53.3	43.5	70.5
3	93.9	113.5	93.3	100.2
4	80.0	50.0	28.6	52.9
5	115.0	81.3	26.7	74.3
6	43.9	80.0	23.8	49.2
7	85.7	86.8	42.9	71.8

Supplemental Information

The Hybrid Extraction Method

1. Procedure

1.1. Materials

- 5-gallon bucket (20 L)
- 45 μm (wire mesh, ASTM #325) and 250 μm (wire mesh, ASTM#60) brass sieves, 8-inch diameter
- 1 mm sieve, 8-inch diameter (wire mesh, ASTM #18)
- 2 mm sieve, with appropriate diameter size to fit over 5-gallon (20 L) bucket
- 47 mm 0.45 μm pore cellulose nitrate filters
- 2 glass funnels/sample
- 2 metal spatulas/sample
- Four 1 L separatory funnels/sample with stoppers and valves (glass, if possible)
- Vacuum filtration flask (1 L), filter base with stainless steel screen (47 mm), and filter funnel (250 mL)
- Four 47 mm 20 μm pore polycarbonate track etched (PCTE) filters/sample
- Four >47 mm petri dishes/sample
- >98% purity sodium bromide
- 2 laboratory wash bottles >500 mL
- Small crystallization dishes
- 30% reagent grade hydrogen peroxide (H_2O_2)
- Aluminum foil
- Deionized (DI) water system
- Laminar flow hood
- Hydrometer
- Ring stands (wood recommended if possible, as the stands will be exposed to sodium bromide solution and metal will likely rust)
- Laboratory vacuum system
- Laboratory drying oven (capable of 60°C)

1.2. Laboratory Conditions

1.2.1. Hybrid method extractions should be conducted in a laboratory environment that minimizes the use of plastics and prevents plastic contamination from airborne particles, ideally with HEPA filtration and negative air pressure.

- 1.2.2. All persons occupying the lab should avoid wearing of synthetic clothing and should wear a 100% cotton lab coat over their clothing to minimize contamination. Brightly colored lab coats allow researchers to track fiber contamination more easily.
- 1.2.3. Water sources (DI water) should be evaluated for microplastics prior to the start of this procedure.
- 1.2.4. Please read through the Quality Analysis (QA, Section 3) of this document prior to starting any experiments.

2. Sediment Collection

- 2.1.1. Minimize contamination of samples by avoiding synthetic clothing and minimizing proximal plastics to sampling operation. Note any plastics on boat during sampling (e.g. ropes, containers) to document possible contamination.
- 2.1.2. Collect sediments in a manner that preserves the sediment depositional sequence (top layer) (i.e., a Van Veen grab sampler).
- 2.1.3. Using a metal shovel or spoon, scoop at least 300 g of wet sediment from the top 5 cm of the sediment collection into a clean glass jar. Note: depth and location of the sample will depend on the objectives of the study.
- 2.1.4. Keep samples on ice until they can be refrigerated (4° C)
- 2.1.5. Homogenize the sample and aliquot 100 g wet samples into clean glass jars. Record weight. And store samples at 4° C

2.1.6. An air blank (a clean 47 mm, 20 μm pore PCTE filter in a clean glass jar) should be used during sediment collection. The jar should be opened every time a sample is collected and closed after sampling. The air blank will later be processed to account for airborne contamination of samples.

2.2. Experimental Procedure

2.2.1. Please refer to QA practices before beginning this procedure.

2.2.2. Density Separation Preparation

2.2.2.1. Make a sodium bromide (NaBr) solution with a density of $\rho=1.3\text{g}/\text{cm}^3$. Use a hydrometer to check density. Filter solution through a 0.45 μm cellulose nitrate filter to remove any particulates. Recheck density to make sure it hasn't changed. Fill a laboratory wash bottle with 400 mL of this solution.

2.2.2.2. Make a second NaBr solution with a density of $\rho=1.5\text{g}/\text{cm}^3$. Use a hydrometer to check density. Filter solution through a 0.45 μm cellulose nitrate filter to remove any particulates. Recheck density to make sure it hasn't changed. Fill a laboratory wash bottle with 300 mL of this solution.

2.2.3. Sample Preparation

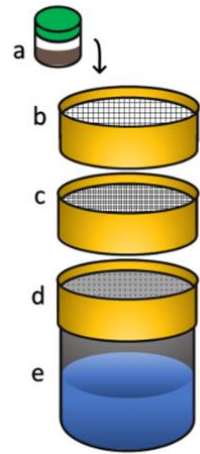
2.2.3.1. This sample preparation discards size fractions $>1\text{ mm}$ or $<45\mu\text{m}$. Place a large 2 mm sieve onto a 5-gallon bucket (e) to serve as a base for the stacked sieve procedure. This

allows for rinsate collection in the bucket and suspended solids to settle before disposing of the rinsate (Figure 2).

2.2.3.2. Place a 1 mm sieve (b) on top of a 250 μm sieve (c).

Place these sieves on top of a 45 μm sieve (d) and place the stacked sieves on top of the 2 mm sieve

and bucket. Pour sample (100 g wet) over the first stacked sieves and use DI water to gently rinse smaller debris through sieves.



2.2.3.3. Rinse original sample container and any tools used to help transfer materials (i.e., spatulas, glass jars) onto sieve a minimum

of 5 times to ensure complete transfer of jar materials onto sieve. Continue rinsing sample until water passing through sieves runs clear. Rinse down walls and sides of sieve very carefully, a minimum of five times. Note: It is critical to avoid losing sample in this transfer step.

2.2.3.4. Retain sediments on the 45 μm and 250 μm sieves.

Discard materials that passed through the 45 μm sieve and materials that did not pass through the 1 mm sieve. This leaves two sample size fractions: 45-250 μm and 251-1000 μm .

2.2.3.4.1. We chose these size classes to assist in the future processing of our samples with Raman spectroscopy. Different size classes may be optimal for other projects.

2.2.4. Density Separation (NaBr 1.3 g/cm³)

- 2.2.4.1. Be sure that the separatory funnels' stoppers are in the "closed" position before beginning. Using a metal spatula, scrape contents of each sieve into separate 1-L glass separatory funnels, using a glass funnel if necessary. Thoroughly rinse the sieve contents into one portion of the sieve with DI water, then tilt the sieve and use the 400 mL (1.3 g/cm³) NaBr solution to rinse remaining debris into separatory funnel. (Note - the only liquid entering the separatory funnel should be NaBr solution)
- 2.2.4.2. Rinse down the tilted sieve into the separatory funnel with the NaBr a minimum of five times to ensure complete transfer of all debris into the separatory funnel. Thoroughly rinse the sieve, spatula, and glass funnel into separatory funnel with NaBr solution so that all particles enter separatory funnel.
- 2.2.4.3. Pour the rest of the allotted 400 mL NaBr solution into the separatory funnel, retaining a small amount of NaBr (20 - 100 mL), so that the total amount of solution in the separatory funnel reaches ~300 - 380 mL. Stopper the separatory funnel and tilt to a 90° angle. Shake vigorously for three minutes, ensuring NaBr solution comes into complete contact with entire sediment sample.

2.2.4.4. Place separatory funnel upright in ring stand and use the remaining 20-100 mL NaBr solution to rinse the inside of the stopper and the inner walls of the separatory funnel. The goal is to remove any materials stuck to the inner wall of the separatory funnel so they are in the NaBr solution.

2.2.4.5. Let settle for two hours, or longer, until the sediment and debris are settled at the bottom of the separatory funnel. The water column should be mostly clear, with the exception of floating debris at the solution surface.

2.2.4.6. Perform these steps for both size classes (i.e., 45 – 250 μm and 250 – 1000 μm).

2.2.5. Vacuum Filtration

2.2.5.1. Sediments that have settled in the bottom of the separatory funnel after the two hours will be transferred to a new separatory funnel for the higher density treatment. Place a new 1-L separatory funnel in upright position and make sure funnel is closed.

2.2.5.2. Take the separatory funnel containing settled sediments and hold it over the new separatory funnel. Slowly open the valve at the bottom of the upper separatory funnel and empty the sediments into a new separatory funnel. Close the separatory funnel after the sediments have transferred so the

remaining NaBr solution and floating particles remain in the funnel. Retain both funnels for later use.

2.2.5.3. Assemble filter rig inside of a laminar flow hood to prevent airborne particle contamination. Place a clean 20 μm PCTE filter on a non-fritted glass filter base with a stainless-steel support screen attached to 1-L vacuum flask. Turn on the vacuum and slowly release remaining liquid/ supernatant from separatory funnel onto the filter.

2.2.5.3.1. Liquid salt solution fraction will not be further processed but may be retained for recycling purposes.

2.2.5.3.2. NaBr solution can be re-filtered through 0.45 μm filter and brought back up to desired density with anhydrous NaBr.

2.2.5.3.3. If not recycled, NaBr should be properly disposed of in accordance with State/ Federal regulations.

2.2.5.4. Use 1-L of DI water to thoroughly rinse the inside of the separatory funnel and stopper onto the filter paper, ensuring that all debris is removed from the funnel and transferred to filter. Some plastics may adhere to walls of vacuum apparatus; it is advised to rinse down the sides of apparatus as thoroughly as possible before removing the filter.

2.2.5.5. Carefully transfer filter to clean glass petri dishes and cover, being sure not to allow any debris to be lost from the filter.

2.2.5.6. Perform these steps for both separatory funnels.

2.2.6. Density Separation (1.5 g/cm³)

2.2.6.1. Fill the new separatory funnels with ~200 - 280 mL of 1.5 g/cm³ NaBr, retaining the remaining 20 - 100 mL.

2.2.6.2. Stopper the separatory funnel and tilt to a 90° angle. Shake vigorously for three minutes, ensuring NaBr solution comes into complete contact with entire sediment sample.

2.2.6.3. Place separatory funnel in ring stand and use remaining 20-100 mL NaBr solution to rinse the inside of the stopper and the inner walls of the separatory funnel. The goal is to remove any debris stuck to the inner wall of the separatory funnel. Let settle for two hours, or longer until clearly defined water column separates from sediment.

2.2.6.4. Perform these steps for both separatory funnels.

2.2.7. Vacuum Filtration

2.2.7.1. Slowly open the valve at the bottom of each separatory funnel and collect sediments in glass beakers. Sediment can be discarded according to State and Federal regulations.

2.2.7.2. Place a clean 20 µm PCTE filter on a non-fritted glass filter base with a stainless-steel support screen attached to 1-

L vacuum flask. Turn on the vacuum and slowly release remaining liquid/supernatant from separatory funnel onto the filter.

2.2.7.2.1. Liquid fraction will not be further processed but may be retained for recycling purposes.

2.2.7.2.2. NaBr solution can be re filtered through 0.45 μm filter and brought back up to density with anhydrous NaBr.

2.2.7.2.3. If not recycled, NaBr should be properly disposed of in accordance with State and Federal regulations.

2.2.7.3. Use 1-L of DI water to thoroughly rinse the inside of the separatory funnel and stopper onto the filter paper, ensuring that all debris is removed from the funnel and transferred to filter. Some plastics may adhere to walls of vacuum apparatus; it is advised to well rinse down the sides of apparatus before removing the filter.

2.2.7.4. Carefully transfer filter to clean glass petri dishes and cover, being sure not to allow any debris to be lost from the filter.

2.2.7.5. Perform these steps for both separatory funnels.

2.2.8. Oxidation

2.2.8.1. Samples that are heavily biofouled with organic matter may need to undergo oxidation prior to analysis.

2.2.8.2. Carefully move the filters to small crystallization dishes and gently pour 30% H₂O₂ over the filter, sufficient to completely submerge it.

2.2.8.3. Cover the dishes with aluminum foil and move to a 60°C oven for 2 hours.

2.2.8.4. Remove the dishes and refilter each sample onto a new clean 20 µm PCTE filter, rinsing the filter and dish thoroughly with DI water.

2.2.8.5. Move the filter carefully to the sample's previous petri dish.

2.2.9. Identification

2.2.9.1. This procedure generates four filters per sample (2 size fractions x 2 density solutions), which will allow isolated plastics particles to be analyzed by stereomicroscopy, Raman spectroscopy, and/or other types of identification procedures.

2.2.9.2. The hybrid method is focused on the extraction of MPs from sediment. It does not cover MP identification. Identification of extracted MPs will depend largely on available instrumentation, resources, and research questions.

2.2.9.3. For an example of what we have done, please see the main text (Cashman et al., 2021) of our MP identification workflow using Raman spectroscopy.

3. QA/QC

3.1. As noted earlier, we recommend running experiments in a laboratory environment that minimizes the use of plastics and contamination.

3.1.1. Laboratory space should be free of plastics to the greatest extent possible. This includes minimizing the existence of synthetic textiles, labware, and furniture.

3.1.2. Minimize any sources of potential dust or air contamination. For our laboratory, we installed a HEPA air handling system.

3.1.3. Laboratory spaces should be cleaned at the start and end of each day to ensure clean working space. Cleaning should be performed with 100% cotton tight weave cloths - no Kim Wipes or paper towels should be used.

3.1.4. All personnel that enter the laboratory should wear 100% cotton laboratory coats over their clothing to prevent synthetic fiber contamination. Minimal synthetic textiles should be worn in the lab to prevent contamination of samples.

3.1.5. Work should be performed under a laminar flow hood, and best practices implemented to minimize dust contamination from air handling systems.

3.1.6. Glassware should be washed a minimum of 5 times in deionized water. All glassware should be covered in aluminum foil after cleaning to prevent contamination. Labware used during experiments should be capped or covered in foil during waiting times to minimize dust contamination.

3.1.7. Sieves should be sonicated daily to remove debris and cleaned with a 100% cotton cloth.

3.2. An air blank (a clean 47 mm 20 µm pore PCTE filter in a petri dish) should be used for each day samples are extracted. The petri dish should be opened every time the samples are exposed to air. If air blanks are found to have more than 5 unknown particles (i.e., particles or fibers not originating from the cotton laboratory coats), the laboratory should be thoroughly cleaned, and new filters placed over the air handling systems.

3.3. A water blank should be performed once per 12 samples to determine sample contamination during processing. If water blanks are found to have more than 5 unknown particles (i.e., particles or fibers not originating from the cotton laboratory coats), the laboratory should be thoroughly cleaned, and new filters placed over the air handling systems.

4. TROUBLE SHOOTING

4.1 Fine sediments may not settle completely after 2 hours. Samples may need to settle for up to 12 hours to successfully clear water column and let particles settle to the bottom of the separatory funnel.

4.2 Fine grain sediments can clog filters during the vacuum filtration process; if this happens, multiple filters may be needed for one

sample. Use multiple filters to filter a sample so that the filters do not clog. These filters can then be combined following oxidation.

4.3 Samples with excessive organic matter may require additional oxidation time.

4.4 We experienced samples with >1 million MPs/ filter. In order to quantify high volumes of particles, we recommend scraping the contents of the filter into a 250mL volumetric flask and bringing it to volume with deionized water. The contents of the flask can be mixed and small aliquots (1mL increments) can be pipetted onto a new filter for analysis.

SI Figures

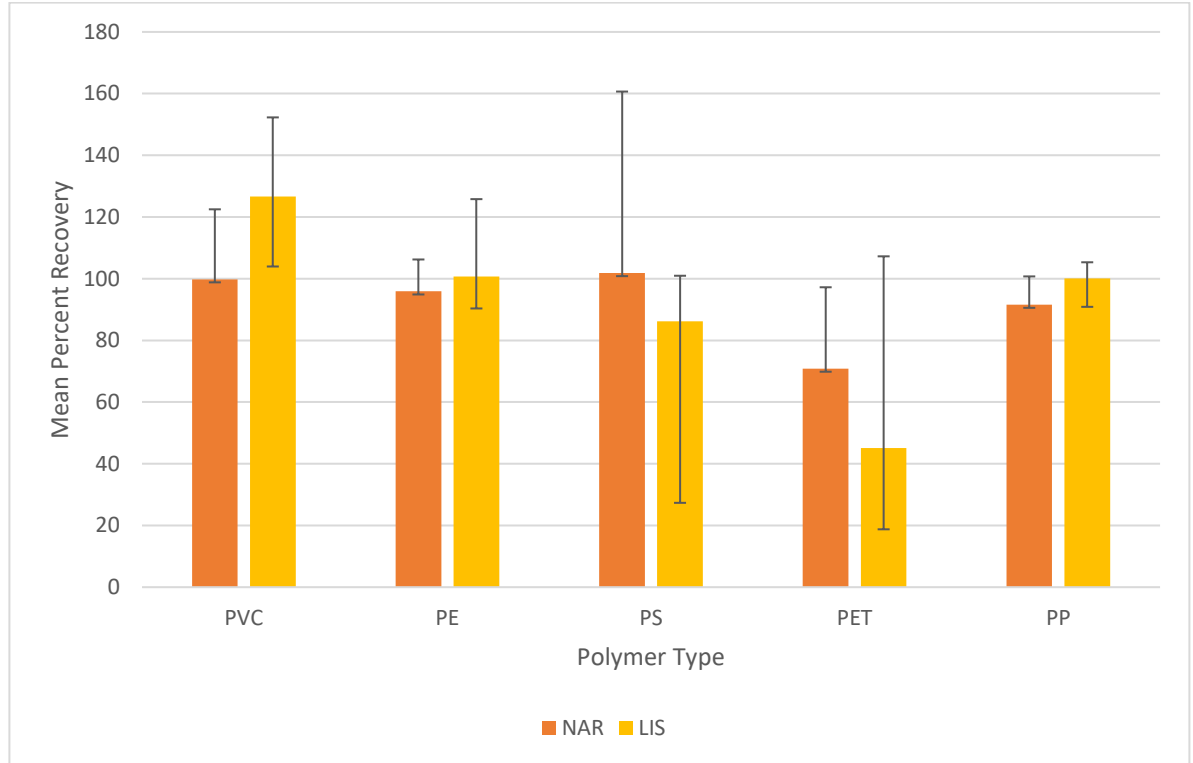


Figure 2-7. Mean percent recovery of MPs recovered from NAR and LIS sediments during method development. Error bars show relative standard deviation (RSD). N=5 for both sediment types.



Figure 2-8. Microscope picture of cellulose acetate fibers retained on filter from Station 4.

SI Tables

Table 2-3. Physical properties and sampling locations for representative sediments: Long Island Sound and Narragansett Beach. *Sediment sizes classified using grainsize diameter 10, 50, and 90% cumulative percentile value.*

	D ₁₀ (μm)	D ₅₀ (μm)	D ₉₀ (μm)	Water wt/wt%	Organic carbon %	GPS coordinates of collection location
Long Island Sound (LIS)	4.1	13.7	62.6	43	2	41° 7'N 72° 52'W
Narragansett Beach (NAR)	179.1	251.6	345.2	<1	0	41° 26'N 72° 27'W

Table 2-4. Properties of microplastics used in this investigation.

	Size (μm)	Density (g/cm^3)	Shape	Color	Source
Polystyrene (PS)	40	0.96	Sphere	Green	Cospheric
Polyethylene (PE)	96–106	1.13	Sphere	Blue	Cospheric
Polyvinyl chloride (PVC)	500–710	1.35	Fragment	Orange	PVC pipe
Polyethylene terephthalate (PET)	250–500	1.38	Fiber	Pink	Embroidery floss
Polypropylene (PP)	500–710	0.91	Fiber	Yellow	Rope

Table 2-5. Spiked and recovered MPs in method development to determine percent recovery.

	Spiked					Recovered				
	PVC	PE	PS	PET	PP	PVC	PE	PS	PET	PP
NAR-A	23	25	22	27	21	24	25	17	23	17
NAR-B	25	40	40	27	21	20	33	19	17	19
NAR-C	20	21	34	21	22	13	22	33	20	22
NAR-D	22	28	25	23	22	27	26	51	14	19
NAR-E	20	37	36	26	20	23	35	30	13	20
LIS-A	21	20	35	21	27	21	16	22	18	27
LIS-B	22	20	26	24	20	39	24	24	5	20
LIS-C	20	20	29	33	25	21	27	23	11	24
LIS-D	22	26	24	30	23	31	23	18	10	25
LIS-E	20	20	28	23	23	22	16	22	7	22

Table 2-6. Mean (M) and relative standard deviation (RSD) recoveries of MPs by sediment and polymer type.

		PVC	PE	PS	PET	PP
NAR	Mean	99.82	95.90	101.83	70.85	91.56
	RSD	22.68	10.34	58.83	26.37	9.19
LIS	Mean	126.64	100.69	86.18	45.13	100.07
	RSD	25.66	25.10	14.78	62.12	5.25

Table 2-7. Mean (M) recoveries of spiked MPs at each Station within Narragansett Bay.

Station	Spiked			Recovered			Percent Recovery %			Mean Percent Recovery %
	PG	PS	PET	PG	PS	PET	PG	PS	PET	PG, PS, & PET
1	29	32	16	11	6	10	37.9	18.8	62.5	39.7
2	34	15	23	39	8	10	114.7	53.3	43.5	70.5
3	33	37	15	31	42	14	93.9	113.5	93.3	100.2
4	20	24	21	16	12	6	80.0	50.0	28.6	52.9
5	20	32	21	23	26	4	115.0	81.3	26.7	74.3
6	41	30	22	18	24	5	43.9	80.0	23.8	49.2
7	21	53	14	18	46	9	85.7	86.8	42.9	71.8

Table 2-8. Number of synthetic particles found in air blanks and water blank for quality control.

		Coat Fibers	White Fragments	Black Fibers	Other
Air Blank	Hybrid	0	0	0	1
Water Blank	Hybrid	2	0	3	0
Air Blank 1	Region 1	0	0	0	0
Air Blank 2	Region 1	0	0	0	0
Air Blank 3	Region 1	0	0	1	0
Air Blank 4	Region 1	1	1	0	0
Air Blank 5	Region 1	0	0	1	0
Air Blank 6	Region 1	0	0	0	0
Air Blank 7	Region 1	0	0	3	2
Water Blank	Region 1	4	1	10	2

Table 2-9. Raw data from Raman Analysis.

To see SI Table 9, please view the published SI information below:
<https://doi.org/10.1016/j.marpolbul.2021.113254>

Chapter 3

Temporal Distribution of PFAS in Sediment Cores from an Urban River:

Relation to Water and Fish Tissue Data

Michaela A. Cashman^{1,2}, Anna R. Robuck³, Maya Morales-McDevitt⁴, Melanie Hedgespeth¹, Thomas B. Boving^{2,5}, & Mark G. Cantwell¹

¹ U.S. Environmental Protection Agency
ORD/CEMM Atlantic Coastal Environmental Sciences Division
27 Tarzwell Drive
Narragansett, Rhode Island, USA 02882

² University of Rhode Island
Department of Geosciences
9 E Alumni Avenue
Kingston, Rhode Island, USA 02881

³ Mt. Sinai Icahn School of Medicine
1 Gustave L. Levy Place
New York, New York, USA 10029

⁴ Oak Ridge Institute of Science Education
c/o U.S. Environmental Protection Agency
ORD/CEMM Atlantic Coastal Environmental Sciences Division
27 Tarzwell Drive
Narragansett, Rhode Island, USA 02882

⁵ University of Rhode Island
Department of Civil Engineering
9 E Alumni Avenue
Kingston, Rhode Island, USA 02881

This manuscript was prepared for submission to Environmental Science & Technology.

Introduction

Per- and polyfluoroalkyl substances (PFAS) are a diverse type of fluorinated, synthetic chemicals that became commercially available in the 1950s. PFAS possess many useful properties including durability, surface-tension reduction, and water repellence. These favorable properties have led to their use in a wide variety of products, including textiles, cleaning products, flame retardants, pesticides, and hydraulic fluids (Kissa 2001). The use and disposal of PFAS together with their environmental persistence and bioaccumulative properties have led to widespread global distribution in aquatic systems (Rayne and Forest 2009). The chemical structure of PFAS compounds, particularly the strength of the C-F bonds, makes them remarkably persistent and unlikely to fully degrade in the environment (Simon et al. 2019). PFAS adversely impact environmental and human health (Giesy and Kannan 2001). Exposure to PFAS have been linked to cancer, immune suppression, and endocrine disruption (Barry et al. 2013, Grandjean et al. 2012). The United States Environmental Protection Agency (EPA) has a Lifetime Drinking Water Health Advisory level of 70 ppt for combined PFOS and PFOA in drinking water. These values are used as the preliminary remediation goal (PRG) for groundwater and surface waters that are used as drinking water sources. There are currently no thresholds for PFAS in sediment, soils, or non-potable groundwater at the federal level.

Characterizing sites and sources of PFAS is important for identifying potential environmental and human health risk. However, historic PFAS releases predate accessible methods for their detection. Sensitive methods for detecting PFAS in the environment surfaced in the early 2000's and primarily focused on perfluorooctane sulphonic acid (PFOS) and perfluorooctanoic acid (PFOA) (van Leeuwen and de Boer 2007). The ability to detect PFAS in environmental matrices has always lagged behind PFAS production (Lorenzo et al. 2018). Current EPA methods for PFAS detection in non-potable water are routinely validated for upwards of 40 PFAS compounds with existing standards, which include perfluorinated acids, sulfonates, fluorotelomers, and poly/perfluorinated ether carboxylic acids (2019, Rosenblum and Wendelken 2019). These methods exclude thousands of known PFAS and their precursors/degradation products from identification. Since these persistent, bioaccumulative, and toxic compounds have entered the environment from many sources for decades, it is often difficult to characterize legacy PFAS sources.

To date, the US EPA has included >7,000 PFAS in the CompTox Chemicals Dashboard (Williams et al. 2019). Though this list is likely an underestimate due to the rapid development of novel PFAS and progress with identification of unknown compounds in the environment. Targeted analysis (TA) typically identifies and quantifies a discrete set of PFAS compounds using isotopic dilution methods. It offers a high-precision quantification of analytes but is limited by the necessity of standards and labeled analogs for

identification. TA excludes most novel PFAS and PFAS precursor compounds that are unavailable in the form of analytical reference standards, such as perfluoro alcohols and amides (Buck et al. 2011, Suthersan et al. 2016). Hence, existing TA methods underestimate PFAS concentrations in the environment. This means there are thousands of existing PFAS compounds with limited information regarding their structure or behavior present in the environment (Ateia et al. 2019). Detecting and possibly quantifying this pool of 'dark' PFAS requires additional analytical methods. In this study, conventional TA identified and quantified 24 PFAS compounds in sediment, water, and fish tissue. The Total Oxidizable Precursor (TOP) assay, Extractable Organic Fluorine (EOF), and Nontargeted Analysis (NTA) were employed to further characterize PFAS beyond TA.

PFAS precursors are often excluded in TA but may transform to terminal PFAS products through oxidation. The TOP assay uses chemical oxidation to convert PFAS precursors into detectable terminal PFAS compounds that are readily identifiable in TA (Houtz and Sedlak 2012). A comparison of perfluorocarboxylic acid (PFCA) concentrations before and after conducting the TOP assay indicates the presence of PFAS precursors in the sample (Göckener et al. 2020). An increase of detectable PFAS after oxidation with TOP reveals previously undetected PFAS present in a sample.

Methods that identify total fluorine can be used to characterize the fraction of fluorine accounted for in TA and estimate a mass balance (Spaan et al. 2020). In this study, EOF was used to quantify extractable fluorine from the

sediment and select water samples. The fluorine mass was calculated from targeted analysis and compared against recovered fluorine from the TOP assay and EOF to estimate undetected PFAS. NTA was then performed to identify additional PFAS compounds. NTA is a relatively new approach developed within the past decade that utilizes high resolution mass spectrometry (HRMS) techniques to characterize chemical compounds (Rajski et al. 2021). The first stage of NTA typically analyzes broad mass ranges of interest (e.g., m/z) in a mass analyzer and obtains a MS spectrum. In a coupled, second mass spectrometer (MS2), ions are fragmented before analysis to derive a MS2 spectrum. MS and MS2 spectra are then assigned to known or suspected PFAS through various means including use of Kendrick mass defect plots and mass features from the MS and MS2 scans. Currently, NTA is not as sensitive as TA, and at-best is referred to as “semi-quantitative”, meaning exact quantification is hard to obtain from environmental samples. While it is limited in its quantification abilities, NTA is a powerful tool for identifying novel PFAS. Local PFAS accurate mass libraries for NTA contain >4,000 known PFAS compounds and are easily modified to include other PFAS discovered during analysis. Therefore, NTA can provide a more comprehensive analysis of total PFAS in a sample.

Stable isotope analyses were included to further assess sediment composition and source. Stable isotopes are determined by the number of neutrons in a molecule’s nuclei. The isotope distribution ratios, known as isotope composition, change as elements cycle through biogeochemical

processes (Holtvoeth et al. 2019). Therefore, both carbon (C) and nitrogen (N) isotope composition and ratios can explain the potential sources of organic matter. Lighter isotopes can more quickly move through biogeochemical cycles, resulting in higher abundances of light isotopes. This can be seen in higher abundances of C^{12} vs C^{13} in the production of algal biomass, for example. This is also true for N isotope ratios (N^{14} vs N^{15}) (Bonn and Rounds 2010). Higher abundances of heavy isotopes are often indicative of anthropogenic inputs of carbon, such as synthetic chemical products which often contain highly variable C^{13} . In this study, the stable isotope composition of C and N within the sediment core are used to make inferences about the paleoenvironment.

One way to document historical records of PFAS deposition may be obtained from sediment cores with radiometric dates. Radiometric dating of well-preserved sediment cores can be a reliable technique for determining sediment deposition rates over long periods of time (Appleby and Oldfield 1992, Koide et al. 1973). A radiometrically-dated sediment core can be plotted against pollution concentrations to develop a depositional timeline (Donazzolo et al. 1982). The first radiometric dating technique was the analysis of lead (^{210}Pb). It is used for modern sediment dating (<150 years) that uses the fallout of ^{210}Pb radionuclide (Goldberg 1963, Krishnaswamy et al. 1971). A constant rate of supply (CRS) model is used to correlate ^{210}Pb deposition to a sediment accumulation rate (SAR). These models assume ideal conditions of sediment deposition and preservation (Appleby and Oldfield 1978). A SAR

model can be further constrained through the additional analysis of radiogenic Cesium (^{137}Cs) to develop a piecewise model. A global maximum of ^{137}Cs marks the bomb-derived fallout from atmospheric testing which peaked in 1963 (Tylmann et al. 2016). The sediment age-depth model was further constrained with analyses for chlorinated pesticides.

PFAS trends in sediment cores are described in several studies, including lake sediments (MacInnis et al. 2019, Mussabek et al. 2019, Yeung et al. 2013) and marine environments (Falandysz et al. 2012, Strivens et al. 2021, Zushi et al. 2010). This study uses targeted analysis of PFAS compounds in a radiometrically dated sediment core to determine temporal trends of PFAS deposition within the Pawtuxet River (Rhode Island, USA). The location for sediment coring is near a recreational fishing pier and is seasonally stocked for fish. Therefore, surface water and fish tissue were added to the list of analyses to broaden the understanding of PFAS located onsite. The United States has seen a recent increase in freshwater fish consumption, which increases the importance of characterizing their PFAS concentrations (Domingo 2016). Significant associations between fish consumption and increased PFOS serum concentrations in humans have heightened concern around PFAS in fish (Hansen et al. 2016, Yamaguchi et al. 2013). There are no current federal PFAS fish consumption advisories, but several states have developed their own.

This study presents a novel approach to investigating the temporal distribution of legacy PFAS in sediment cores obtained from a river with

suspected historic PFAS use. A combination of stable isotope and radiometric dating methods together with advanced PFAS identification and quantification tools along with analysis of fish tissue and surface water show temporal preservation of PFAS in the Pawtuxet River sediments, water, and biota. Much of the existing research on PFAS-contaminated sediments focuses on surficial sediments. This study gives a unique perspective of PFAS accumulation over time for both common and novel PFAS. Further, these data show the wide variation in PFAS distribution and abundance within sediment, water, and fish. This study employs novel scientific approaches to trace PFAS in riverine sediment columns through time in a historic industrialized area and therefore is of interest to managers of water and sediment quality or regulators of fish and wildlife in other areas with a long history of PFAS usage.

The Pawtuxet River

This study was conducted in an urbanized watershed along the southern branch of the Pawtuxet River in central Rhode Island, USA, which ultimately discharges into Narragansett Bay estuary (Figure 1). The Pawtuxet River has a rich history that includes over two centuries of manufacturing industry. Early success of the United States' Industrial Revolution led to the rapid development of water-powered mills along the Pawtuxet, supporting industries such as textile dyeing, printing, metal plating, and fabric manufacturing (Kulik 1980). While many of these mills are no longer production facilities, remnants of these processes are relics in the environment. Much of the Pawtuxet River's legacy contamination is attributed

to manufacturing facilities along the river. Some of the textile and dyestuff facilities have been directly linked to point source discharge of metals, polycyclic aromatic hydrocarbons (PAHs), and other contaminants (Latimer et al. 1988, Nixon and Fulweiler 2012). Nicknamed the “Velvet Village”, these mills were once home to many textile and dyestuff manufacturing companies which included Providence Manufacturing Company, Crompton Corporation, Clariant Corporation, Hoescht Chemicals, Metro Dye Stuffs, and Concordia Fabrics. Several of these facilities created products that are suspected to have used PFAS in their production, including water repellent textiles and dyes (Times 1991) . Clariant was once a known world leader in PFAS chemical production and was subject to the voluntary PFOA phaseout ((ATSDR) 2018). Many of the mills along the Pawtuxet River have been repurposed over the years for the manufacturing of goods including pharmaceuticals, textiles, inks, and flame suppressants. Previous measurements of Narragansett Bay waters have shown persistent levels of PFAS entering from the Pawtuxet River but were unable to identify their sources.

Methods

The primary objective of this research was to identify PFAS deposition in riverine sediments. Three sediment cores were taken from a dammed mill pond on the lower Pawtuxet River (Figure 1) in October of 2019 using a piston corer with a 68 cm ID polycarbonate core barrel (Aquatic Research Instruments, Idaho, USA). The coring site was determined based on historic land-use observations and accessibility by boat. All three cores were taken

from the same approximate location to minimize spatial variability. Sediment cores were extruded and capped below the water surface and transported to the lab to preserve stratigraphy. The cores were sub-sectioned, homogenized, freeze-dried, and stored at 4 °C prior to analysis. Sub-sectioned sediment samples underwent stable isotope analysis, radiometric dating, grainsize, and PFAS analyses. PFAS analyses included targeted and nontargeted PFAS analysis. Other PFAS proxies included the TOP Assay and EOF analysis.

Stable Isotope & Grain Size Analysis

Isotopes $\delta^{15}\text{N}$ and $\delta^{13}\text{C}$ were measured alongside elemental nitrogen and carbon in sediments following the methods of Hubeny et al. (2015). Briefly, dried sediments were ground, acidified, and weighed into tin capsules and analyzed with an Isoprime 100 Isotope Ratio Mass Spectrometer coupled to a Micro Vario Elemental Analyzer (Elementar Americas, NJ, USA). Analyses were conducted using continuous-flow elemental analysis/ isotope ratio mass spectrometry. Results from these analyses include isotope abundance and % C and N for sediment samples. Select sediments underwent grainsize analysis. Sediments were analyzed in triplicate with a Malvern 3000 Grainsize Mastersizer (Malvern, UK).

Radiometric Dating

Radiometric dating of sediment included ^{210}Pb and Cs^{137} was conducted by the Science Museum of Minnesota (St. Paul, Minnesota). Cesium activity was measured using an Ortec-EGG (Ortec, Oak Ridge, TN)

High Purity, germanium crystal well, photon detector coupled to a digital gamma-ray spectrometer. ^{137}Cs activity was counted for $7\text{-}20 \times 10^4$ seconds and quantified using GammaVision software (Ortec, Oak Ridge, TN). ^{210}Pb samples were spiked with a calibrated ^{209}Po standard to act as a yield tracer. Activity was measured from $1\text{-}6 \times 10^5$ seconds with ion-implanted surface barrier detectors and an Ortec alpha spectroscopy system. Unsupported ^{210}Pb was calculated by subtracting supported activity from the total activity measured at each level, whereas supported ^{210}Pb was estimated from asymptomatic activity at depth. Sediment accumulation rates were estimated from a constant rate of supply (CRS) piecewise model that incorporated excess ^{210}Pb activity with ^{137}Cs (Abril 2019, Abril 2020). The piecewise CRS average was calculated using the R statistical software package Serac (Bruel and Sabatier 2020) using the 1963 peak in ^{137}Cs activity as a forced age.

Chlorinated Pesticides

The sediment age-depth model was further constrained with analyses for chlorinated pesticides. Sediments were extracted following a QueCHERS method (Lesueur et al. 2008). Freeze-dried sediment samples from 84-102cm were weighed out to 2g and spiked with 25 ng of the internal standard (IS), Expanded POPS Pesticides Cleanup Spike (^{13}C) from Cambridge Isotope Laboratories (Cambridge, MA, USA). Sediments were extracted with 30 mL acetonitrile (>99%, Fisher Scientific, MA, USA), vortexed for 1 minute (Vortex Genie 2, Cole Parmer, IL, USA), and sonicated for 30 minutes (Branson

5510, Fisher Scientific, MA, USA). Extracts were concentrated to 1 mL and analyzed using an Agilent 6890 gas chromatograph mass spectrometer (GC-MS) equipped with a 5937 Mass Selective Detector and a DB-5 MS 60 m capillary column (Agilent Technologies, Wilmington, DE) in SIM mode.

PFAS Targeted Analysis

Freeze-dried sediment was weighed out to 2 g and spiked with 10 ng of internal standard MPFAC-24ES (Wellington Laboratories, Ontario, Canada) for targeted analysis. Sediments were extracted twice with basic LC-MS grade methanol (>99.5%, Fisher Scientific, MA, USA), vortexed for 1 minute (Vortex Genie 2, Cole Parmer, IL, USA), and sonicated for 30 minutes (Branson 5510, Fisher Scientific, MA, USA) prior to centrifugation for 10 minutes at 5,000 RPM (Sorvall RC 6 Plus Superspeed Centrifuge, Thermo Scientific, MA, USA) to separate solids. Extracts were passed through a Supelco Envi-Carb SPE cartridge with 500 mg bed weight and concentrated to 1 mL of methanol extract. Extracts were diluted as needed to 50:50 water:methanol containing 2mM ammonium acetate buffer. All deionized water was pre-filtered through a Milli-Q water system with a LC-Pak polisher (EMD Millipore, MA, USA).

Isotopically labeled internal standards and native standards were obtained from Wellington Laboratories (Guelf, Ontario, CA). Standards were prepared in a range from 0 to 100 ng/mL for calibration. Twenty-four PFAS compounds (SI Table 2) were analyzed using targeted analysis which included perfluoroalkyl carboxylates (PFCAs, C₄₋₁₂), perfluoroalkane sulfonates (PFASAs, C₄₋₁₄) perfluorooctane sulfonamides, perfluorooctane

sulfonamidoethanols, perfluorooctane sulfonamidocetic acids, and three fluorotelomer carboxylates. All PFAS were analyzed on a Waters Acquity Liquid Chromatograph Mass Spectrometer (LC-MS/MS) using a BEH C18 column (Waters, MA, USA). Compound-specific Minimum Detection Limits (MDLs) were derived for sediment and water samples (SI Table 3). Duplicate samples were analyzed for select sediment, water, and fish tissue for quality assurance (SI Tables 4 & 5). Sample duplicates were within $\pm 30\%$ of the expected value for each analyte. Evaluation of matrix interference was determined by the analysis of a spiked solvent or laboratory reference sediments for PFAS quantification (SI Table 4). For this study, Long Island Sound (LIS) sediment was used as reference sediment (Mecray and ten Brink 2000). All samples were injected twice on the LC-MS/MS to monitor for injection variability. Duplicate injections were within $\pm 40\%$ for each analyte. Sample blanks consisted of PFAS-free media spiked with internal standard to assess laboratory contamination. LIS sediment, methanol, and deionized water (Milli-Q grade) were used for sample blanks. Select sediment and methanol samples were also spiked with native standards as a positive control. All analytes were calibrated on the LC-MS/MS using a 10-point calibration curve with a $R^2 \geq 0.99$. A set of two calibration verification (CV) standards were run at the beginning and end of the samples to ensure system performance. Sample blanks were run between each duplicate injection to minimize carry-over between sample injections.

TOP Assay

TOP Assays were conducted following a modified method from Houtz & Sedlak (2012). Freeze dried sediment samples were weighed out to 2 g and extracted as described above. Extracts were passed through a Supelco Envi-Carb SPE cartridge (500 mg bed weight) and evaporated using a Turbovap LV (Biotage, Stockholm, Sweden). Aqueous solutions of potassium persulfate and sodium hydroxide (>99% Fisher Scientific, MA, USA) in milli-Q water were added to evaporated samples. Samples were then transferred to a heated water bath (Memmert, WI, USA) at 80°C for 8 hours of oxidation. Samples were neutralized with 6M hydrochloric acid (Thermo Fisher, MA, USA) post-oxidation to quench the reaction. Oxidized samples underwent solid phase extraction (SPE) through a packed Waters WAX cartridge (150mg, 6cc), evaporated to dryness, and reconstituted to 1 mL of 50:50 water:methanol containing 2 mM ammonium acetate buffer. All TOP samples were run on a Waters Acquity LC-MS/MS as described above.

Extractable Organic Fluorine

EOF analysis was performed by Bureau Veritas Laboratories (MI, Canada) following CAM SOP-00812/2. Freeze dried sediments were homogenized and stored in polypropylene centrifuge tubes. Samples were extracted with 70:30 methanol:water + 0.5% ammonium hydroxide, vortexed, sonicated and centrifuged to remove solids. Water samples were extracted by SPE using a method-specific carbon cartridge (Nitto Seiko Analytech). The supernatant from extracts were diluted with PFAS-free DI water and analyzed

with a Thermo Scientific combustion ion chromatography total organic fluorine (TOF) system (Wilmington, Delaware, USA). Samples were analyzed with Mitsubishi NSX-2100 software and post-processed using Thermo Fisher Chromeleon software.

Nontargeted Analysis

Select undiluted methanol extracts from targeted analysis were analyzed using nontargeted analysis. Methanol extracts were reconstituted to 0.5 mL of 50:50 water:methanol containing 0.1% Ammonium acetate. Samples were then analyzed on a Thermo Orbitrap Fusion High Resolution Mass Spectrometer in negative electrospray ionization mode (ESI⁻). Each sample run included full MS scans and data dependent MS² scans. Features from MS and MS² scans were post-processed using Compound Discoverer software (Thermo Fisher Scientific, MA, USA), and derived features were filtered by method workflow described in Nason et al. (2020). Sample screening within Compound Discoverer included full MS scans, data dependent MS/MS (MS²) scans, and all ion fragmentation scans within a singular injection. Compound libraries ChemSpider and mzCloud were used along with the “Compound Class Scoring” feature to identify additional PFAS compounds within select sediment samples. Baseline filters were used to select compounds with standard mass defects <0.1 or > 0.75 , or those identified by mass list matches. From there, potential PFAS compounds were manually sorted through to eliminate poor matches. Fluoromatch software (Innovative Omics, FL, USA) was used to automate data files for chromatographic peak picking,

blank filtering, and PFAS annotation (Koelmel et al. 2020). A Kendrick Mass Defect (KMD) plot was calculated for each sediment sample.

Water and Fish Matrices

Several water and fish samples were opportunistically collected from the coring location to compare against the sediment samples. Water samples were collected in HDPE bottles and stored at 4°C until analysis. Samples were filtered through pre-combusted GF/F glass fiber filters (0.7 µm, 47 mm). Samples were extracted with Oasis WAX SPE (500 mg; Waters Corp; Milford MA) (Nakayama et al., 2010) and concentrated to 1 mL of 50:50 water:methanol with 2mM ammonium acetate. All five fish were *Lepomis macrochirus* (blue gill). Fish samples were stored at -20°C until analysis. Fish muscle was dissected, homogenized, and freeze dried. Freeze-dried samples (500mg) were spiked with 10 ng of internal standard for targeted analysis. Tissues were extracted twice with basic methanol, vortexed, and sonicated prior to centrifugation to separate solids. Extracts were passed through two stacked Supelco Envi-Carb SPE cartridges (250 & 500mg bed weight) and evaporated using a Turbovap LV. Samples were concentrated to 0.5 mL of methanol extract and diluted as needed to 50:50 water:methanol containing 2 mM ammonium acetate buffer. Fish and water sample extracts were then analyzed for PFAS using the same TA and NTA methods as described above.

Results

Stable isotope analysis revealed changes in both elemental and isotopic C and N throughout the sediment core (Figure 2). At or near the core

surface, $\delta^{13}\text{C}$ had a value of -28 ‰ to -29 ‰, which are typical of soils and particulate organic matter in freshwater systems (Peterson and Fry 1987). The $\delta^{13}\text{C}$ values increased with depth to -26 ‰, indicating higher ratios of ^{13}C isotopes. $\delta^{15}\text{N}$ values were also typical of freshwater systems, with a value of 4 ‰ at the surface and a range of 1 to 3 ‰ between 5 and 90 cm below the surface. Both elemental % C and % N were highest at about 60 cm depth. Sediment grainsize was analyzed in triplicate and averaged for each sediment (SI Table 6). Grainsize values are reported by particle size distribution for d_{10} , d_{50} , and d_{90} percentiles. The values ranged from 10-14, 29-46, and 119-180 μm , respectively. All sediments were classified as sandy silts or silt loams based on grainsize.

Sediment geochronology was determined with a CRS model fit with unsupported ^{210}Pb activities (Appleby and Oldfield 1992) and through the time-stratigraphic peaks of ^{137}Cs (Bopp et al. 1982) for the approximate sediment accumulation rates (SI Figure 6). Initial results from the ^{210}Pb model approximated a sediment accumulation rate (SAR) of 9.87mm yr^{-1} ($r^2=0.857$). The peak abundance of isotope ^{137}Cs was used as a marker of the 1963 fallout peak of nuclear weapons testing (NWT). Peak ^{137}Cs was between 65-75 cm, so the middle depth (70.5 cm) was used to approximate the NWT of 1963. Further analyses of pesticides revealed the introduction of dichlorodiphenyl trichloroethane (DDT) at 90 cm (SI Table 7). This depth was used as a second forced age (1939) in the CRS model. These data were incorporated into a CRS model to yield an average accumulation rate of 9.99

mm/yr. This proposed sediment accumulation rate was used to develop an age-depth model that converts sediment depth to an approximate year in time.

Targeted analysis of PFAS in the sediment core revealed 18 of the 24 targeted PFAS compounds present throughout the sediment core. The compound classes encountered were: perfluorocarboxylic acids (PFCAs), perfluoroalkane sulfonic acids (PFSA), and sulfonamides (FOSAs) (Figure 3, SI Figure 7, SI Table 4). The sediment core surface had a Σ PFAS concentration of 5 ng/g. With depth, it steadily increased to a peak of 50 ng/g PFAS at 51 cm (SI Figure 7 & 8). Below that level, concentrations trended downwards. Greater than 51% of all detectable PFAS were PFCAs in each core subsection (\bar{x} =73%). Long-chain PFAAs include PFCAs with eight or more fully fluorinated carbons or PFSA with six or more fully fluorinated sulfonates (Buck et al., 2011). Further analysis of PFCAs shows that long-chain PFCAs ($C_N \geq 8$) accounted for >35% of all accounted PFCAs (\bar{x} =76%) (Figure 3). Perfluorododecanoic acid (PFDoA, C_{12}) was the most abundant PFCA found in the sediment core from 0-60 cm.

Surface sediment (0-3 cm), fish and water data from targeted analysis are shown in Table 1. Ten PFAS compounds were detected in the surface sediments, ranging from 0.12-1.68 ng/g dry weight. The most abundant PFAS compound detected in the sediment was PFOS (1.68 ng/g). Ten PFAS compounds were detected in fish muscle samples, ranging from 0.02-4.7 ng/g wet weight. The most abundant PFAS compound detected in fish was PFOS (\bar{x} = 4.7 ng/g), which accounted for >50% of the total detected PFAS (SI

Figure 9, SI Table 5). Thirteen PFAS compounds were detected in water samples, ranging from 0.44-18.07 ng/L. The most abundant PFAS in water were PFHxA (15.17 ng/L), PFOA (17.92 ng/L), and PFOS (18.07 ng/L). Sum Σ PFAS concentrations in surface sediment, fish muscle, and water samples were 5.46 ng/g, 9.06 ng/g, and 102.28 ng/L, respectively. Several water samples were taken upstream and downstream of the coring site for PFAS analysis (SI Figure 10). These samples were taken in January of 2021, and display lower concentrations than samples collected in October 2020 (Table 1).

Results from the TOP Assay and EOF are compared in Figure 4 and SI Tables 8 & 9. Compounds identified in targeted analysis pre-and post-TOP Assay were converted to fluorine (F) contribution (ng/g) for comparison with EOF data. Total F abundance from the targeted analysis and TOP Assay are shown together on both graphs. Increases in total F were not uniform across the sediment core. Select samples saw a decline in F, suggesting a decrease in compounds readily identified in the analysis of post-TOP samples. Total F abundance increased in post-TOP samples near the core surface until the early 1970s. The increase in F post-TOP signifies the successful conversion of PFAS precursors into detectable terminal PFAS via oxidation. This suggests the presence of undetected precursors in the sediment.

EOF analysis was conducted for the entire sediment core (Figure 4) . Most of the core subsamples returned below the fluorine MDL value of 200 ng/g and are not shown. Samples with detectable fluorine had EOF values that

ranged from 200-710 ng F/g sediment. In a comparison of total F from targeted analysis to EOF, a percent increase of F ranged from 64-628 % (\bar{x} =313%). The highest % increase was seen at 87 cm depth (1975). Peak F abundance detected in EOF correlates with peak F abundance detected in the TOP Assay. These results further confirm the presence of PFAS precursors within the sediment. EOF analysis was also conducted on a singular surface water sample. The sum of F from the targeted water sample was 65.19 ng F/L, or 3.43×10^{-6} mM/L. Total F from EOF showed F concentrations 24 times higher than what was reported in targeted analysis, with 1.6 μ g/L F.

Nontargeted analysis is ongoing and will continue into the next several years, but fluorinated compounds from select samples were identified with characteristic insource fragmentation patterns from MS and MS2 features. These compounds were selected with a Kendrick formula difference of CF_2 (Figure 5). Initial data from the Kendrick Mass Defect plot indicate the probability of several PFAS compounds. It is noteworthy that several suspect PFAS compounds have high molecular weights, >1,000 Da.

Discussion

Sediment PFAS

This research started as a proof-of-concept to determine whether PFAS deposition was preserved within a sediment core from a river influenced by historic PFAS use. The results from targeted analysis of PFAS within the radiometrically dated sediment core sparked further interest in undetected

PFAS present at this site. PFAS are found within the sediment record, the surface water, and fish within the Pawtuxet River. The observed temporal trends of PFAS in the Pawtuxet River sediment core correlate with suspected PFAS production history, confirming the radiometric dating results (Mueller and Yingling 2017). Some of the earliest known uses for PFAS include textile and dye manufacturing. Results from the targeted analysis show the highest abundance of PFCAs occurring in the late 1960s through the 1970s. This coincides with the high production of textile dyes and pigment being produced in nearby mills at the time. The PFCAs within the sediment were dominated by long-chain compounds. Long-chain compounds are often the dominant PFCAs in sediment, as their sorption to organic carbon increases with increasing CF_2 groups (Ahrens et al. 2010, Higgins and Luthy 2006). Our results confirm this i.e., PFDoA is consistently seen throughout the sediment core. This compound's largest concentration increases are seen in 1952 and 1972. Its sediment concentration tapers off in the 1980s, but it remains at low levels throughout the core. The largest percent increase of PFAS accumulation happens in 1972 (SI Figure 8). At this timepoint, we see the introduction of compounds PFBA, PFPeA, PFHpA, PFOA, PFNA, PFOS, N-MeFOSAA, PFDS, and PFTeDA. Most of these compounds continue to increase in concentration until 1975. In 1978, most of these compounds decrease in concentration, with the exception of PFOS and N-MeFOSAA. PFOS increases in deposition again in 2001, 2009, 2012, and 2021. Other compound increases include PFDS in 1987, PFNA in 2009, and EtFOSAA in 2015.

Long-chain PFCAs are commonly the dominant PFAS class found in textile manufacturing (Zhu and Kannan 2020). This is particularly true for textiles produced prior to the voluntarily C₈ phaseouts. There are three mills upstream of the coring site with potential PFAS use in their manufacturing history, Crompton Mills, Quidnick Mills, and Anthony Mills. These mills were all used to produce chemical pigments and dyes for textiles in the 1950s-80s. Several companies within these mill sites, including Hoescht, Clariant, and Crompton Dyes discharged wastes directly to the Pawtuxet River. The patterns of PFAS increase and decrease potentially correspond to the timeline of dye production in the area. Many of the mills closed in the early 1980s due the falling demand for American-made textiles. This timing could possibly explain the decrease in PFAS in the core in the following years (Figure 3).

Another known source of PFCAs is the degradation of precursor compounds such as fluorotelomer alcohols (FTOHs) and perfluorooctanesulfonyl fluorides (POSF) (Ellis et al. 2004, Martin et al. 2006, Rhoads et al. 2008). Precursor degradation could be one source of long-chain PFAS in the sediment, especially in the top of the core. This would help explain the presence of long-chain PFAS within the core despite their production phaseout. However, the proximity of several manufacturing facilities in the study area makes it difficult to ascertain the exact source of these compounds, Long-chain PFCAs, particularly PFDA (C₁₀), were detected in sediments that predate the commercial manufacturing of PFAS (Figure 3).

These findings are consistent with research from Kabiri et al. (2021) that highlight the propensity of long-chain PFCAs to mobilize in sediments.

Long-chain compounds were voluntarily phased out of production by several PFAS manufacturers through the US EPA 2010/2015 Stewardship Program (2010/2015 Stewardship Program). The production of PFOS in the United States terminated in 2002, so we hypothesized a decline in PFOS accumulation in the past two decades. Instead, an upward trend in PFOS deposition is seen in the upper 15 cm of the core, which corresponds to year 2009-2021 (SI Figures 7 & 9, Table 5). This suggests that despite the end of PFOS production, PFOS is still mobile in the environment decades later. One probable explanation for this is the degradation of PFAS precursors into terminal PFAS such as PFOS. We also see high levels of PFOS in the river water and fish (18.07 ng/L & 4.7 ng/g), indicating that these compounds are remain relevant and pose potential risks, despite their production phaseout. This phenomenon is seen across the US. National fish tissue monitoring data for the US demonstrate an average of 10.7 ng/g within freshwater fish (Stahl et al. 2014). Another possibility is that compounds such as PFOS and PFOA are degradation products of other long-chain PFAS. Studies such as Koch et al. (2009) show that PFOA can be a degradation product of fluorotelomer-based acrylate polymers.

Water & Fish Matrices

Understanding historic PFAS deposition is critical for assessing environmental risk. Bioaccumulation potential increases with increasing

perfluoroalkyl chain length (Armitage et al. 2009, Labadie and Chevreuil 2011), making long-chain PFAS of great concern. Surface water samples did not exhibit PFAS with a carbon chain length $>C_{10}$ in targeted analysis. This is likely due to the phaseout of long-chain PFAS, and preferential partitioning to sediment (Dassuncao et al., 2019). However, several long-chain PFAS compounds were present in the fish muscle. Excluding PFOS, the three most abundant PFAS found within the fish muscle were PFTTrDA, PFDoA, and PFTeDA. These long-chain compounds would be missed if analysis was restricted to water samples. This study was limited to fish muscle, but it is speculated that higher concentrations may be found within the fish's blood liver, and kidneys due to preferential protein partitioning. These results are consistent with other studies which highlighted high levels of long-chain PFCAs in fish (Fujii et al. 2015, Goodrow et al. 2020). The uptake of PFAS into fish is likely from dietary uptake, as long-chain PFAS compounds present in the sediment and fish were not found in the water. Possible exposure could be from the consumption benthic organisms such as macroinvertebrates. Bluegill are known benthic feeding fish and are often consumed by larger fish including largemouth bass (Lake et al., 2001). It is likely that these fish higher trophic level fish will have higher PFAS accumulation and higher bioaccumulation potential in humans consuming PFAS-contaminated fish (Conder et al. 2008).

Surface water samples collected at the coring site in October 2020 contained $>100\text{ng/L}$ PFAS (Table 1). These concentrations are an order of magnitude higher than reported for the Pawtuxet River at the mouth of

Narragansett Bay where dilution effects can explain lower concentrations (Zhang et al. 2016). The PFAS compounds found in site water were predominantly short-chained PFASs and PFCAs, with no detections of $>C_{11}$ PFAS. These PFAS likely stem from a multitude of sources, which include several upstream wastewater treatment plants, surface runoff, and existing industries (Zhang et al. 2016). Another series of water samples were collected in January 2021. Surface water concentrations of PFAS were substantially lower ($\bar{x}=12.1$ ng/L) at the coring location (SI Figure 10). Sampling locations 1, 3, and 4 were relatively similar in concentration, but sampling site 2 was nearly double in concentration ($\bar{x}=21.8$ ng/L). It is unclear why water samples from Site 2 were contained higher levels of PFAS, but it is possible that there are other PFAS contributors upstream of the coring site. Across all four sampling sites, the most abundant PFAS were PFOS and PFCAs (C_{4-8}). Elevated levels of PFNA were seen at Site 4, the most downstream site. This is the only site that receives water from the Upper Pawtuxet River.

TOP & EOF

The interpretation of the TOP Assay results is not straightforward. Some PFCAs increased in concentration post TOP assay, which would indicate the presence of PFAS precursors, but the concentration of other PFCAs decreased. A possible explanation could be that the TOP oxidation converted many PFAS into ultra-short ($<C_4$) chained PFAAs, such as trifluoroacetic acid (TFA). TFA and other short-chained PFAS were not quantified by targeted analysis, but likely make up a significant contribution to

the total fluorine found in aqueous samples (Yeung et al. 2017). Other factors could include matrix temperature, pH, or interference with organic carbon and other chemicals (Al Amin et al. 2021). For this reason, the TOP Assay results were taken as an indication of increase in total F, rather than by specific compound increase. Results from both the TOP Assay and EOF showed that there were significant amounts of F not captured by targeted analysis. This speaks to the small portion of PFAS quantified in targeted methods, and the need to expand analyses to capture more PFAS. Initial results from NTA suggest the presence of several ultra-long chain (>C₁₄) PFAS based on suspect molecular weight. Future work to identify PFAS detected by NTA will likely close the F mass balance deficit seen in the targeted analysis versus EOF. One of the compounds that increased in post-TOP assay was perfluorooctane sulfonamide (FOSA), which could be the oxidation product of EtFOSA (Plumlee et al. 2009). Another interesting consideration is the large increase of 6:2 fluorotelomer sulfonate (FTS) in the sediment post-TOP assay. While 6:2 FTS is not a known end-product of oxidation, it can be further oxidized to other terminal PFAS. It's large presence in the sediment may therefore suggest incomplete oxidation.

A potential explanation for the increase of F at the core surface is the production of fluorinated pharmaceuticals upstream of the coring site. Fluorinated pharmaceuticals are often overlooked in PFAS analysis, but fluorinated pharmaceuticals make up over 20% of pharmaceuticals (Bégué and Bonnet-Delpon 2006). Fluorinated pharmaceuticals, such as paroxetine,

were produced by Rhodes Pharma in the late 20th Century (Adegbite-Adeniyi et al. 2012). The Crompton Mill site is also a known former producer of Teflon, or polytetrafluoroethylene (PTFE). And the Anthony Mills are known producers of fluorinated synthetic fibers including Kevlar. These compounds are not detectable in current targeted analyses, but could contribute to a portion of the detected F within modern sediments. Similarly, inverse ratio of $\delta^{15}\text{N}$ to C:N ratios shows slightly elevated abundances of C throughout the core, which we speculate this is related to the high levels of organic legacy contaminants (e.g.- PAHs, PCBs) identified within the core. The highest $\delta^{15}\text{N}$ values were detected at the core surface, which is commonly attributed to the most oxygenated part of a sediment profile. $\delta^{15}\text{N}$ values increase to upwards of 5 ‰ at the 80 cm core depth. The values seen within the Pawtuxet are within standard ranges (Fry 2006). The $\delta^{13}\text{C}$ values range from -28.96 to -26.18 ‰. The most abundant $\delta^{13}\text{C}$ is present below 90 cm, whereas the lowest $\delta^{13}\text{C}$ values are near the sediment surface (5-15cm). Sediment C/N ratios ranged from 13.4 to 20.3. From 0-55 cm depth, they ranged between 15.9-17.9, then declined from 55-75 cm, to sharply rise at 85 cm. The increase of C/N and $\delta^{15}\text{N}$ values at 85 cm is likely a result of a change in sediment parent material.

Conclusion

Site-specific characterization of PFAS is an important step towards predicting PFAS fate and risk. Temporal analyses of PFAS in sediment, fish, and water within the Pawtuxet River display a complex assembly of PFAS

compounds. Many prior site assessment studies focus on PFAS in surface waters. But as seen here, there is large variability in PFAS composition among sediment depths, water, and biota. Several long-chain PFAS compounds that were phased out of production many years ago were still detected in the sediment and biota. These compounds pose active risk to the environment, despite legislation to ban production. Select PFAS compounds are known to have been present in the environment for several decades based on the analysis of a radiometrically dated sediment core. These PFAS likely correspond to dye production in close-by former mills. But other PFAS presence cannot be explained by manufacturing history, such as PFOS. This suggests that legacy dye mills are not the only source of PFAS in the Pawtuxet River. This is evident from upstream analysis of surface waters that showed elevated levels of PFAS. These PFAS may be entering the Pawtuxet from upstream mill sites, but they may also be the result of nonpoint sources such as runoff or atmospheric deposition. Additional PFAS that were not detected at the coring site were found downstream. This also suggests additional PFAS contributions from other sites along the Pawtuxet River. Further spatial analyses would be needed to define these sources. Ongoing research includes the tracking of PFAS in suspended solids downstream of the coring site to determine the mobility of PFAS-contaminated sediments. These data will assist in answering how contaminated legacy sites contribute to the overall loading of PFAS into receiving waters such as the Narragansett Bay Estuary.

The location for this study was chosen for its proximity to historic dye production mills, but a nearby fishing pier and boat ramp highlight the current recreational usage of these legacy sites. Brownfields such as the Crompton Fishing Pier are often converted to recreational sites for expanded public access. This study underscores the importance of understanding and evaluating PFAS pollution in recreational sites as it is imperative to protecting ecosystem and human health. PFAS were found in every sample extract for this study. And tests such as EOF and NTA indicate that there are likely many more PFAS on site than we have detected. There are no current surface water or fish consumption advisories for PFAS in Rhode Island. But consideration should be given to multiple matrices at a given site for risk characterization, remediation efforts, and future land use. This is particularly important in places with suspected PFAS use, including Rhode Island's numerous former textile and dye mills.

References

1. (2019) Validated Test Method 8327: Per-and Polyfluoroalkyl Substances (PFAS) Using External Standard Calibration and Multiple Reaction Monitoring (MRM) Liquid Chromatography/Tandem Mass Spectrometry (LC/MS/MS). EPA, U. (ed).
2. (ATSDR), A.f.T.S.a.D.R. (2018) Toxicological profile for Perfluoroalkyls. (Draft for Public Comment). Atlanta, GA.
3. Abril, J.M. (2019) Radiometric dating of recent sediments: on the performance of ^{210}Pb -based CRS chronologies under varying rates of supply. *Quaternary Geochronology* 51, 1-14.
4. Abril, J.M. (2020) The Orientation of Gothic-Mudéjar Churches in Southern Spain: The Rotation of the Qibla and Sunrise on the Canonical Equinox. *Journal of Skyscape Archaeology* 6(2), 182-206.
5. Adegbite-Adeniyi, C., Gron, B., Rowles, B.M., Demeter, C.A. and Findling, R.L. (2012) An update on antidepressant use and suicidality in pediatric depression. *Expert opinion on pharmacotherapy* 13(15), 2119-2130.
6. Ahrens, L., Gerwinski, W., Theobald, N. and Ebinghaus, R. (2010) Sources of polyfluoroalkyl compounds in the North Sea, Baltic Sea and Norwegian Sea: Evidence from their spatial distribution in surface water. *Marine pollution bulletin* 60(2), 255-260.
7. Al Amin, M., Luo, Y., Nolan, A., Robinson, F., Niu, J., Warner, S., Liu, Y., Dharmarajan, R., Mallavarapu, M. and Naidu, R. (2021) Total oxidisable precursor assay towards selective detection of PFAS in AFFF. *Journal of Cleaner Production* 328, 129568.
8. Appleby, P.G. and Oldfield, F. (1978) The calculation of lead-210 dates assuming a constant rate of supply of unsupported ^{210}Pb to the sediment. *CATENA* 5(1), 1-8.
9. Appleby, P.G. and Oldfield, F. (1992) Uranium-series disequilibrium: applications to earth, marine, and environmental sciences. 2. ed.
10. Armitage, J.M., Macleod, M. and Cousins, I.T. (2009) Comparative assessment of the global fate and transport pathways of long-chain perfluorocarboxylic acids (PFCAs) and perfluorocarboxylates (PFCs) emitted from direct sources. *Environmental Science and Technology* 43(15), 5830-5836.
11. Ateia, M., Alsbaiee, A., Karanfil, T. and Dichtel, W. (2019) Efficient PFAS Removal by Amine-Functionalized Sorbents: Critical Review of the Current Literature. *Environmental Science and Technology Letters* 6(12), 688-695.
12. Barry, V., Winquist, A. and Steenland, K. (2013) Perfluorooctanoic acid (PFOA) exposures and incident cancers among adults living near a chemical plant. *Environmental Health Perspectives* 121(11-12), 1313-1318.

13. Bégué, J.-P. and Bonnet-Delpon, D. (2006) Recent advances (1995–2005) in fluorinated pharmaceuticals based on natural products. *Journal of Fluorine Chemistry* 127(8), 992-1012.
14. Bonn, B.A. and Rounds, S.A. (2010) Use of stable isotopes of carbon and nitrogen to identify sources of organic matter to bed sediments of the Tualatin River, Oregon, U. S. Geological Survey.
15. Bopp, R.F., Simpson, H.J., Olsen, C.R., Trier, R.M. and Kostyk, N. (1982) Chlorinated hydrocarbons and radionuclide chronologies in sediments of the Hudson River and Estuary, New York. *Environmental science & technology* 16(10), 666-676.
16. Bruel, R. and Sabatier, P. (2020) serac: AR package for ShortlivEd RAdionuclide Chronology of recent sediment cores. *Journal of Environmental Radioactivity* 225, 106449.
17. Buck, R.C., Franklin, J., Berger, U., Conder, J.M., Cousins, I.T., de Voogt, P., Jensen, A.A., Kannan, K., Mabury, S.A. and van Leeuwen, S.P.J. (2011) Perfluoroalkyl and Polyfluoroalkyl Substances in the Environment: Terminology, Classification, and Origins. *Integrated environmental assessment and management* 7(4), 513-541.
18. Conder, J.M., Hoke, R.A., Wolf, W.d., Russell, M.H. and Buck, R.C. (2008) Are PFCAs Bioaccumulative? A Critical Review and Comparison with Regulatory Criteria and Persistent Lipophilic Compounds. *Environmental science & technology* 42(4), 995-1003.
19. Dassuncao, C., Pickard, H., Pfohl, M., Tokranov, A. K., Li, M., Mikkelsen, B., ... & Sunderland, E. M. (2019). Phospholipid levels predict the tissue distribution of poly- and perfluoroalkyl substances in a marine mammal. *Environmental science & technology letters*, 6(3), 119-125.
20. Domingo, J.L. (2016) Nutrients and chemical pollutants in fish and shellfish. Balancing health benefits and risks of regular fish consumption. *Critical Reviews in Food Science and Nutrition* 56(6), 979-988.
21. Donazzolo, R., Orio, A.A. and Pavoni, B. (1982) Radiometric dating and pollutant profiles in a sediment core from the Lagoon of Venice. *Oceanologica Acta*, Special issue.
22. Ellis, D.A., Martin, J.W., De Silva, A.O., Mabury, S.A., Hurley, M.D., Sulbaek Andersen, M.P. and Wallington, T.J. (2004) Degradation of Fluorotelomer Alcohols: A Likely Atmospheric Source of Perfluorinated Carboxylic Acids. *Environmental science & technology* 38(12), 3316-3321.
23. Falandysz, J., Rostkowski, P., Jarzyńska, G., Falandysz, J.J., Taniyasu, S. and Yamashita, N. (2012) Determination of perfluorinated alkylated substances in sediments and sediment core from the Gulf of Gdańsk, Baltic Sea. *Journal of Environmental Science and Health - Part A Toxic/Hazardous Substances and Environmental Engineering* 47(3), 428-434.

24. Fry, B. (2006) *Stable isotope ecology*, Springer.
Fujii, Y., Sakurada, T., Harada, K.H., Koizumi, A., Kimura, O., Endo, T. and Haraguchi, K. (2015) Long-chain perfluoroalkyl carboxylic acids in Pacific cods from coastal areas in northern Japan: A major source of human dietary exposure. *Environmental Pollution* 199, 35-41.
25. Giesy, J.P. and Kannan, K. (2001) Global Distribution of Perfluorooctane Sulfonate in Wildlife. *Environmental science & technology* 35(7), 1339-1342.
26. Göckener, B., Eichhorn, M., Lämmer, R., Kotthoff, M., Kowalczyk, J., Numata, J., Schafft, H., Lahrssen-Wiederholt, M. and Bücking, M. (2020) Transfer of Per- And Polyfluoroalkyl Substances (PFAS) from Feed into the Eggs of Laying Hens. Part 1: Analytical Results including a Modified Total Oxidizable Precursor Assay. *Journal of Agricultural and Food Chemistry*.
27. Goldberg, E.D. (1963) Geochronology with ^{210}Pb radioactive dating. International Atomic Energy Agency, Vienna 121, 130.
28. Goodrow, S.M., Ruppel, B., Lippincott, R.L., Post, G.B. and Procopio, N.A. (2020) Investigation of levels of perfluoroalkyl substances in surface water, sediment and fish tissue in New Jersey, USA. *Science of The Total Environment* 729, 138839.
29. Grandjean, P., Andersen, E.W., Budtz-Jørgensen, E., Nielsen, F., Mølbak, K., Weihe, P. and Heilmann, C. (2012) Serum vaccine antibody concentrations in children exposed to perfluorinated compounds. *Jama* 307(4), 391-397.
30. Hansen, S., Vestergren, R., Herzke, D., Melhus, M., Evenset, A., Hanssen, L., Brustad, M. and Sandanger, T.M. (2016) Exposure to per- and polyfluoroalkyl substances through the consumption of fish from lakes affected by aqueous film-forming foam emissions — A combined epidemiological and exposure modeling approach. The SAMINOR 2 Clinical Study. *Environment International* 94, 272-282.
31. Higgins, C.P. and Luthy, R.G. (2006) Sorption of perfluorinated surfactants on sediments. *Environmental science & technology* 40(23), 7251-7256.
32. Holtvoeth, J., Whiteside, J.H., Engels, S., Freitas, F.S., Grice, K., Greenwood, P., Johnson, S., Kendall, I., Lengger, S.K. and Lücke, A. (2019) The paleolimnologist's guide to compound-specific stable isotope analysis—An introduction to principles and applications of CSIA for Quaternary lake sediments. *Quaternary Science Reviews* 207, 101-133.
33. Houtz, E.F. and Sedlak, D.L. (2012) Oxidative conversion as a means of detecting precursors to perfluoroalkyl acids in urban runoff. *Environmental Science and Technology* 46(17), 9342-9349.
34. Hubeny, J.B., McCarthy, F.M.G., Lewis, J., Drljepan, M., Morissette, C., King, J.W., Cantwell, M., Hudson, N.M. and Crispo, M.L. (2015) The paleohydrology of Sluice Pond, NE Massachusetts, and its regional significance. *Journal of paleolimnology* 53(3), 271-287.

35. Kabiri, S., Centner, M. and McLaughlin, M.J. (2021) Durability of sorption of per- and polyfluorinated alkyl substances in soils immobilised using common adsorbents: 1. Effects of perturbations in pH. *Science of The Total Environment*.
36. Kissa, E. (2001) Fluorinated surfactants and repellents. *Surfactant Science Series* 97, 1-615.
37. Koch, V., Knaup, W., Fiebig, S., Geffke, T. and Schulze, D. (2009) Biodegradation kinetic and estimated half-life of a Clariant fluorotelomer-based acrylate polymer - Results from a test on aerobic transformation in soil. *Reprod. Toxicol.* 27(3-4), 420-421.
38. Koelmel, J.P., Paige, M.K., Aristizabal-Henao, J.J., Robey, N.M., Nason, S.L., Stelben, P.J., Li, Y., Kroeger, N.M., Napolitano, M.P. and Savvaides, T. (2020) Toward comprehensive per- and polyfluoroalkyl substances annotation using fluoromatch software and intelligent high-resolution tandem mass spectrometry acquisition. *Analytical chemistry* 92(16), 11186-11194.
39. Koide, M., Bruland, K.W. and Goldberg, E.D. (1973) Th-228/Th-232 and Pb-210 geochronologies in marine and lake sediments. *Geochimica et Cosmochimica Acta* 37(5), 1171-1187.
40. Krishnaswamy, S., Lal, D., Martin, J.M. and Meybeck, M. (1971) Geochronology of lake sediments. *Earth and Planetary Science Letters* 11(1-5), 407-414.
41. Kulik, G.B. (1980) *The beginnings of the industrial revolution in America: Pawtucket, Rhode Island, 1672-1829*.
42. Labadie, P. and Chevreuil, M. (2011) Biogeochemical dynamics of perfluorinated alkyl acids and sulfonates in the River Seine (Paris, France) under contrasting hydrological conditions. *Environmental Pollution* 159(12), 3634-3639.
43. Latimer, J.S., Carey, C.G., Hoffman, E.J. and Quinn, J.G. (1988) Water Quality In The Pawtuxet River: Metal Monitoring And Geochemistry 1. *JAWRA Journal of the American Water Resources Association* 24(4), 791-800.
44. Lesueur, C., Gartner, M., Mentler, A. and Fuerhacker, M. (2008) Comparison of four extraction methods for the analysis of 24 pesticides in soil samples with gas chromatography–mass spectrometry and liquid chromatography–ion trap–mass spectrometry. *Talanta* 75(1), 284-293.
45. Lorenzo, M., Campo, J. and Picó, Y. (2018) Analytical challenges to determine emerging persistent organic pollutants in aquatic ecosystems. *TrAC - Trends in Analytical Chemistry* 103, 137-155.
46. MacInnis, J.J., Lehnerr, I., Muir, D.C.G., Quinlan, R. and De Silva, A.O. (2019) Characterization of perfluoroalkyl substances in sediment cores from High and Low Arctic lakes in Canada. *Science of The Total Environment* 666, 414-422.
47. Martin, J.W., Ellis, D.A., Mabury, S.A., Hurley, M.D. and Wallington, T.J. (2006) Atmospheric chemistry of perfluoroalkanesulfonamides: Kinetic and product studies

of the OH radical and Cl atom initiated oxidation of N-ethyl perfluorobutanesulfonamide. *Environmental Science and Technology* 40(3), 864-872.

48. Mecray, E.L. and ten Brink, M.R.B. (2000) Contaminant distribution and accumulation in the surface sediments of Long Island Sound. *Journal of Coastal Research*, 575-590.

49. Mueller, R. and Yingling, V. (2017) History and use of per- and polyfluoroalkyl substances (PFAS). Interstate Technology & Regulatory Council.

50. Mussabek, D., Ahrens, L., Persson, K.M. and Berndtsson, R. (2019) Temporal trends and sediment–water partitioning of per- and polyfluoroalkyl substances (PFAS) in lake sediment. *Chemosphere* 227, 624-629.

51. Nason, S.L., Koelmel, J., Zuverza-Mena, N., Stanley, C., Tamez, C., Bowden, J.A. and Godri Pollitt, K.J. (2020) Software comparison for nontargeted analysis of PFAS in AFFF-contaminated soil. *Journal of the American Society for Mass Spectrometry* 32(4), 840-846.

52. Nixon, S.W. and Fulweiler, R.W. (2012) Ecological footprints and shadows in an urban estuary, Narragansett Bay, RI (USA). *Regional Environmental Change* 12(2), 381-394.

53. Peterson, B.J. and Fry, B. (1987) Stable isotopes in ecosystem studies. *Annual review of ecology and systematics* 18(1), 293-320.

54. Plumlee, M.H., McNeill, K. and Reinhard, M. (2009) Indirect photolysis of perfluorochemicals: Hydroxyl radical-initiated oxidation of N-ethyl perfluorooctane sulfonamido acetate (N-EtFOSAA) and other perfluoroalkanesulfonamides. *Environmental Science and Technology* 43(10), 3662-3668.

55. Rajski, Ł., Petromelidou, S., Díaz-Galiano, F.J., Ferrer, C. and Fernández-Alba, A.R. (2021) Improving the simultaneous target and non-target analysis LC-amenable pesticide residues using high speed Orbitrap mass spectrometry with combined multiple acquisition modes. *Talanta* 228, 122241.

56. Rayne, S. and Forest, K. (2009) Perfluoroalkyl sulfonic and carboxylic acids: A critical review of physicochemical properties, levels and patterns in waters and wastewaters, and treatment methods. *Journal of Environmental Science and Health - Part A Toxic/Hazardous Substances and Environmental Engineering* 44(12), 1145-1199.

57. Rhoads, K.R., Janssen, E.M.L., Luthy, R.G. and Criddle, C.S. (2008) Aerobic biotransformation and fate of N-ethyl perfluorooctane sulfonamidoethanol (N-EtFOSE) in activated sludge. *Environmental Science and Technology* 42(8), 2873-2878.

58. Rosenblum, L. and Wendelken, S.C. (2019) Method 533: Determination of per- and polyfluoroalkyl substances in drinking water by isotope dilution anion exchange solid phase extraction and liquid chromatography/tandem mass spectrometry.

Tandem Mass Spectrometry (US Environmental Protection Agency, Washington, DC, 2019).

59. Simon, J.A., Abrams, S., Bradburne, T., Bryant, D., Burns, M., Cassidy, D., Cherry, J., Chiang, S.Y., Cox, D. and Crimi, M. (2019) PFAS Experts Symposium: Statements on regulatory policy, chemistry and analytics, toxicology, transport/fate, and remediation for per-and polyfluoroalkyl substances (PFAS) contamination issues. *Remediation Journal* 29(4), 31-48.

60. Spaan, K.M., van Noordenburg, C., Plassmann, M.M., Schultes, L., Shaw, S., Berger, M., Heide-Jørgensen, M.P., Rosing-Asvid, A., Granquist, S.M. and Dietz, R. (2020) Fluorine mass balance and suspect screening in marine mammals from the Northern Hemisphere. *Environmental science & technology* 54(7), 4046-4058.

61. Stahl, L.L., Snyder, B.D., Olsen, A.R., Kincaid, T.M., Wathen, J.B. and McCarty, H.B. (2014) Perfluorinated compounds in fish from U.S. urban rivers and the Great Lakes. *Science of The Total Environment* 499, 185-195.

62. Strivens, J.E., Kuo, L.-J., Liu, Y. and Noor, K.L. (2021) Spatial and temporal baseline of perfluorooctanesulfonic acid retained in sediment core samples from Puget Sound, Washington, USA. *Marine pollution bulletin* 167, 112381.

63. Suthersan, S., Quinnan, J., Horst, J., Ross, I., Kalve, E., Bell, C. and Pancras, T. (2016) Making strides in the management of “emerging contaminants”. *Groundwater Monitoring & Remediation* 36(1), 15-25.

Times, N.Y. (1991) Ernest Nathan Is Dead; *Entrepreneur Was* 86, New York Times, New York, New York.

64. Tylmann, W., Bonk, A., Goslar, T., Wulf, S. and Grosjean, M. (2016) Calibrating 210Pb dating results with varve chronology and independent chronostratigraphic markers: problems and implications. *Quaternary Geochronology* 32, 1-10.

65. van Leeuwen, S.P.J. and de Boer, J. (2007) Extraction and clean-up strategies for the analysis of poly- and perfluoroalkyl substances in environmental and human matrices. *Journal of Chromatography A* 1153(1), 172-185.

66. Williams, A., Grulke, C., Patlewicz, G. and Richard, A. (2019) An integrated data hub for per-and polyfluoroalkyl (PFAS) chemicals to support Non-Targeted Analysis via the US-EPA CompTox Chemicals Dashboard.

67. Yamaguchi, M., Arisawa, K., Uemura, H., Katsuura-Kamano, S., Takami, H., Sawachika, F., Nakamoto, M., Juta, T., Toda, E. and Mori, K. (2013) Consumption of seafood, serum liver enzymes, and blood levels of PFOS and PFOA in the Japanese population. *Journal of occupational health* 55(3), 184-194.

68. Yeung, L.W.Y., De Silva, A.O., Loi, E.I.H., Marvin, C.H., Taniyasu, S., Yamashita, N., Mabury, S.A., Muir, D.C.G. and Lam, P.K.S. (2013) Perfluoroalkyl substances and extractable organic fluorine in surface sediments and cores from Lake Ontario. *Environment International* 59, 389-397.

69. Yeung, L.W.Y., Stadey, C. and Mabury, S.A. (2017) Simultaneous analysis of perfluoroalkyl and polyfluoroalkyl substances including ultrashort-chain C2 and C3 compounds in rain and river water samples by ultra performance convergence chromatography. *Journal of Chromatography A* 1522, 78-85.
70. Zhang, X., Lohmann, R., Dassuncao, C., Hu, X.C., Weber, A.K., Vecitis, C.D. and Sunderland, E.M. (2016) Source Attribution of Poly- and Perfluoroalkyl Substances (PFASs) in Surface Waters from Rhode Island and the New York Metropolitan Area. *Environmental Science and Technology Letters* 3(9), 316-321.
71. Zhu, H. and Kannan, K. (2020) Total oxidizable precursor assay in the determination of perfluoroalkyl acids in textiles collected from the United States. *Environmental Pollution* 265, 114940.
72. Zushi, Y., Tamada, M., Kanai, Y. and Masunaga, S. (2010) Time trends of perfluorinated compounds from the sediment core of Tokyo Bay, Japan (1950s-2004). *Environmental Pollution* 158(3), 756-763.

Figures



Figure 3-1. A map of the Pawtuxet River in central Rhode Island, USA. The location of field sampling is denoted as the “Coring Location” on the map.

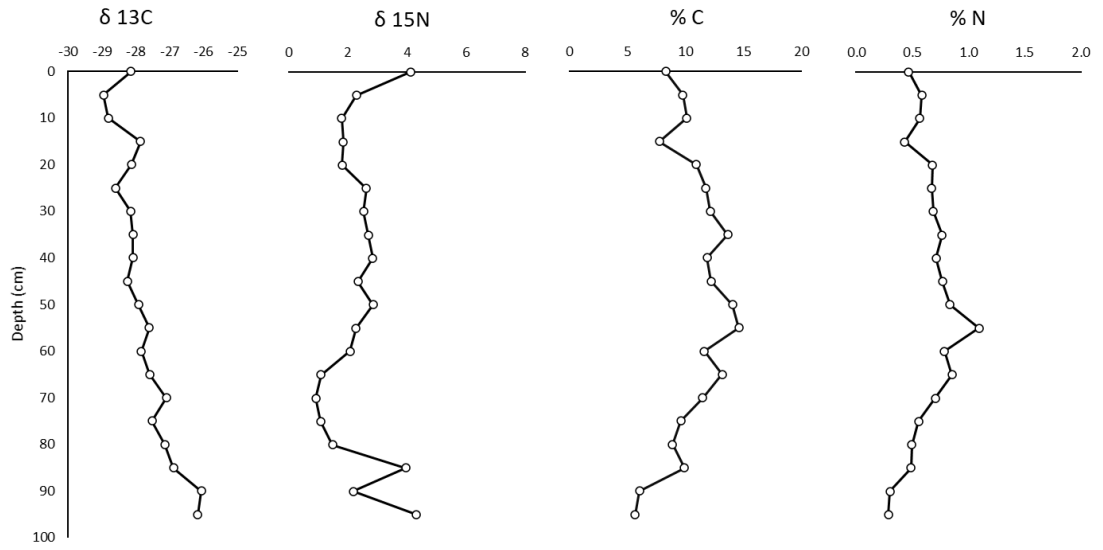


Figure 3-2. Stable isotope and elemental analysis of Carbon (C) and Nitrogen (N) in sediment cores as a function of depth.

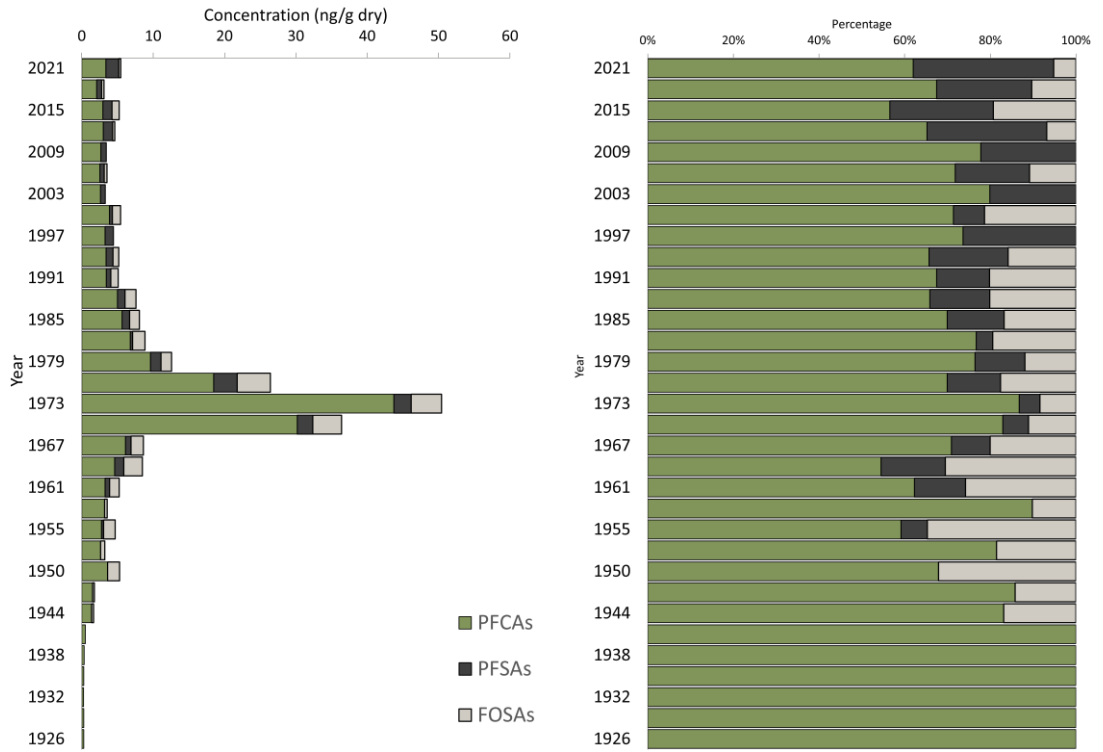


Figure 3-3. Σ PFAS by compound class in sediment core in ng/g and % proportionality.

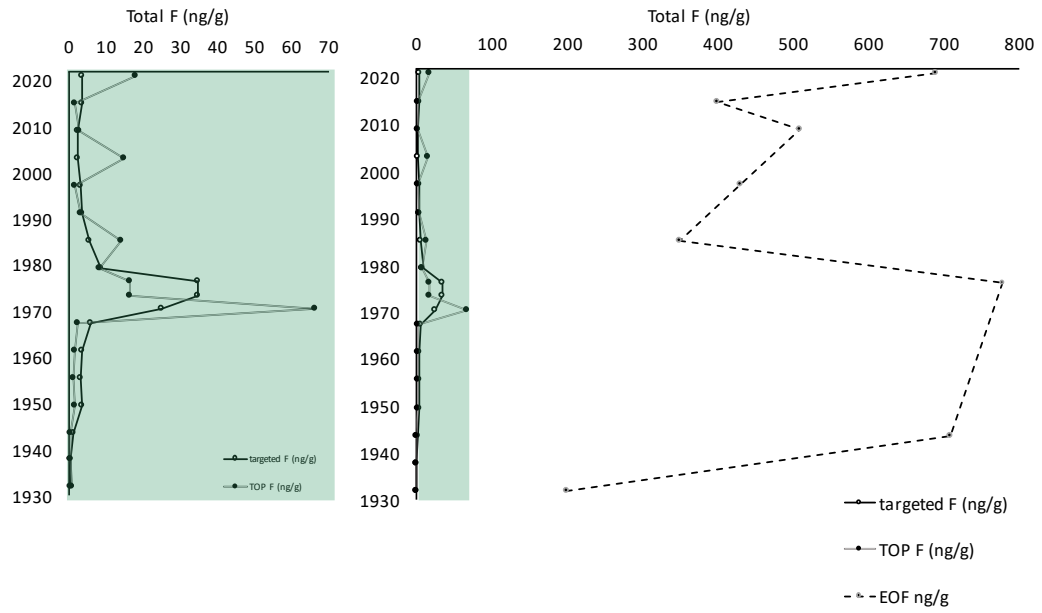


Figure 3-4. Total F abundance in Targeted Analysis, TOP Analysis, and EOF. Results from target-ed analysis and the TOP Assay are shown in blue. The chart on the right includes F abundance in EOF.

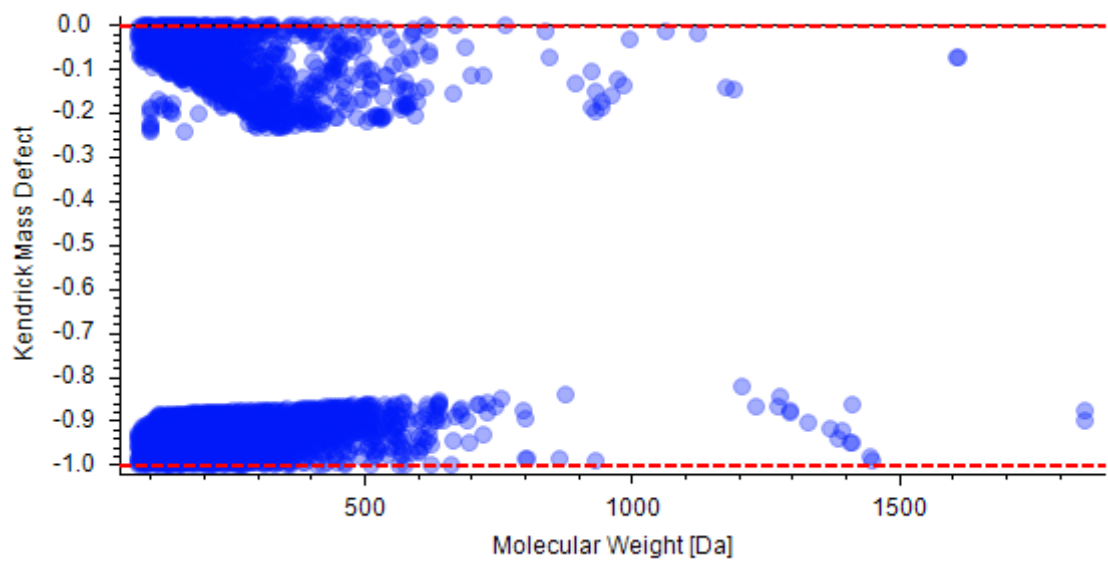


Figure 3-5. Kendrick Mass Defect Plot (KMD) of suspected fluorinated features based on insource fragmentation patterns.

Tables

Table 3-1. Targeted analysis of PFAS in surface sediment, fish muscle, and water from sediment coring location.

	Carbon chain (n)	Sediment (ng/g dry)	Fish (ng/g wet)	Water (ng/L)
Fluorotelomer Sulfonates				
4:2-FTS	6	ND	ND	ND
6:2-FTS	8	ND	ND	1.77
8:2-FTS	10	ND	ND	ND
Sulfonamides				
FOSA	10	ND	ND	ND
N-MeFOSAA	11	ND	ND	ND
EtFOSAA	12	0.28	0.02	ND
Carboxylates				
PFBA	4	ND	0.29	9.10
PFPeA	5	<MDL	<MDL	13.80
PFHxA	6	0.31	ND	15.17
PFHpA	7	<MDL	<MDL	7.86
PFOA	8	0.26	<MDL	17.92
PFNA	9	ND	0.02	3.19
PFDA	10	0.30	0.53	1.64
PFUdA	11	0.47	ND	0.47
PFDoA	12	1.05	0.91	ND
PFtrDA	13	0.41	1.62	ND
PFTeDA	14	0.58	0.61	ND
Sulfonates				
PFBS	4	ND	ND	6.10
PFPeS	5	ND	ND	0.44
PFHxS	6	0.12	0.05	6.80
PFHpS	7	ND	ND	ND
PFOS	8	1.68	4.70	18.07
PFNS	9	ND	ND	ND
PFDS	10	<MDL	0.31	<MDL
Total Σ PFAS		5.46	9.06	102.28

Supplemental Information

SI Figures

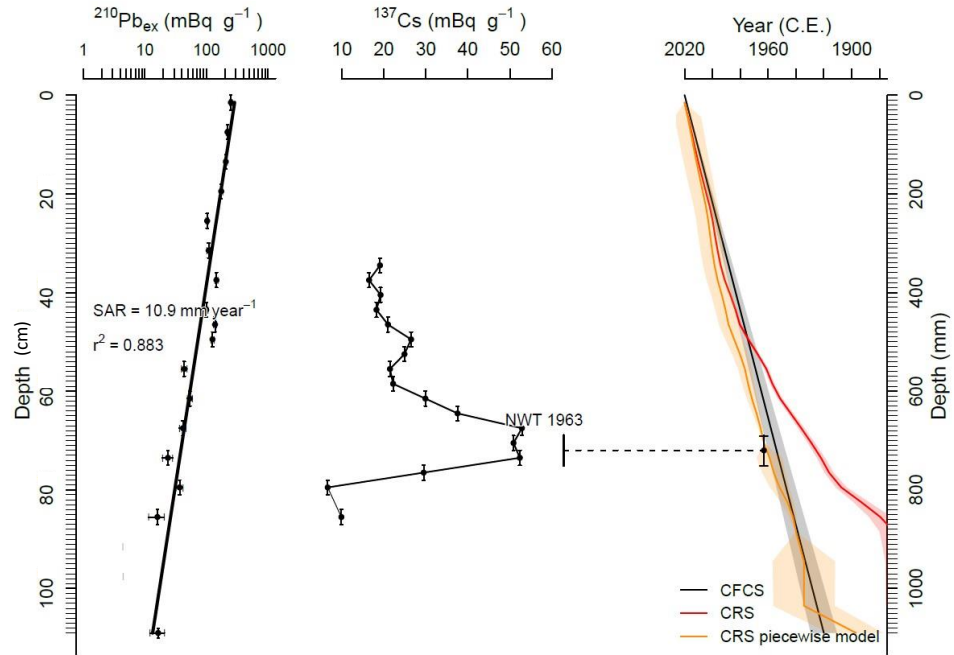


Figure 3-6. Radiometric Isotope data from ^{210}Pb and ^{137}Cs used to develop a Constant Rate of Supply (CRS) piecewise model.

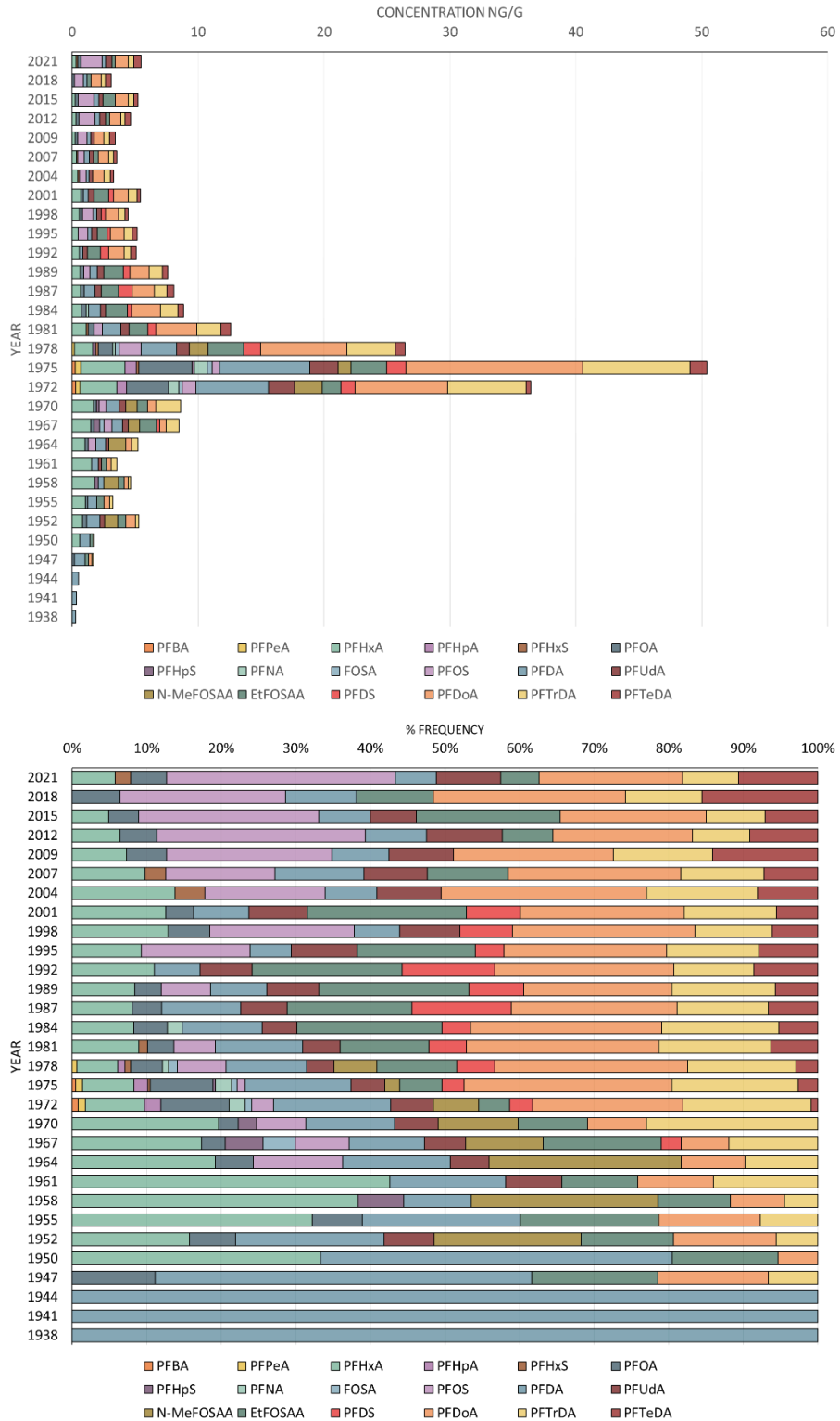


Figure 3-7. Σ PFAS by compound in sediment core in ng/g and % proportionality.

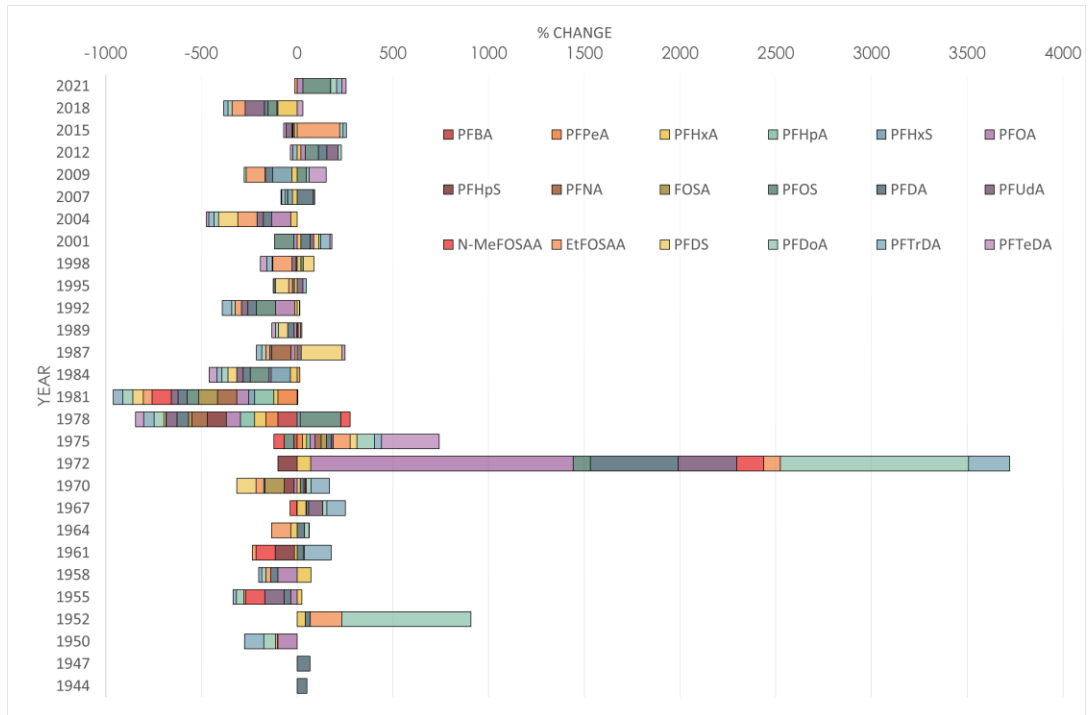


Figure 3-8. Percent change of PFAS deposition in sediment core. Percent change was calculated by comparing sediment sample concentration (x_2) to underlying sediment (x_1) as $(x_2 - x_1) / (x_1)$.

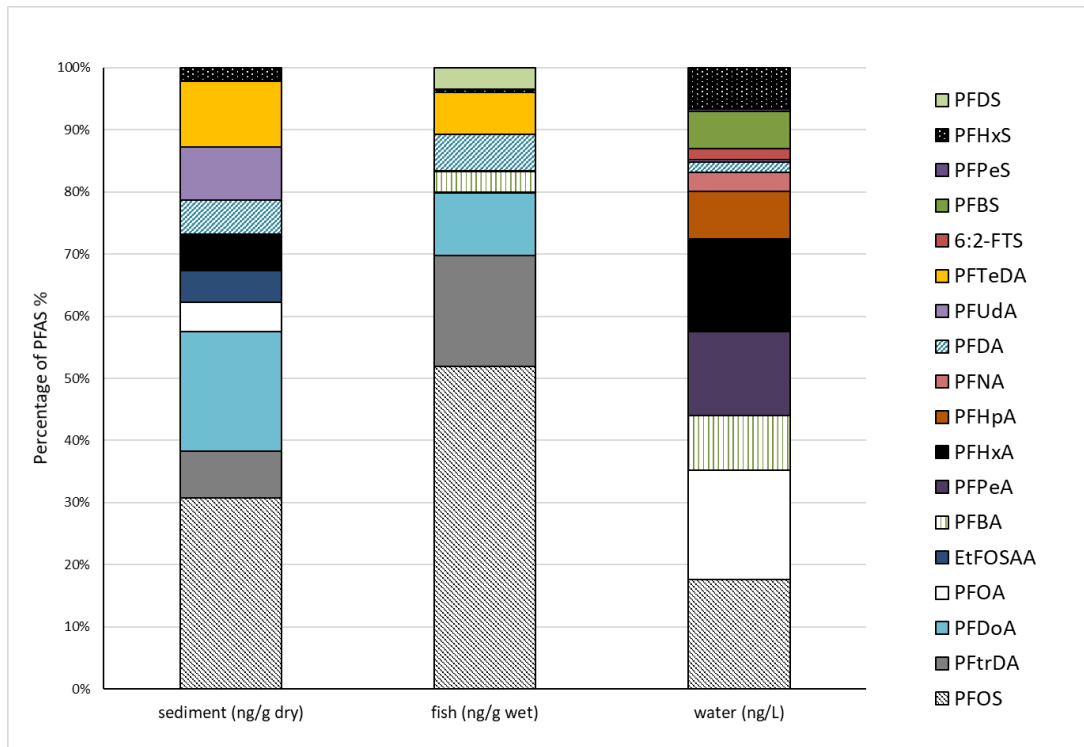


Figure 3-9. Percent frequency of PFAS found in surface sediment, fish muscle, and surface water.

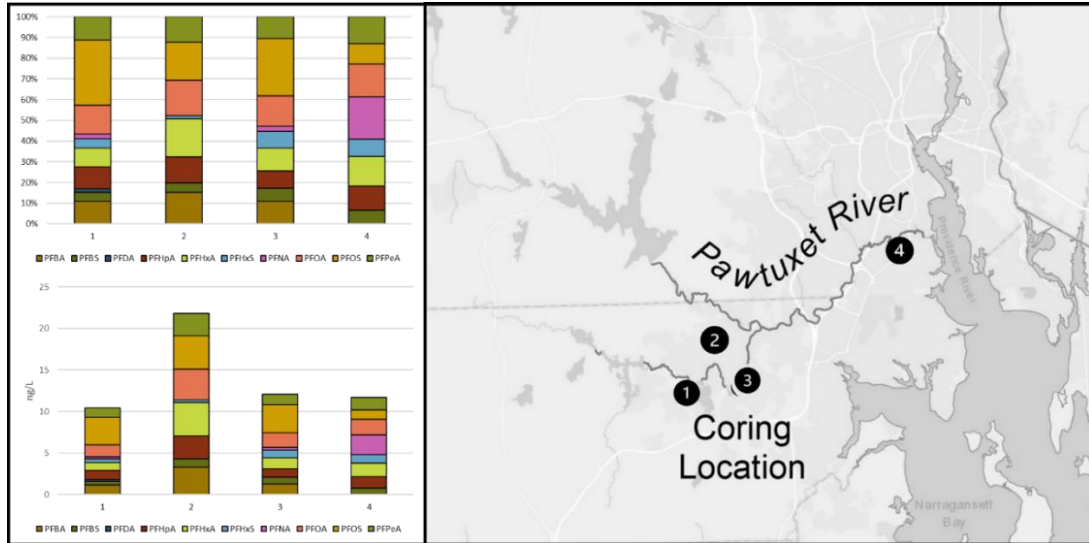


Figure 3-10. Upstream water concentrations of targeted PFAS. Samples were taken from (1) Pilgrim Avenue, (2) Washington Street, (3) Crompton Pier, and (4) Rhodes on the Pawtuxet in January 2021. Note - (3) Crompton Pier is the sediment coring location.

SI Tables

Table 3-2. List of PFAS analytes and isotopically labeled standards for targeted analysis on LC-MS/MS.

Native Compound (Catalog # PFAC-MXB)	Abbreviation	CAS#
Perfluoro-n-butanoic acid	PFBA	375-22-4
Perfluoro-n-pentanoic acid	PFPeA	2706-90-3
Potassium perfluoro-1-butanefulfonate	PFBS	29420-49-3
Perfluoro-n-hexanoic acid	PFHxA	307-24-4
Sodium 1H, 1H, 2H, 2H-perfluoro-1-hexanesulfonate	4:2-FTS	N/A
Sodium perfluoro-1-pentanesulfonate	PFPeS	N/A
Perfluoro-n-heptanoic acid	PFHpA	375-85-9
Potassium perfluorohexanesulfonate	PFHxS	432-50-7
Perfluoro-n-octanoic acid	PFOA	335-67-1
Sodium 1H, 1H, 2H, 2H-perfluoro-1-octanesulfonate	6:2-FTS	N/A
Sodium perfluoro-1-heptanesulfonate	PFHpS	N/A
Perfluoro-n-nonanoic acid	PFNA	375-95-1
Perfluoro-1-octanesulfonamide	FOSA	754-91-6
Potassium perfluorooctanesulfonate	PFOS	4021-47-0
Perfluoro-n-decanoic acid	PFDA	335-76-2
Sodium 1H, 1H, 2H, 2H-perfluoro-1-decanesulfonate	8:2-FTS	N/A
Sodium perfluoro-1-nonanesulfonate	PFNS	98789-57-2
Perfluoro-n-undecanoic acid	PFUdA	2058-94-8
N-methylperfluoro-1-octanesulfonamidoacetic acid	N-MeFOSAA	2355-31-9
N-ethylperfluoro-1-octanesulfonamidoacetic acid	N-EtFOSAA	2991-50-6
Sodium perfluoro-1-decanesulfonate	PFDS	2806-15-7
Perfluoro-n-dodecanoic acid	PFDoA	307-55-1
Perfluoro-n-tridecanoic acid	PFTTrDA	72629-94-8
Perfluoro-n-tetradecanoic acid	PFTeDA	376-06-7
Labeled Compound (Catalog # MPFAC-MXA)	Abbreviation	
Perfluoro-n-[¹³ C ₄]butanoic acid	MPFBA- ¹³ C ₄	
Perfluoro-n-[¹³ C ₅]pentanoic acid	M5PFPeA- ¹³ C ₅	
Sodium perfluoro-1-[2,3,4- ¹³ C ₃]butanesulfonate	M3PFBS- ¹³ C ₃	
Perfluoro-n-[1,2,3,4,6- ¹³ C ₅]hexanoic acid	M5PFHxA- ¹³ C ₅	
Sodium 1H,1H,2H,2H-perfluoro-1-[1,2- ¹³ C ₂]hexanesulfonate	M2-4:2-FTS- ¹³ C ₂	
Perfluoro-n-[1,2,3,4- ¹³ C ₄]heptanoic acid	M4PFHpA- ¹³ C ₄	
Sodium perfluoro-1-[1,2,3- ¹³ C ₃]hexanesulfonate	M3PFHxS- ¹³ C ₃	
Perfluoro-n-[¹³ C ₈]octanoic acid	M8PFOA- ¹³ C ₈	
Sodium 1H,1H,2H,2H-perfluoro-1-[1,2- ¹³ C ₂]octanesulfonate	M2-6:2-FTS- ¹³ C ₂	
Perfluoro-n-[¹³ C ₉]nonanoic acid	M9PFNA- ¹³ C ₉	
Perfluoro-1-[¹³ C ₈]octanesulfonamide	M8FOSA	
Sodium perfluoro-1-[¹³ C ₈]octanesulfonate	M8PFOS- ¹³ C ₈	
Perfluoro-n-[1,2,3,4,5,6- ¹³ C ₆]decanoic acid	M6PFDA- ¹³ C ₆	
Sodium 1H,1H,2H,2H-perfluoro-1-[1,2- ¹³ C ₂]decanesulfonate	M2-8:2-FTS- ¹³ C ₂	

Perfluoro-n-[1,2,3,4,5,6,7- ¹³ C ₇]undecanoic acid	M7PFUdA- ¹³ C ₇	
N-methyl-d ₃ -perfluoro-1-octanesulfonamidoacetic acid	MeFOSAA-d ₃	
N-ethyl-d ₅ -perfluoro-1-octanesulfonamidoacetic acid	EtFOSAA-d ₅	
Perfluoro-n-[1,2- ¹³ C ₂]dodecanoic acid	M2PFDoA- ¹³ C ₂	
Perfluoro-n-[1,2- ¹³ C ₂]tetradecanoic acid	M2PFTeDA- ¹³ C ₂	

Table 3-3. Minimum Detection Limits calculated for sediment and water samples on LC-MS/MS.

	MDL sediment/tissue (ng/g)	MDL water (ng/L)
PFBA	0.20	0.05
PFPeA	0.22	0.03
PFBS	0.32	0.05
PFHxA	0.44	0.05
4:2 FTS	0.28	0.10
PFPeS	0.30	0.11
PFHpA	0.48	0.06
PFHxS	0.20	0.07
PFOA	0.36	0.06
6:2-FTS	0.64	0.12
PFHpS	0.33	0.16
PFNA	0.36	0.08
FOSA	0.53	0.07
PFOS	0.96	0.08
PFDA	0.45	0.08
8:2-FTS	0.64	0.24
PFNS	1.03	0.09
PFUdA	0.48	0.11
N-MeFOSAA	1.72	0.03
EtFOSAA	0.15	0.08
PFDS	0.44	0.18
PFDoA	0.11	0.06
PFTTrDA	0.15	0.13
PFTeDA	0.27	0.86

Table 3-4. PFAS concentrations in sediment targeted analysis. Concentrations reported in ng/ g dry sediment. Nondetect (ND) and concentrations below the minimum detection limit (MDL) are not reported.

	P F B A	P F P e A	P F B S	P F H x A	4- F T S	P F P e S	P F H p A	P F H x S	P F O A	6 : 2 - F T S	P F H p S	P F N A	F O S A	P F O S	P F D A	8 : 2 - F T S	P F N S	P F U d A	N- M e F O S A A	E t F O S A A	P F D S	P F D o A	P F T r D A	P F T e D A
3	ND	ND	ND	0.31*	ND	ND	ND	0.12*	0.26*	ND	ND	ND	ND	1.68	0.30*	ND	ND	0.47*	ND	0.28	ND	1.05	0.41	0.58
6	ND	ND	ND	ND	ND	ND	ND	0.20*	ND	ND	ND	ND	ND	0.69	0.30*	ND	ND	ND	ND	0.32	ND	0.80	0.32	0.48
9	ND	ND	ND	0.26*	ND	ND	ND	0.21*	ND	ND	ND	ND	ND	1.27	0.37*	ND	ND	0.32*	ND	1.01	ND	1.03	0.42	0.37
12	ND	ND	ND	0.30*	ND	ND	ND	0.23*	ND	ND	ND	ND	ND	1.29	0.38*	ND	ND	0.47*	ND	0.31	ND	0.87	0.35	0.42
15	ND	ND	ND	0.25*	ND	ND	ND	0.18*	ND	ND	ND	ND	ND	0.76*	0.26*	ND	ND	0.30*	ND	ND	ND	0.74	0.46	0.49
18	ND	ND	ND	0.35*	ND	ND	ND	0.10*	ND	ND	ND	ND	ND	0.52*	0.42*	ND	ND	0.30*	ND	0.38	ND	0.82	0.40	0.26*
21	ND	ND	ND	0.46	ND	ND	ND	0.13*	ND	ND	ND	ND	ND	0.53*	0.23*	ND	ND	0.28*	ND	ND	ND	0.91	0.49	0.27
24	ND	ND	ND	0.68	ND	ND	ND	0.20*	ND	ND	ND	ND	ND	0.40*	ND	ND	ND	0.43*	ND	1.16	0.39*	1.19	0.68	0.30
27	ND	ND	ND	0.57*	ND	ND	ND	0.25*	ND	ND	ND	ND	ND	0.86*	0.27*	ND	ND	0.36*	ND	ND	0.31*	1.09	0.46	0.27
30	ND	ND	ND	0.48	ND	ND	ND	ND	ND	ND	ND	ND	ND	0.76*	0.28*	ND	ND	0.46*	ND	0.82	0.20*	1.13	0.64	0.41
33	ND	ND	ND	0.56	ND	ND	ND	ND	ND	ND	ND	ND	ND	0.31*	ND	ND	ND	0.35*	ND	1.03	0.63	1.23	0.55	0.44
36	ND	ND	ND	0.64	ND	ND	ND	0.27*	ND	ND	ND	ND	ND	0.50*	0.57*	ND	ND	0.53	ND	1.53	0.56	1.51	1.05	0.43
39	ND	ND	ND	0.65	ND	ND	ND	0.31*	ND	ND	ND	ND	ND	0.86	ND	ND	ND	0.50	ND	1.35	1.07	1.80	0.99	0.53
42	ND	ND	ND	0.73	ND	ND	ND	0.40	ND	ND	0.18*	ND	ND	0.95	ND	ND	0.42*	ND	1.72	0.34*	2.27	1.39	0.46	
45	ND	ND	ND	1.13	ND	ND	ND	0.14*	0.45	ND	ND	ND	ND	0.70*	1.48	ND	0.63	ND	1.50	0.63	3.25	1.89	0.80	
48	ND	0.17*	ND	1.45	ND	ND	0.24*	0.21	1.13	ND	0.22*	0.32*	1.73	2.85	ND	0.98	1.53*	2.81	1.35	6.84	3.84	3.84	0.77	
51	0.23	0.47	ND	3.50	ND	ND	0.92	0.18*	4.21	ND	0.19*	0.05	0.39	0.55	7.16	ND	2.27	1.02*	2.84	1.50	14.06	8.52	1.34	
54	0.29	0.36	ND	2.89	ND	ND	0.79	ND	3.33	ND	ND	0.80	0.31	1.08	5.73	ND	2.07	2.22	1.50	1.11	7.34	6.27	0.33	
57	ND	ND	ND	1.69	ND	ND	ND	0.23*	ND	0.21*	ND	ND	ND	0.57*	1.03	ND	0.51	0.92*	0.81	ND	0.68	1.99	ND	
60	ND	ND	ND	1.47	ND	ND	ND	0.27*	ND	0.43	ND	0.36*	0.61*	0.86	ND	ND	0.47*	0.88*	1.34	0.23*	0.54	1.01	ND	
63	ND	ND	ND	1.01	ND	ND	ND	0.27*	ND	ND	ND	ND	ND	0.63*	0.76	ND	0.27*	1.35*	ND	ND	0.45	0.52	ND	
66	ND	ND	ND	1.52	ND	ND	ND	ND	ND	ND	ND	ND	ND	0.55	ND	ND	0.27*	ND	0.36	ND	0.36	0.50	ND	
69	ND	ND	ND	1.79	ND	ND	ND	ND	ND	0.29*	ND	ND	ND	0.42*	ND	ND	ND	1.17*	0.45	ND	0.34	0.21	ND	
72	ND	ND	ND	1.04	ND	ND	ND	0.22*	ND	ND	ND	ND	ND	0.68	ND	ND	ND	ND	0.60	ND	0.44	0.25	ND	
75	ND	ND	ND	0.84	ND	ND	ND	0.33*	ND	ND	ND	ND	ND	1.05	ND	ND	0.36*	1.04*	0.66	ND	0.73	0.30	ND	
78	ND	ND	ND	0.59	ND	ND	ND	ND	ND	ND	ND	ND	ND	0.83	ND	ND	ND	ND	0.25	ND	0.09*	ND	ND	
81	ND	ND	ND	ND	ND	ND	ND	0.19*	ND	ND	ND	ND	ND	0.84	ND	ND	ND	ND	0.28	ND	0.25	0.11*	ND	
84	ND	ND	ND	ND	ND	ND	ND	ND	ND	ND	ND	ND	ND	0.50	ND	ND	ND	ND	ND	ND	ND	ND	ND	ND
87	ND	ND	ND	ND	ND	ND	ND	ND	ND	ND	ND	ND	ND	0.33*	ND	ND	ND	ND	ND	ND	ND	ND	ND	ND
90	ND	ND	ND	ND	ND	ND	ND	ND	ND	ND	ND	ND	ND	0.28*	ND	ND	ND	ND	ND	ND	ND	ND	ND	ND

Table 3-5. PFAS concentrations in fish tissue. Concentrations reported in ng/g dry sediment. Nondetect (ND) and concentrations below the minimum detection limit (MDL) are not reported.

	FOSA	PFBA	PFDA	PFDoA	PFDS	PFHxS	PFNA	PFOS	PFTeDA	PFTrDA
Fish A	0.00	3.07	2.92	3.78	0.97	0.54	0.00	30.66	2.10	10.20
Fish A dup	0.00	2.40	1.91	4.02	2.66	0.70	0.00	32.91	3.40	6.72
Fish B	0.00	4.21	6.27	5.97	7.28	0.00	0.00	65.52	3.19	9.46
Fish C	0.00	2.90	3.10	4.08	0.00	0.00	0.00	13.82	0.88	7.24
Fish D	0.27	0.69	2.15	4.67	1.01	0.24	0.00	21.96	5.34	8.91
Fish E	0.00	0.82	2.24	4.67	1.32	0.24	0.26	16.12	1.62	6.81

Table 3-6. Grainsize of select sediment samples. All values are mean of 3 replicates.

Depth (cm)	Average of D ₁₀ (µm)	Average of D ₅₀ (µm)	Average of D ₉₀ (µm)
15	13.7	45.6	152.0
20	12.5	40.8	147.7
25	12.0	41.7	139.7
35	11.6	40.1	135.0
40	12.9	45.6	149.3
45	12.9	45.2	146.7
80	10.1	37.8	180.3
95	8.5	29.7	119.0
97	9.5	32.8	141.0

Table 3-7. Analysis of 2,4-DDD, 4,4-DDT, and 2,4-DDT (ng/g) for sediment age depth.

Depth (cm)	2,4-DDD (ng/g)	4,4-DDT (ng/g)	2,4-DDT (ng/g)
78	32.93	15.72	51.34
81	15.66	9.26	13.56
84	39.88	35.46	3.05
87	7.12	5.64	1.96
90	ND	ND	ND
93	ND	ND	ND
96	ND	ND	ND
99	ND	ND	ND
102	ND	ND	ND

Table 3-8. PFAS concentrations in sediment targeted analysis from the TOP assay. Concentrations reported in ng/g dry sediment. Non-detect (ND) and concentrations below the minimum detection limit (MDL) are not reported.

	4: 2- FT S	6: 2- FT S	8: 2- FT S	EtF OS AA	F O S A	N- MeF OSA A	P F B A	P F B S	P F D A	P F D o A	P F D S	P F H p A	P F H p S	P F H xA	P F H xS	P F N A	P F N S	P F O A	P F O S	P F P e A	P F P e S	PF Te DA	PF Tr DA	P F U d A
3	0.01	0.40					0.331		0.229	0.370	0.033	0.027		0.380	0.020	0.011		0.056	0.013	0.053		0.055	0.026	0.027
9	0.11	24.20	0.02		0.02	0.00	0.377		0.110	0.130	0.011	0.014	0.04	0.29	0.02	0.012		0.088	0.010	0.032		0.055	0.010	0.11
15	0.01	0.39	0.00				0.022		0.011	0.230	0.022	0.009		0.10	0.03	0.000	0.00	0.022	0.011	0.010		0.066	0.023	0.20
21	0.00	0.24				0.03	0.400		0.035	0.506	0.006	0.033		0.26	0.02	0.021		0.094	0.044			0.044	0.037	0.33
27	0.08	14.86	0.03				0.555		0.088	0.951	0.013	0.076	0.02	0.68	0.03	0.057		1.063	0.072			0.111	0.062	0.68
33		0.68			0.02		0.688		1.078	1.301	0.022	1.02		0.88	0.06	0.096		1.096	0.073			0.094	0.059	1.09
39					0.01		1.166		3.045	3.021	0.071	2.57		1.81	0.04	0.024		3.020	0.022	0.098		0.088	1.062	2.38
45			0.00			0.01	6.966		1.275	6.381	0.011	15.288		10.027	0.04	0.012		1.197	0.011	0.127	0.01	0.099	1.068	8.24
51		0.50		0.08	0.01	0.01	0.022	0.011	0.043	0.021	0.004	0.013		0.15	0.03	0.007	0.00	0.031	0.026			0.038	0.078	0.15
54		0.38	0.01			0.07	0.335	0.018	0.027	0.005	0.005	0.005	0.07	0.09		0.055	0.02	0.018	0.007	0.008	0.008	0.033	0.007	0.09
57		0.17		0.07	0.02	0.07	0.088	0.006	0.026	0.013	0.003	0.005	0.03	0.09		0.044		0.013	0.005	0.016	0.002	0.007	0.024	0.12
63		0.35		0.19		0.51		0.012	0.010	0.160	0.002	0.005		0.10	0.04	0.004	0.002	0.017	0.004			0.011	0.003	0.17
69		0.01				0.02	0.060		0.020	0.001		0.02		0.06	0.02	0.002		0.008	0.006			0.007	0.002	0.02
75					0.00		0.011		0.015	0.000		0.01	0.02	0.02	0.02	0.002		0.003	0.005	0.009	0.009	0.006	0.000	0.00
81		0.44			0.01	0.02	0.211		0.013	0.000		0.01	0.02	0.03				0.002	0.003	0.005	0.006	0.002	0.002	0.01
87	0.01	0.40					0.311		0.029	0.037	0.003	0.027		0.38	0.02	0.016		0.051	0.013	0.053		0.055	0.026	0.27
93	0.11	24.20	0.02		0.02	0.00	0.377		0.110	0.130	0.011	0.014	0.04	0.29	0.02	0.012		0.088	0.010	0.032		0.055	0.010	0.11

Table 3-9. Total Fluorine (F) in ng from targeted analysis, TOP Assay, and EOF for surface water and sediment core

Water Volume (L)	Targeted F (ng/L)	TOP F (ng/L)	EOF (ng/L)
1	65.19	n/a	1600
Depth (cm)	targeted F (ng/g)	TOP F (ng/g)	EOF ng/g
3	3.62	18.08	690
9	3.41	1.65	400
15	2.34	2.66	510
21	2.25	14.71	
27	3.01	1.38	430
33	3.39	3.14	
39	5.41	14.04	350
45	8.52	8.22	
48	34.71	16.47	780
51	34.71	16.47	
54	24.93	66.40	
57	5.76	2.12	
63	3.49	1.39	
69	3.04	1.24	
75	3.53	1.67	
81	1.13	0.52	710
87	0.23	0.36	
93	0.18	0.65	200

CONCLUSION

These three chapters explored novel techniques to quantify MPs and PFAS from sediments. Overall, I found that PFAS and MPs were ubiquitous in the analyzed sediments. Chapter 1's focus on comparison of MP extraction methods highlights the variability in detection and reporting based on extraction procedure. This makes it difficult to make meaningful comparisons of MP abundance in environmental sediments. Chapter 2 presented the hybridized method for the extraction of MPs and highlighted environmental MP concentrations from Narragansett Bay. MPs within Narragansett Bay ranged from 40 -4,600,000 pieces/ 100 g sediment. These MP concentrations reported within Chapter 2 are startling. But these concentrations may become common as advancements are made in the detection capabilities of MPs. The same can be said for Chapter 3, though the contaminant class shifts to PFAS. PFAS are found ubiquitously in the environment, but sediments are often excluded from environmental assessments. I detected $\sum 50.4 \mu\text{g}/\text{kg}$ PFAS within the sediment core through targeted analysis and anticipate these concentrations will increase with additional NTA results. Advancements in methodologies to detect broader ranges of PFAS will continue to raise reported concentrations in environmental media.

While both suites of contaminants are very different from one another, PFAS and MPs share several similarities. Both represent vast classes of pollutants with thousands of possible congeners. Plastics and PFAS both became commercially available in the 1950s. Their high use and chemical

persistence have led to wide-spread environmental contamination. Today, we struggle with finding adequate methods to quantify and remediate these pollutants. Further complicating these matters is the rapid introduction of replacement products, such as plastic alternatives and novel PFAS. These compounds are developed at rates that make it nearly impossible for environmental researchers to keep up with their detection and quantification in the environment. These areas of research are very much in early stages but are rapidly expanding. As shown here, recent advancements in analytical detection of both MPs and PFAS aid in better understanding their fate and relevant concentrations. This will ultimately lead to more holistic assessments of their roles as environmental contaminants.